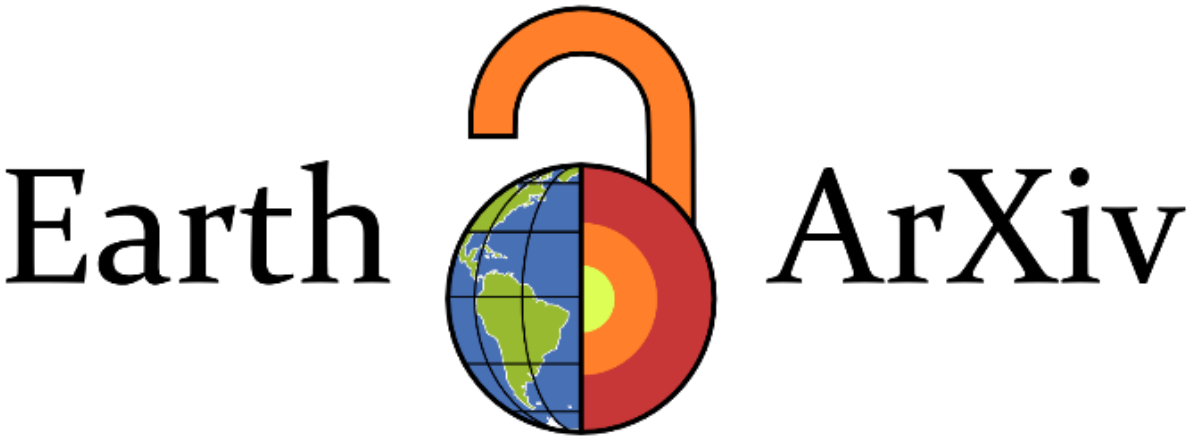

Submitted to Gondwana Research

Reconstruction of plate tectonic evolution and orogenesis of the Central Tethysides (Iran, Afghanistan) since the Permian

Nalan Lom[1,2,3*], Douwe J.J. van Hinsbergen[1]

1. Department of Earth Sciences, Utrecht University, Princetonlaan 8A, 3584 CB Utrecht, the Netherlands
2. Institute of Earth Sciences, Heidelberg University, Heidelberg, Germany
3. Department of Earth and Environmental Sciences, School of Arts and Sciences, University of Central Asia, Khorog, Tajikistan

*Corresponding author: nalan.lom@ucentralasia.org

For: Gondwana Research [Focus Review]

Abstract

The Central Tethysides constitute the Iranian and Afghan section of the Alpine-Himalayan orogenic belt. Two large sutures in the north and south are widely considered to represent the closed Paleo- and Neotethys ocean, respectively, with a 'Cimmerian' continent in between that traveled from Gondwana-Land to Eurasia in the Permo-Triassic and reconnected with Arabia in the late Oligocene. However, the smaller Sabzevar-Nain-Baft and Sistan Sutures in Iran have not been kinematically reconstructed in detail before. Here, we review geological constraints on the architecture of the Central Tethysides and provide a GPlates-based reconstruction of its (plate) tectonic history. We show that the Sabzevar-Nain-Baft ocean basin opened by late Jurassic-early Cretaceous N-S back-arc extension that also formed the continental Central Basin, in tandem with opening of the South Caspian-Kopet Dagh basin to the north. The Sabzevar-Nain-Baft basin closed in late Cretaceous-Eocene time by westwards extrusion of the Central-East Iranian Microcontinent (CEIM) and its eastward extension, the Farah Rud Block. The Sistan Ocean closed simultaneously by faster westwards extrusion of the Helmand Block, originally part of the Tibetan Qiangtang terrane. Extrusion exceeded 1000 km and was likely initiated by Cretaceous shortening in the Tibetan Plateau. Early Cretaceous opening of the Sistan Ocean and simultaneous closure of the Waser Suture between Helmand and Farah Rud accommodated the final collision of the China Blocks with Eurasia. Whilst we reconcile known evidence with Tethyan plate tectonic history, key information remains hidden in the spectacular geology of Iran and Afghanistan, awaiting future detailed mapping and analysis.

Introduction

The Alpine-Himalayan Mountain belt comprises continent-derived accretionary fold-thrust belts and more or less intact continental fragments, bounded by east-west trending suture zones that contain deformed remains of oceanic lithosphere (Stöcklin, 1968, 1974a; Schreiber et al., 1972; Berberian and King, 1981; Abdullah and Chmyriov, 2008; Shafaii Moghadam and Stern, 2014, 2015). This mountain belt has long been recognized as the remnant of several ~E-W trending and eastward widening oceanic basins and intervening continental fragments, collectively referred to as the ‘Cimmerian Continent’, that formed and closed since Paleozoic times between Gondwana-Land-derived continents in the south (Africa, Arabia, India) and Eurasia and its precursor continents to the north (Stöcklin, 1974a; Şengör, 1979, 1984, 1990;

Savostin et al., 1986; Boulin, 1988; Şengör et al., 1988). The orogen that resulted from the closure of the Tethys oceans is referred to as the Tethysides (Şengör, 1987). But when studied in more detail, first-order along-strike heterogeneity in tectonic architecture and deformation patterns become apparent. The sizes of continental units between sutures, the ages of opening and closure of ocean basins, and even the number of suture zones that formed since the Paleozoic vary and change abruptly over lineaments that are at high angle to the overall E-W orogen strike (e.g., Stöcklin, 1974a; Şengör, 1987, 1990; Stampfli, 2000; Stampfli and Borel, 2002; Yin, 2010) (Fig. 1). Based on the distinct tectonic architectures and histories, the orogen can be subdivided at first-order into three segments, from west to east, these are the (eastern) Mediterranean, Iranian-Afghan, and Indian-Tibetan segments, whose boundaries likely represent former transform plate boundaries that existed within the Tethyan oceans. Reconstructing the deformation history within each segment is then key to unravel the plate kinematic history of these Tethyan plates, and the dynamics that drove ocean closure and orogenesis.

The Himalaya-Tibetan and eastern Mediterranean segments of this orogenic system show dominantly E-W trending suture zones and continental fragments that are contiguous throughout each segment. Even though orogen-lateral motions in the eastern Mediterranean and Tibetan regions are well-known (e.g., Dewey and Şengör, 1979; Tapponnier et al., 1982; Şengör, 1984; Leloup et al., 1995; Şengör et al., 2005; Li et al., 2017; Whitney et al., 2025), these orogenic systems were predominantly deformed by overall north-south convergence and shortening that governed ocean closure and orogenesis (e.g., Kapp and DeCelles, 2019; van Hinsbergen et al., 2019; 2020). However, the Iranian and Afghan segments display Paleogene sutures that closed mid-late Mesozoic ocean basins, and these sutures are at high angles, to even orthogonal to the east-west trending overall system (Camp and Griffis, 1982; Tirrul et al., 1983; Bagheri and Stampfli, 2008; Bagheri and Gol, 2020) (Fig. 2). These discontinuous sutures are puzzling and have only provisionally been placed in a kinematic framework (Van der Voo, 1993; Fourcade et al., 1995; Dercourt et al., 2000; Stampfli, 2000; Golonka, 2004). An important implication of the orientation of these sutures is that a considerable amount of east-west shortening must be inferred to generate the modern pattern (e.g., Bagheri and Gol, 2020). Although this shortening component has been realized in previous studies that focused on Iran (e.g., Tirrul et al. 1983; Bröcker et al., 2013; Jentzer et

al., 2017), the kinematic implications that such orogen-parallel motions must have for the kinematic history of western Tibet and adjacent areas (e.g., Tapponnier et al., 1981) has not been accounted for in plate reconstructions.

In this paper, we review the available structural and stratigraphic constraints from sutures and intervening continental fragments on the architecture of the Central Tethysides and use this to reconstruct the kinematic evolution of the opening and closure of the ocean basins in Iran and Afghanistan. We attempt at restoring the deformation since the Jurassic in detail and illustrate the Permian and Triassic history in a wider context of the evolution of the Tethyan oceans. We will use our reconstruction to discuss the opening and closure history of back-arc basins in the Central Tethyan region and the role of orogen-lateral tectonic extrusion therein. Finally, we will use our results to discuss how the evolution of the Central Tethysides may aid the reconstruction of the enigmatic closure history of the final intra-Asian oceans between the China and Tibetan Blocks and Eurasia.

1. Regional Geological Setting

The region including Iran and Afghanistan constitutes the central part of the Alpine-Himalayan mountain belt and the Tethyan paleogeographic domain. Its first-order architecture is defined by continental fragments that are separated from Eurasia by a Triassic suture zone adorned with Paleozoic oceanic rocks, interpreted as the remains of the Paleo-Tethys, and by a Cenozoic suture with Mesozoic oceanic rocks, interpreted as the remains of the Neo-Tethys Ocean (Stöcklin, 1974a, 1989; Berberian and King, 1981; Tapponnier et al., 1981; Şengör 1990a,b; Stampfli, 2000; Torsvik and Cocks, 2017) (Supplementary Information 1). The continental fragments exposed in Iran and Afghanistan between these sutures contain crystalline basement that underwent similar Precambrian histories as basement in Arabia and that shares no similarities with Eurasian basement to the north, based on which they have long been interpreted as formed along the northern or/and northeastern margin of Gondwana-Land (e.g., Şengör et al., 1988; Davydov and Arerifard, 2007; Shakerardakani et al., 2021). The stratigraphic constraints from the suture zones shows that these 'Cimmerian' continental fragments detached from Gondwana-Land in the Permian and accreted to Laurasia in the late Triassic (Şengör et al., 1988; Stampfli and Borel, 2002), as also shown by paleomagnetic data that reveal a Permo-Triassic paleolatitudinal drift from the Gondwana-

Land to the Eurasian margin (Wensink et al., 1978; Van der Voo, 1993; Muttoni et al., 2009). Subsequent closure of the Neo-Tethys was underway by Jurassic time, as shown by the long-lived Sanandaj-Sirjan magmatic arc on the southern part of the Cimmerian continent (e.g., Hassanzadeh and Wernicke, 2016) and was finalized in late Oligocene time (McQuarrie and van Hinsbergen, 2013; Koshnaw et al., 2019; Cai et al., 2021), after which convergence was accommodated by shortening and strike-slip deformation within Iran, and underthrusting of the Arabian continental margin (Vernant et al., 2004a,b; Agard et al., 2011; Mouthereau, 2011; McQuarrie and van Hinsbergen, 2013).

In between the laterally continuous and widely recognized Paleo-Tethys and Neo-Tethys sutures, the 'Cimmerian' continental units in Iran and Afghanistan are broken into blocks separated by major fault zones (thrusts and strike-slip faults) and separated by ophiolite-bearing sutures (Figs. 1 and 2). These are overlain sedimentary basins or intruded by arcs. These suture zones contain Mesozoic oceanic rocks and are sealed by middle Eocene and younger volcano-sedimentary covers (e.g., Babazadeh, 2013; Camp and Griffis, 1982).

2. Approach

The prime constraint on plate reconstructions is the restoration of the modern oceanic basins using marine magnetic anomalies and fracture zones/transform faults. Relative Arabia-Eurasia motion back to the times of Pangea are based on the Eurasia-North America-Africa-Arabia plate circuit (e.g., Seton et al., 2012; McQuarrie and van Hinsbergen, 2013 - we use the latest rendition summarized in Vaes et al., 2023). However, these reconstructions are only of limited use for the reconstruction of the Mesozoic-Paleogene deformation within Iran: The Eurasia-Arabia plate circuit only constrains the net area lost between Arabia and Eurasia but cannot account for area gained and lost by intra-Iranian extension and subsequent closure.

Our reconstruction thus relies on the restoration of the modern orogenic architecture of Iran and Afghanistan, starting from the present-day by removing deformation, from young to old. For the youngest time, mostly restricted to the Neogene, there are abundant strike-slip faults, as well as some extensional basins and core complexes with quantified or estimated displacements, which we review below and restore. Subsequently, the shortening record of fold-and thrust-belts that are known from the balanced cross sections (e.g., Woodward et al., 1989) are used to estimate minimum convergence.

For times prior to the Eocene, quantified fault displacements are restricted to a few major strike-slip faults, but deformation is mostly concentrated in the suture zones in which convergence, and the preceding divergence that made the ocean floor, cannot be directly constrained. There, we estimate the timing of extension and convergence through stratigraphic data and correlations. Our reconstruction does not use geochemical data as primary input to build the kinematic reconstruction, except for the geochemistry of ophiolites to infer whether they formed above subduction zone or at a regular mid-ocean ridge. Where independent evidence for subduction exists from structural records, we use adjacent calc-alkalic magmatism to infer e.g., subduction polarity or timing of activity, but no plate boundaries are inferred based on geochemistry of magmatic rocks alone. Combined, geological data from suture zones and adjacent continental margins constrain timing, and general direction and location of spreading and subduction, as well as subduction polarity, but cannot directly quantify the associated horizontal motions.

An independent source of quantitative kinematic information comes from paleomagnetic data. Paleolatitudinal motions within Iran and Afghanistan after the Triassic were typically within typical paleomagnetic error bars of ~±5-10°, but the information of vertical axis rotations is valuable. We compiled the available paleomagnetic constraints and adjust our reconstruction according to these within the constraints posed by geological data.

Our final model is a best-fit kinematic scenario that obeys the constraints as we understand them. This may be used as basis for future refinement (or correction), and we will assess realistic uncertainties in the discussion. For the reconstruction, we used the free GPlates software to create polygons which define blocks that behave as coherent units (http://www.gplates.org; Boyden et al., 2011; Müller et al., 2018). These polygons are almost always subject of internal deformation: where constrained, we used polylines that move relative to each other to be able to reshape the polygons (see e.g., van Hinsbergen and Schmid, 2012, for approach). The rotation and shape files are provided in the appendix.

Below, we review the first order orogenic features of the Iran-Afghan region between the Neo-Tethys and Paleo-Tethys sutures. We illustrated our individual tectonic units on geological maps of the present-day and trace them on our paleogeographic maps. The kinematic constraints we used in our restoration and the timing of the emplacement or juxtapositions of key order units are shown in charts and tables.

3. Main Tectonic Units and Structural Discontinuities

The geology of Iran and Afghanistan, exposed in an arid to semi-arid environment, forms an orogenic belt that bridges the Afro-Arabian and Eurasian continents. It consists of continental blocks and delimiting oceanic relics (Fig. 1). The remnants of a Paleozoic Ocean (also known as Paleo-Tethys) are exposed mostly in northern Iran, in the Alborz Mountains, Kopet Dagh, and western part of Yazd Block (Fig. 2). They are observed as strongly deformed and metamorphosed Paleozoic sedimentary rocks with tectonically interspersed serpentinized ultramafic rocks. To the east, the suture itself is less well mapped, and harder to follow in Afghanistan, but also there lenses of ultramafic rocks and abundant calc-alkaline magmatism to its north have been found to delineate the suture (Natal'in and Şengör, 2005).

The Neo-Tethyan suture separates the Cimmerian blocks in the south from the Arabian continental margin-derived Zagros fold-thrust belt to the south (Berberian and King, 1981; Şengör, 1990) (Fig. 2). The Arabian continental margin units were obducted by ophiolites prior to the collision with Eurasia (Agard et al., 2011). To the east of Strait of Hormuz, in the Makran region, continental collision between Arabia and the Cimmerian blocks has not happened yet, and instead an active subduction zone is still consuming oceanic lithosphere of the Arabian Plate (Peyret et al., 2009) (Fig. 2).

To the west, the Cimmerian blocks of Iran are separated by a N-S trending fault zone from the orogenic collage of Anatolia. This boundary has acted as transform fault, oblique subduction zone, and in its latest motions since the Eocene, as the sinistral Araks Fault (ArF in Fig. 2). The ocean closure history to the west of the Araks fault differs from the Iranian segment, owing to a much different paleogeographic and subduction zone configuration (see; van Hinsbergen et al., 2020, 2024). For instance, the Neo-Tethys Ocean in the Anatolian segment opened later (late Triassic to Jurassic) than in the Iranian segment (Permian-late Triassic) (Şengör, 1979; Barrier et al., 2018; van der Boon et al., 2018; van Hinsbergen et al. 2020). The eastern boundary of our study area is formed by the Chaman Fault that separates Indian plate-derived units (including the Kabul Block) that accreted to Eurasia in late Cenozoic times in the east from Cimmerian units of Afghanistan in the west.

In the geological literature about Iran, it is common that names of geographical features are also loosely used to identify tectonic units. The first detailed tectonic division of Iran, of Stöcklin (1968), used geography to define stable and tectonically mobile regions by

elaborating the simplified perception of “a median mass and two bordering mountain ranges”. He defined the Turan Plateau (i.e., the southern part of Eurasia), the Arabian Platform, and the Lut Block as stable areas, and Kopet Dagh, the Alborz Mountains, Central Iran, and the Sanandaj-Sirjan region as Alpine structural zones with Mesozoic and Cenozoic deformation. This first-order division is still used today but has been expanded. In this study, we adopted the acknowledged names for these regions and review and reconstruct their architecture and kinematic history. To avoid the confusion in terms, we will use the Central-East Iranian Microcontinent (CEIM) for the central and eastern part Central Iran as widely accepted, and we prefer to use the name ‘the Central Basin’ for the western part of Central Iran. Thus, Central Iran will represent the geographical name of the triangle area between the geographic belts of the Zagros-Makran mountain ranges in the south and the Alborz and Kopet Dagh ranges in the north (Fig. 2).

We describe the tectonic architecture of Iran in terms of tectonic units and structural discontinuities. Tectonic units are defined by spatially continuous, coherent lithostratigraphies that share a similar tectonic and paleogeographic origin and evolution. They form by deterministic tectonic processes that develop in the same way and produce similar products, and they can generate a lithosphere which supports their long-term existence. These lithostratigraphies are at first order subdivided into ocean-derived units (Ocean Plate Stratigraphy (OPS), which in its simplest form comprises oceanic magmatic crustal rocks (mostly pillow lavas), radiolarian cherts, and foreland basin clastics (Isozaki et al., 1990) and continent-derived units (Continental Plate Stratigraphy (CPS), which in its simplest form may comprise crystalline basement from a previous orogeny, syn-rift clastics, passive margin (hemi-) pelagic or platform sediments, and foreland basin clastics, plus post-orogenic cover (van Hinsbergen and Schouten 2021; Advokaat and van Hinsbergen 2024). Where these units were broken and displaced by faults, we call them “blocks”. These blocks are still part of a greater tectonic unit that overall dominates the tectonic evolution, but locally they have moved independently. When two tectonic units or blocks juxtapose with each other and the continuity of the original structural trend and lithostratigraphy is interfered or can no longer be followed, their intersection is classified as “structural discontinuity”, either individual faults or wide fault zones.

3.1 The South Caspian Basin

The South Caspian Basin, surrounded by Greater Caucasus, Talesh, Alborz, and Kopet Dagh mountains, is a rigid block likely underlain by oceanic crust and a ~20-25 km thick sedimentary cover (Berberian, 1983; Khain and Bogdanov, 2005; Kaz'min and Verzhbittskii, 2011). Although the age of the oldest deposits in the basin is not known, and often presumed late Jurassic, borehole data confirm presence of Cretaceous strata in the Apsheron-Kyupam and Gilyavar uplifts (Khain and Bogdanov, 2005). Towards the west, the South Caspian Sea likely continued into the hyper-extended or thinned continental Greater Caucasus Basin (Saintot et al., 2006; McCann et al., 2010) that was lost to Cenozoic subduction and whose sedimentary remains are exposed in the south Caucasus (Cowgill et al., 2016; Forte et al., 2022). The northern boundary of the South Caspian Basin is the Apsheron Sill, a fault zone where Caspian ocean floor is thought to be starting to subduct beneath the Central Caspian Sea that is underlain by Eurasian continental crust (Jackson et al., 2002) (Fig. 2). The estimated shortening orthogonal to the Apsheron Sill is calculated ~17-35 km and the dextral displacement parallel to Apsheron Sill is 22-45 km (Walker et al., 2021).

The origin of the South Caspian Basin was interpreted as a Mesozoic back-arc (Zonenshain and Le Pichon, 1986) or a remnant of Paleo-Tethys that was trapped in continental collision zones such as the eastern Mediterranean (Berberian, 1983) or a pull-apart basin between the Caucasus and Kopet Dagh strike slip zone (Şengör, 1990). The Kura Depression in the west is the onshore continuation of the South Caspian Basin (KD in Fig. 2).

3.2 The Kopet Dagh

The Kopet Dagh is a WNW-ESE trending mountain range in southern Turkmenistan and northeastern Iran from the Caspian Sea in the west to the Afghanistan border in the east (Fig. 2). The Kopet Dagh fold-and-thrust belt formed since the Neogene (Stöcklin, 1968; Tchalenko, 1975) by the inversion of the Kopet Dagh basin that formed in Jurassic time, likely linked to the opening of the adjacent South Caspian Basin, and remained a depocenter until into the Cenozoic (Robert et al., 2014) (Fig. 3). The thickness of the Mesozoic and Cenozoic strata of the basin exceeds 10 km (Lybéris et al., 1998).

The basement of the basin crops out in the Aghdarband erosional window and consists of north-verging nappes of Upper Devonian and Lower Carboniferous metasedimentary and -volcanic rocks that thrust over Triassic strata (Baud and Stampfli, 1989; Ruttner et al., 1991; Eftekharnezhad and Behroozi, 1991). Along the northeastern side of the Mashhad-Fariman-Torbat-e-Jam depression, and in the Darrehanjir Mountain (Fig. 4), OPS units comprising Lower Permian radiolarites intercalated with turbidites, mafic lavas, and gabbros are exposed (Alavi, 1992; Zanchi et al., 2009a). Gabbros in Mashhad were dated at Permian (282-288 Ma; Ghazi et al., 2001) and gabbros in the Darrehanjir Mountain are Devonian in age (380-382 Ma; Shafaii Moghadam et al. 2014). These mafic rocks and the accompanying sediments are attributed to the Paleo-Tethys, and the Mashhad-Fariman-Torbat-e-Jam lineament is thus considered as the suture between the Iranian Cimmerides and the Turan platform of Eurasia (Hsü, 1977; Şengör, 1979).

Highly deformed and faulted Lower-Middle Triassic volcaniclastic rocks, associated with shallow water carbonates around Aghdarband, and granitoids near Mashhad (Fig. 4) are interpreted as a volcanic arc on the Eurasian margin that formed during closure of the Paleo-Tethys (Ruttner et al., 1991; Balini et al., 2009, 2019; Mirnejad et al., 2013; Zanchi et al., 2016). Upper Triassic granitoids of Mashhad (ca. 217-200 Ma; Mirnejad et al., 2013) intruding into the accreted OPS units that demarcate the suture have been interpreted as sealing the suture (Alavi, 1992; Karimpour et al., 2010, 2011a; Zanchetta et al., 2013).

Table 1: Types and amount of tectonic displacement documented in the Kopet Dagh–Alborz Mountains from published studies.

Region	Fault Name	Type of displacement	Amount of displacement	Since	Method	Reference
Kopet Dagh	The Main Kopet Dagh Fault	Dextral	35 km	~5 Ma	resolving 75 km of N-S shortening across the western Kopet Dagh	1
		Shortening (N-S)	70 km	~5 Ma	resolving 75 km of N-S shortening across the western Kopet Dagh	1

		Shortening (N-S)	60 km	10 Ma		2
Kopet Dagh-Binalud	Farhadan Fault system	Sinistral	7.3 ± 0.8 km	Pliocene	restoration of total offset in upper Eocene volcanic units	3
Kopet Dagh-Binalud	the Sar'akhor Fault	Dextral	2.7 ± 0.3 km	Quaternary	displacement in Cretaceous limestone (Tirgan Formation) and Plio-Quaternary lavas	3
Alborz Mountains	Takab (Geynardjeh-Chahartagh) Fault	Dextral	15 km	late Quaternary	offset in volcanics	4
	east of Tehran	Shortening	~53 ± 2 km	late Miocene	restored cross sections	5
		Shortening	25–30 % / 30km displacement at the longitude of Tehran	late Sarmatian (~13 Ma)	balanced cross section	6
	Mosha Fault	Sinistral	~30 – 35 km	late Miocene	offset of geological and geomorphic markers	6
Southern Talesh		Shortening	25-30%		restored cross sections	7
Central Talesh		Shortening	13–16%		restored cross sections	7
Northern Talesh		Shortening	22%		restored cross sections	7
Talesh Mountains		Shortening	120km	Eocene	restoration of vertical axis rotations	8
Western Alborz Mountains	Lahijan Fault	Sinistral	12km		morphotectonic evidence of offsetting thrust sheets	9
1: Lyberis and Manby (1999); **2**: Hollingsworth et al. (2006); **3**: Shabanian et al. (2009); **4**: Allen et al. (2011); **5**: Guest et al. (2006a); **6**: Allen et al. (2003a); **7**: Madanipour et al. (2018); **8**: van der Boon et al. (2018); **9**: Safari et al. (2013)						

Following the late Triassic closure of the Paleo-Tethys, the Middle Jurassic Kashaf-Rud Formation unconformably covered the older deformed successions (Fürsich et al., 2009a; Taheri et al., 2009; Berberian, 2014; Balini et al., 2019) (Fig. 3). The formation starts with conglomerates and siliciclastics at the base indicating a deltaic depositional environment and passes into deep-marine siliciclastic strata and was deposited in a deepening environment owing to syn-depositional extension (Robert et al., 2014) increasing westwards towards the South Caspian Basin (Fürsich et al., 2009a). Facies and thickness of lithologies vary as a result of paleotopography changes shaped by major extensional faults (Lybéris and Manby, 1999). The Upper Jurassic to Lower Cretaceous interval is characterized by post-rift shallow marine limestones, and dolomites with intercalations of shales and evaporates. The shallow marine to fluviodeltaic conditions dominated the post-Cretaceous and several erosional levels with angular unconformity are recognized in the late Cretaceous and Paleogene as indicators of uplift (Moussavi-Harami and Brenner, 1992) (Fig. 3). The last phase of marine deposition is recorded by the Lower Eocene Khangiran Formation, which was deformed during the late Eocene, leading to regional uplift and denudation that persisted until the late Miocene (VahdatiRad et al., 2016; Aghababaei et al., 2022).

N-S shortening of the Kopet Dagh basin led to a north-vergent fold-thrust belt that forms a northward-convex orocline together with the Binalud Mountains in the west. In the northeast, the Neogene Kopet Dagh fold-thrust belt is bounded by the seismically active, 350 km-long, dextral, NW-SE striking Main Kopet Dagh Fault zone (Berberian, 1981; Hollingsworth et al., 2006) (Fig. 4). Estimates of overall northward motion amount ~60-75 km since ~5 Ma (Table 1), based on balanced cross sections (Lybéris and Manby, 1999) morphological observations of individual faults (Lybéris and Manby, 1999; Hollingsworth et al., 2006), reconstructions based on paleomagnetic rotation (Ruh et al., 2019), and on extrapolating modern GPS motions (Hollingsworth et al., 2010). Hollingsworth et al. (2006) estimates ~30 km of along strike extension during oroclinal bending and Lybéris and Manby (1999) estimated ~35 km of dextral displacement on the Main Kopet Dagh Fault.

3.3 The Alborz Mountains

The Alborz (or Elburz) Mountains and their western continuation in the Talesh (or Talysh, or Talish) Mountains form a gentle, southward convex arcuate mountain range in northwestern

Iran, south and southwest of the Caspian Sea and reaching from the Kopet Dagh in the east to the Lesser Caucasus in the west (Stöcklin, 1974a, b; Alavi, 1992; Ruh et al., 2019) (Fig. 2). The Talesh Mountains are bounded in the west by the Araks (or Arax) fault (Fig. 5).

The northern Alborz mountains and the southern margin of the South Caspian Sea belong to the Turan Platform, which covered by Mesozoic and younger sedimentary rocks (Popkov, 1992; Natal'in and Şengör, 2005). The Paleo-Tethys suture is marked by ultramafic rocks (serpentinite, dunite, peridotite, pyroxenite, gabbro) and Lower Permian radiolarites intercalated with turbidites in Gorgan and southwest of Rasht (Alavi, 1991; Sheikholeslami and Kouhpeyma, 2012; Rossetti et al., 2017), and Upper Permian metamorphic rocks (greenschists, amphibolites, and gneisses). The suture runs through the northern Alborz mountains (Stöcklin 1974a, b; Şengör, 1990; Alavi, 1991; Ruttner, 1993) (Fig. 5).

To the west in the Talesh Mountains, the Paleo-Tethys suture is marked by deformed OPS units, serpentinized peridotite, as well as and eclogite lenses emplaced onto sheared and deformed slates, phyllites, gneisses, amphibolites, and eclogites of the Shanderman metamorphic complex. This complex is considered as an allochthonous nappe of the subducted Turan Platform (Davies et al., 1972; Alavi, 1996; Zanchi et al., 2009a; Rossetti et al., 2017). The Shanderman eclogites have Carboniferous ages (315±9 Ma, $^{40}Ar/^{39}Ar$ ages of white micas; Zanchetta et al. 2009; 350 Ma, Sm-Nd isochron in garnet; Pastor-Galán et al., 2025) while middle to late Devonian (382±48 Ma and 375±12 Ma) metamorphism has been recorded by the gneisses and schistose phyllites of the Gasht metamorphic complex (Crawford, 1977; Alavi, 1996). Triassic (226 ± 24 and 229 ± 25 Ma) amphibolite facies metamorphism (Rezaei et al., 2021) suggests a ~160 Ma span of subduction-related burial and metamorphism. Towards the northwest, the Paleo-Tethys suture has been deformed by opening of the Greater Caucasus Basin and the Black Sea and is more challenging to follow (Şengör and Yılmaz, 1981; Şengör et al., 1984, 2019; van Hinsbergen et al., 2020 and references therein). Although the composition and evolution of the Gasht and Shanderman complexes differ from each other, the Pre-Jurassic metamorphism links them both to the same active margin along the Paleo-Tethys (Alavi, 1996).

To the south of the Paleo-Tethys suture in the Alborz Mountains, the northern margin of the Iranian Cimmerian continent exposes a 12 km thick stratigraphic succession, spanning from the Upper Precambrian to Quaternary with minor unconformities (Zanchi et al., 2009a).

Neoproterozoic crystalline rocks are represented by low-grade siliciclastic rocks of the Kahar Formation (Etemad-Saeed et al., 2015), the Lahijan granite in the north of the Central Alborz Mountains (Lam, 2002; 551±9 Ma; Hassanzadeh et al., 2008), and a granite from the Gasht Metamorphic Complex (551 ± 2.5 Ma U/Pb zircon age; Rezaei et al., 2021). These ages that are similar to Pan-African basement units of Arabia (Hassanzadeh et al., 2008). Widespread and voluminous late Ordovician-Silurian mafic magmatism in Soltan Maidan Complex has been interpreted as rift-related, and may have been associated with the opening of the Paleo-Tethys Ocean (Derakhshi and Ghasemi, 2015) (Fig. 3). The succeeding Upper Paleozoic shallow marine environment evolves into carbonate platforms in middle Triassic both in the Talesh Mountains and the Alborz Mountains (Zanchi et al., 2009a; Madanipour et al. 2018). The Upper Triassic-Lower Jurassic terrigenous Shemshak Formation unconformably overlies the basement units in the north of the Alborz mountain range, as well as the thrusted and metamorphosed units of the Iranian Cimmerian continental sequence, sealing the suture (Zanchetta et al., 2009; Fürsich et al. 2009b; Madanipour et al. 2017). The intrusion of Lower Jurassic pegmatitic granites (175±10 Ma: Crawford, 1977 in Berberian and King, 1981) into the Gasht Complex further confirms pre-middle Jurassic suturing. The middle Jurassic and early Cretaceous interval is dominated by shallow to deep-marine carbonate deposition during regional extension, followed by Upper Cretaceous carbonate deposition intercalated with basaltic and andesitic, arc-related volcanics (Madanipour et al., 2017) (Fig. 3). The Cretaceous limestones in the Alborz mountains are faulted and folded and resulted in NNE-SSW shortening and limited late Cretaceous to Paleocene basin closure in the area (Huber, 1977; Ehteshami-Moinabadi et al., 2012, 2016). In the Talesh Mountains, the structural trend changes from a WNW-ESE to NNW-SSE and is cut by right-lateral strike-slip faults. Paleocene to Eocene volcanic and sedimentary rocks are widely exposed in the Talesh Mountains, and ended in the late Eocene, around 38 Ma, after which clastic deposition remained (van der Boon et al., 2017). The ~8 km thick Eocene volcanic-sedimentary deposits and basalt eruptions are thought to have formed in an extensional environment during this period, in the upper plate of the Neo-Tethys subduction zone (Vincent et al., 2005). An angular unconformity between the Lower Cenozoic volcanics and clastic rocks of Upper Cenozoic sequences were interpreted as related to the inception of the shortening documented in the Caucasus fold-thrust belt (Madanipour et al., 2013). The eastern boundary of the Talesh fold-thrust belt is defined by the sinistral Lahijan fault in the south and by the West Caspian fault in the north

(Safari et al., 2013). Although the West Caspian fault is not visible at the surface, the eastern margin of the N-S trending Talysh–Vandam gravity high, the western extent of a series of mud volcanoes, and the thickness contrast within Cenozoic strata are used to locate the fault (Kadirov, 2000; Allen et al., 2003b; Vincent et al., 2005; Rezaeian et al., 2020).

The Alborz Mountain range is a relatively young topographic feature formed by N-S shortening (Guest et al., 2006a, b). Uplift and exhumation were underway by the late Oligocene and accelerated in the late Miocene to early Pliocene as revealed by apatite fission track data (Rezaeian et al., 2012; Madanipour et al., 2017). The Alborz Mountains displays a symmetrical structure with thrust faults dipping southward in the north and northward in the south (Stöcklin 1974a, b; Afaghi et al., 1977; Allen et al., 2003a; Djamour et al., 2010). The structural trend changes from WNW-ESE in the west to ENE-WSW in the east as associated with oblique-slip transpression, dextral in the west and sinistral in the east (Allen et al., 2003a; Guest et al., 2006a).

The amount of shortening was estimated from balanced cross sections that suggested 53 ± 2 km of shortening in the east of Tehran since late Miocene (Guest et al. 2006a), and ~30 km at the longitude of Tehran, alongside ~30–35 km of left lateral displacement (Allen et al., 2003a) (Table 1). Paleomagnetic data suggests CW rotation (17.7°±4°) for the western part and CCW rotation (37°±7°) for the eastern part of the Alborz Mountains, with an indication of almost straight E-W elongation for the Alborz Mountains prior to 7 Ma (Cifelli et al., 2015; Rashid, 2016) (Fig. 11) (Supplementary Information 2).

Towards the west, the Alborz fold-thrust belt continues into the Talesh Mountains that display a striking “2” shape where the N-S trending central part continues with curved ends (Madanipour et al., 2018). Paleomagnetic studies revealed the Talesh mountains underwent clockwise vertical-axis rotations (van der Boon et al., 2018) (Fig. 11). Restoration of these rotations and kinematic reconstruction of the Caucasus fold-thrust belt suggest that ∼120 km of convergence was accommodated in the Talesh Mountains since the Eocene, as the eastern part of an orocline that formed during the closure of the Greater Caucasus Basin (Cowgill et al., 2016; van der Boon et al., 2018).

3.4 The Central Basin

To the south of the Alborz Mountains is a large, triangle-shaped area in west-central Iran that has low topography and is occupied by intracontinental sedimentary basins of Qom, Great Kavir, and Garmsar (Fig. 6) (Jackson et al., 1990; Bin and Meiyin, 2010; Arian and Noroozpour, 2015). This region is loosely defined as the Central Basin (but also known as the Great Kavir Block)(Jackson et al. 1990; Morley et al. 2009). It is bounded in the west by the Araks Fault, in the south by the magmatic/metamorphic belt of the Sanandaj-Sirjan Zone, in the east by Central-East Iranian Microcontinent (CEIM) and surrounding structural discontinuities, and in the northeast by the chaotically deformed Sabzevar Suture (Fig. 4).

Mostly on the periphery of the basin, pre-Cenozoic rocks are exposed that are correlated to the units of the Kopet Dagh, Alborz, and Talesh mountains (Jackson et al., 1990). Precambrian orthogneisses and amphibolites (547 ± 7 Ma, U-Pb zircon age) occur north of the E–W trending Shotur Kuh-Biarjmand metamorphic complex (Rahmati-Ilkhchi, 2011, Malekpour-Alamdari, 2017) (Fig. 4), as well as in the Takab-Zanjan region in northwest Iran (576± 13 Ma) (Honarmand et al., 2020) (Fig. 5), i.e. with similar basement ages as those in the Iranian Cimmerides of the Alborz and Talesh mountains.

The Central Basin hides horst-and-graben structures beneath its desert cover. It contains Turonian and older graben fill that consists of marls, calcarenites, tuffs (140.7±4.8 Ma, U-Pb geochronology on zircon), shales, and radiolarites, indicating pre-late Cretaceous rifting (Jackson et al., 1990; Rahimpour-Bonab et al., 2007; Malekpour-Alamdari, 2017). Aptian-Albian limestones are exposed on major horsts that are located between the intracontinental basins. Thermal models obtained from $^{40}Ar/^{39}Ar$ thermochronology of Shotur Kuh-Biarjmand metamorphic complex suggest late Cretaceous-early Tertiary rapid cooling related to the exhumation of the core (Malekpour-Alamdari, 2017). The younging of cooling ages from south to north has been explained with a N dipping detachment fault system that may have accommodated as much as 135 km extension (Malekpour-Alamdari, 2017). Neogene red beds unconformably cover the basement rocks. The last deformation that affected the Central Basin was SW-NE shortening in the last 10 Ma with a cross-section reconstruction suggesting 38-40 km of shortening (Morley et al., 2009).

3.5 The Sanandaj-Sirjan Zone

The Sanandaj-Sirjan Zone is a NW-SE elongated magmatic and metamorphic belt that is bounded in the south by the Main Zagros thrust (i.e., the Neo-Tethys suture) (Fig.2). It runs from the western margin of the Iranian Cimmerian continent around the Iranian-Turkish border (Stöcklin, 1968) and is recognized as far east as the North Makran Zone, where Paleozoic metamorphic rocks and Mesozoic carbonates of the Bajgan-Durkan complex likely represent the easternmost parts of the Sanandaj-Sirjan Zone (McCall, 2002; Hunziker et al. 2015; Dorani et al. 2017) (Figs. 6 and 7).

The crystalline basement of the Sanandaj-Sirjan Zone is composed of granites, granodiorite, and mafic igneous rocks, in places overprinted by greenschist to amphibolite facies metamorphism. Many of these igneous complexes have the same Neoproterozoic-Cambrian ages as the crystalline rocks underlying the Central Basin and exposed in the Talesh, Alborz, and Kopet Dagh mountains that are characteristic of northern Gondwana-Land (Badr et al., 2018): for instance, the Sheikh Chupan granodiorite (551±25 Ma, Hassanzadeh et al., 2008) (Fig. 5) and the Galeh–Doz Granite, June Complex (568 ± 11 Ma, Nutman et al., 2014) (Fig. 6). Non-metamorphic epicontinental shelf successions of Paleozoic age are similar as in the other complexes south of the Paleo-Tethys suture (Fig. 3). These, and Paleozoic metamorphic rocks are separated by an angular unconformity from overlying Permian-Triassic sequences consisting of shallow-marine carbonate, shale and dolomite (Taraz et al., 1981; Sheikholeslami, 2015, 2016). These rocks are folded and unconformably covered by Jurassic successions indicating a phase of shortening in the late Triassic–early Jurassic (Shafiei Bafti and Mohajjel 2015; Sheikholeslami, 2015).

The Sanandaj-Sirjan Zone hosts abundant Jurassic and Cretaceous plutons (the Podataksasi zone in Şengör et al., 1991; Bea et al., 2011; Shafaii Moghadam et al., 2015; Shakerardakani et al. 2015; Chui et al., 2017; Jamei et al. 2021a, b). Most researchers interpreted the Jurassic magmatism in the Sanandaj-Sirjan Zone as a subduction-related arc (e.g., Berberian and Berberian, 1981; Şengör et al., 1988; Ahmadi Khalaji et al., 2007; Fazlnia et al., 2009, 2013; Shahbazi et al., 2010; Ahadnejad et al., 2011; Esna-Ashari et al., 2012; Deevsalar et al., 2017; Sepahi et al., 2018; Jamaliashtiani et al. 2024), although some favour a rift-related origin (Hunziker et al., 2015; Azizi et al., 2017, 2020; Azizi and Stern, 2019) or both with a transition from passive margin to an arc environment (Hassanzadeh and Wernicke, 2016).

The Jurassic-late Cretaceous magmatism was in places associated with regional amphibolite and greenschist-facies metamorphism (near Hamadan and Dorud-Azna (Berberian and Berberian, 1981; Rachidnejad-Omran et al. 2002; Agard et al., 2011; Davoudian et al., 2016; Shakerardakani et al., 2017; Monfaredi et al. 2020). Amphibolite-facies metabasalts from southwest of Sirjan revealed a cooling age of 170 ± 15 (Sadegh et al., 2021) and high-temperature eclogites from the north Shahrekord region yield 184 ± 1 Ma ($^{40}Ar/^{39}Ar$ mica ages, Davoudian et al., 2016).

During the late Cretaceous and Paleogene, arc magmatism shifted northwards and developed the ~150 km wide Urumieh-Dokhtar Magmatic Arc (UDMA) (Alavi, 1994; Kafshdouz, 1997; Verdel et al., 2011). This shift was associated with shortening and uplift of the Sanandaj-Sirjan Zone (Shafaii Moghadam et al., 2009). The UDMA forms a topographic high between the Sanandaj-Sirjan Zone and the Central Basin, or the Central-East Iranian Microcontinent. It exposes tholeiitic, adakitic, calc–alkaline, and K- rich alkaline extrusive and intrusive rocks (Honarmand et al., 2013) (Figs. 5 and 6). Calc-alkaline magmatism ceased in the early Miocene in the northwest and lasted until the late Miocene in the southwest (Chiu et al. 2013). To the northwest, UDMA also merges with volcanics of the Central Basin, Talesh, and Alborz mountains.

Since the late Cretaceous the Sanandaj-Sirjan Zone was deformed by transpressional deformation that produced a WNW trending thrust and fold system (Tillman et al., 1981; Shafiei Bafti and Mohajjel, 2015; Lei et al., 2025). In late Cenozoic time, the Sanandaj-Sirjan zone was cut by dextral strike-slip faults that accommodated block rotations of some ~10° (Song et al., 2023), interpreted as distributed transpression during oblique Arabia-Iran convergence (Allen et al., 2011).

3.6 The Nain-Baft Ophiolitic Belt

The eastern Sanandaj-Sirjan Zone is separated from the Central-East Iranian Microcontinent (see next section) by a belt of Upper Cretaceous ophiolitic rocks from Nain in the northwest to Baft in the southeast (Shafaii Moghadam et al., 2009) (Figs. 6 and 7). This Nain-Baft ophiolitic belt (also known as the Coloured Mélanges or the Inner Zagros Belt) is characterized by dismembered ophiolitic rock assemblages and mélanges including massifs such as the Ashin, Nain, Dehshir, Shahr-e Babak, Balvard, and Baft ophiolites (Shafaii Moghadam and Stern

2011) (Figs. 6, 7 and 8). The ophiolites contain mantle sequences of mainly depleted harzburgite with minor lherzolite, and crustal sequences with pegmatitic and isotropic gabbros whereas a well-developed layered cumulate sequence have not been reported (Ghazi and Hassanipak, 2000; Shafaii Moghadam et al., 2013; Shafaii Moghadam and Stern, 2015). Sheeted dike complexes are poorly developed and dacitic and plagiogranite dikes are mostly found in tectonic slices or as separated dike swarms in mantle rock (Rahmani et al., 2007; Shafaii Moghadam et al. 2009, 2010; Ghazi et al. 2012). Pillow or massive lava flows are present in each section and radiolarites are often found as thin chert layers (Rahmani et al., 2007; Shafaii Moghadam et al., 2009; Pirnia et al., 2020). The ophiolitic sections are covered by *Globotruncana*-bearing Cenomanian-Maastrichtian pelagic, shallow marine limestones and evaporites in some places extending into the Paleocene (Stöcklin 1977; Shafaii Moghadam et al., 2009; Shafaii Moghadam and Stern, 2015).

U/Pb ages of intrusions yield ages of 99-103 Ma for the formation of plagiogranites and tonalites of the Nain and Dehshir Ophiolites (Shafaii Moghadam et al., 2013) (Table 2). The geochemistry of the Nain-Baft ophiolitic belt implies an arc-tholeiitic to calc-alkaline affinity as an indicator of a setting above a subduction zone (Shafaii Moghadam et al., 2009; Rahmani et al. 2007).

The Nain-Baft ophiolite belt continues into the North Makran Zone (Hunziker et al., 2015), which to the north of the Bajgan-Durkan complex comprises a tectonic mélange with serpentinite, amphibolite, layered and isotropic gabbro, diabase dykes, andesite flows, pillow basalts, tuff, as well as and cherty and argillitic radiolarites. The mélange contains exotic blocks that are up to several kilometers wide, and some contain Albian limestones (McCall, 2002; Shahabpour, 2010). The north Makran mélanges also contain blueschists on the southern margin of the Jaz Murian depression which are underlain by the southern tip of Tabas and Lut blocks (McCall, 2002; Shahabpour, 2010). Delaloye and Desmons (1980) reported an 88±5 Ma $^{40}Ar/^{39}Ar$ age from a sodic amphibole from the Fannuj complex. Similar Rb–Sr mineral isochrons ages (81-84 Ma) reported from the blueschists of Iranshar (Bröcker et al., 2021) (Fig. 7).

Table 2: Radiometric data from the Nain-Baft Ophiolitic Belt

Region	Unit/Massif	Sample Number	Lithology	Dated mineral	Dating Method	Age	Error	Reference
Nain-Baft Ophiolitic belt	Nain ophiolite	BKB 05-7	Amphibolite	Amp	Ar-Ar	93.4	3.6	1
		N09-21	Tonalitic dike in amphibolite	Zr	U-Pb	101.2	0.2	2
		N09-28	Plagiogranite			102.7	0.2	
	Dehshir ophiolite	AZ 06-28	Gabbro	Amp	Ar-Ar	93.8	8.7	1
		D 06-6				79.4	7.6	
		D 06-2				67.0	6.4	
		DZ05-6	Tonalitic plugs	Zr	U-Pb	99.0	1.1	2
		AZ06-25	Plagiogranite dike			100.4	0.1	
		AZ06-24	Diorite			100.9	0.2	
	Baft ophiolite	BT 06-35	Gabbro	Amp	Ar-Ar	72.3	8.5	1
		BT 06-34				93.8	11.2	
	Ashin ophiolite	A142	Amphibolitic dike	Zr	U-Pb	97.3	1.8	3
		A144		Zr	U-Pb	97.4	1.3	
		A135	Amphibolite	Zr	U-Pb	104.4	1.2	
			Plagiogranite		K-Ar	98.0		4
Amp: Amphibole, WR: Whole Rock, Zr: Zircon.								
1: Shafaii Moghadamet al. (2009); **2**: Shafaii Moghadamet al. (2013); **3**: Shirdashtzadeh et al. (2022); **4**: Sharkovski et al. 1984 (as cited in Pirnia et al. 2020)								

3.7 The Central-East Iranian Microcontinent

The Central-East Iranian Microcontinent (CEIM) was first mentioned by Stöcklin (1968) and became defined by Takin (1972) as a fault bounded continental geological tectonic province, including the Lut Desert, surrounded by “coloured mélange-ophiolites”, between the two main trends of the Alborz and Zagros-Makran Mountain ranges. The eastern boundary of the CEIM is the Sistan suture that separates it from continental tectonic units of Afghanistan, the northern limit is Doruneh Fault and the Sabzevar ophiolites, and the northwestern limit is the Great Kavir Fault, which is mostly covered by the young sediments of the Central Basin. The southwestern and southern boundary is defined by the Nain-Baft suture.

The CEIM has a similar Pan-African crystalline basement as the Kopet Dagh, Alborz, Talesh, and Sanandaj-Sirjan regions, characterized by Ediacaran–Cambrian granitic to tonalitic gneisses intruded into the metamorphic host rocks and overlain by Paleozoic stable platform facies of siliciclastic and limestone sequences with only local deformation (Ramezani and Tucker, 2003; Hassanzadeh et al., 2008; Arefifard and Isaacson, 2011; Rossetti et al., 2015; Shafaii Moghadam et al., 2017; Ranjbar Moghadam et al., 2018; Shirdashtzadeh et al., 2018; Mollai et al., 2019; Sepidbar et al., 2020; Samadi et al., 2021; Nouri et al., 2022) (Fig. 7). This was followed by late Carboniferous and early Permian hiatus interpreted to result from erosion (Dastanpour, 1996). Sedimentation again starts with Lower Permian red coloured clastic sediments that develops into a deeper marine environment with dolomite and limestone sedimentation (Ruttner and Ruttner-Kolisko, 1972; Yarahmadzahi and Leven, 2021). The clastic sediments of the Norian-Bajocian Shemshak Formation that seals the Paleo-Tethys suture, is also widespread across the CEIM (Şengör, 1990; Wilmsen et al., 2003). The Jurassic and Cretaceous cover of the CEIM, however, shows a discontinuous pattern with regional thickness and facies variations related to the normal faulting between the blocks.

The CEIM is separated by major, active, N-S trending faults into four north-south orientated blocks: from west to east the Yazd, Posht-e Badam, Tabas, and Lut blocks, respectively (Takin, 1972; Berberian 1981; Berberian and King, 1981; Davoudzadeh et al., 1997). The geological and paleomagnetic records of the blocks within the CEIM suggests major (~90°) counter-clockwise rotation since the Jurassic (Stöcklin, 1968; Soffel and Förster, 1984; Fürsich et al., 2016) (Figure 10). We describe the history block-by-block below.

3.7.1 The Yazd Block

The Yazd Block is bounded by the (curvi)linear Doruneh fault to the north, the Chapedony fault to the east and southeast, the Shahr-e Babak and Dehshir faults to the southeast (Fig. 6). Lower Cambrian granitoids of the Pan-African basement (~518.2 ± 4.9 Ma and 535–530 Ma U-Pb zircon U/Pb ages (Shirdashtzadeh et al. 2018; Nouri et al. 2021)) are overlain by a discontinuous sedimentary sequence of shallow marine limestones and dolomites and clastics (Ghorbani, 2019). An upper Triassic marine turbiditic deposits and intercalating tuffs of Nakhlak group (in Anarak region, Fig. 6) form a deepening sequence that unconformably

overlies the Paleozoic sequence and is interpreted as a foreland basin adjacent to an active margin (Alavi et al. 1997) (Fig.3).

In the west and east of the Yazd Block, ophiolites and accretionary complexes are found of late Paleozoic to Triassic age, i.e. considerably older than those of the Nain-Baft belt. In the west, in the Anarak region, a dismembered ophiolite consisting of serpentinite, harzburgite, hornblende gabbros (~387 Ma, zircon dating), and diabases are reported. On the eastern part of the Yazd Block lies the Bayazeh ophiolite that also consists of serpentinized peridotites and metagabbros (Nosouhian et al., 2019). These ophiolites are overlain by sedimentary rocks that became metamorphosed and yielded 333-320 Ma $^{40}Ar/^{39}Ar$ cooling ages (Bagheri and Stampfli, 2008; Buchs et al., 2013). In addition, Bagheri and Stampfli (2008) identified a thrusted sequence of marble, phyllite, quartzite, and metavolcanics that they interpreted as remnants of an accretionary wedge. This 'Doshakh' sequence overthrusted in Triassic time Permian–Lower Triassic gneiss, amphibolite, micaschist, quartzite, and marbles (Chah Gorbeh unit). To the northeast of this complex, in the Jandaq area, arc to collisional type granites (215±15 Ma) intrude into these metamorphic rocks. This association of ophiolites and stacked oceanic and continental margin rocks of Triassic age are interpreted as remnants of the Paleo-Tethys suture, that was far displaced into central Iran (Davoudzadeh et al. 1969; Davoudzadeh and Schmidt 1982, 1984; Ruttner, 1984; Vaziri, 2001; Bagheri and Stampfli, 2008; Zanchi et al., 2009b).

The ophiolitic rocks thrusts over the Paleozoic cover units along south verging faults and folds and is unconformably overlain either by the Upper Triassic- Middle Jurassic Shemshak Formation or by younger, Upper Jurassic-Lower Cretaceous conglomerates and sandstones (Bagheri and Stampfli, 2008; Wilmsen et al., 2015). Jurassic rocks are largely absent (Wilmsen et al., 2013), suggesting that the Yazd Block had emerged and acted as a sediment source for the neighbouring Tabas Block from where Jurassic clastic sedimentation is known (Wilmsen et al., 2009). Present-day strike-slip faults delimiting the blocks are thought to reactivate normal faults of a Jurassic horst and graben system (Cifelli et al., 2013). Following late Jurassic syn-rift continental clastic sedimentation (the Chah Palang Formation), a marine transgression led to shallow-marine (Lower Cretaceous Noqreq Formation) and subsequent deep-marine limestone deposition (the Shah Kuh, Bazyaq, Debarsu and Haftoman formations) (Wilmsen et al., 2015) (Fig. 3). Upper Campanian–Maastrichtian shallow-water limestones and marls are

truncated along an angular unconformity at the base of the Paleocene Chupanan Formation showing late Cretaceous deformation (Wilmsen et al., 2015, Fig. 3), coincident with tectonic activity recorded by rocks in the adjacent Nain-Baft suture. Finally, the block was deformed since the middle Oligocene by shortening and strike-slip deformation that is widespread in Central Iran (Arfania and Hamedani, 2008).

3.7.2 The Posht-e Badam Block

The N-S trending Posht-e Badam Block is ~80 km wide and is separated by the Chapedony Fault from the Yazd Block in the west and by the Kalmard and Kuh Banan faults from the Tabas block in the east (Fig. 2). The Posht-e Badam block exposes Neoproterozoic and Lower Paleozoic basement units (the Boneh-Shurow, Sarkuh, Posht-e Badam and Chapedony complexes) consisting of migmatites, amphibolites, gneisses, schists, marbles, and quartzites intruded by Ediacaran-Cambrian alkaline and calcalkaline plutons (Zarigan Leucogranite, 525±7 Ma Pb-Pb age; Zeber-Kuh granite, 534±6 Ma U-Pb zircon ages) (Berberian and King, 1981; Ramezani and Tucker, 2003; Nadimi, 2007; Mollai et al., 2021) (Figs. 6 and 7).

The Posht-e Badam Block is also overlain by Paleozoic ophiolitic mélange, consisting of peridotite, metagabbro, serpentinite and listwaenite, and associated with amphibolites, west of Posht-e Badam city (the Posht-e Badam ophiolite, Khalili et al., 2016) (Fig. 6). In Esmailabad, Upper Triassic granites and granodiorites intrude into the metamorphosed mélange and its metamorphic cover (Esmailabad Granite, 218±3 Ma U-Pb zircon age, Ramezani and Tucker (2003), Fig. 6).

Triassic sedimentary rocks are only exposed on the periphery of the block. Most of the Triassic sediments were likely removed by erosion due to uplift and eastward tilting in the Jurassic (Haghipour, 1974). During the middle Jurassic, the Posht-e Badam Block experienced NE-SW (in modern orientation) extension and exhumation of the crystalline basement along NE-dipping detachment faults (Soleimani et al., 2021). Hornblende from amphibolites of the Esmailabad area yielded a 187.6 ± 1.8 Ma $^{40}Ar/^{39}Ar$ plateau age (Bagheri and Stampfli 2008), interpreted as cooling ages that recorded extensional exhumation.

The late Jurassic to early Cretaceous is associated with folding, low grade metamorphism, deformation and uplift. Lower Cretaceous formations rests on Jurassic and older rocks with an

angular unconformity (Haghipour, 1974) and sedimentation resumed with continental clastics followed by shallow marine limestones in a subsiding environment (Haghipour, 1974). This was followed by another phase of folding and uplift in the late Cretaceous until Oligocene which resulted in reactivation of the Jurassic normal faults, formation of new NW-SE striking thrusts, and low-grade metamorphism of tectonically buried rocks (Haghipour, 1974). Ramezani and Tucker (2003) reported a peak metamorphism in the middle Eocene in the Chapedony Complex, associated with late-to post metamorphic diorite and granite intrusions of similar age (Khoshoumi Granite and Daranjir Granodiorite, Daranjir Mountain, Fig. 6).

3.7.3 The Tabas Block

The Tabas block is separated from the Posht-e Badam Block to the west by the Kalmard and Kuh Banan faults and from the Lut block to the east by the dextral Nayband and Gowk strike-slip faults (Figs. 2 and 7). Pre-Mesozoic rocks crop out in the central and northern parts along the narrow Shotori and Kuh-e Bam mountain ranges, where the Precambrian Pan-African basement is represented by granite, gneiss, slate, phyllite, and limestone (Ruttner and Ruttner-Kolisko, 1972), and the Paleozoic units are comparable to the Yazd Block. The Mesozoic sequence starts with carbonates, sandstones, and evaporites (the Lower Triassic Sorkh Shale Formation, Ruttner and Ruttner-Kolisko, 1972; Lasemi et al., 2008) and unconformably overlying Middle Triassic platform carbonates (the Shotori Formation, Wilmsen et al., 2009), in turn unconformably covered by the terrestrial clastic rocks of the Upper Triassic Shemshak Formation (Wilmsen et al., 2003, 2009) (Fig. 3). Middle Jurassic regional subsidence led to transgression and deposition of carbonates under deepening marine conditions (the Magu Group in the northwest and the Bidou Group in the southern Tabas) (Wilmsen et al., 2009). Upper Jurassic limestones are unconformably overlain by Kimmeridgian-Tithonian red beds (the Garedu Formation) or gypsum (the Magu Formation) (Wilmsen et al., 2009; Ghorbani, 2019; Fig.3). The Tabas Block mostly remained emergent until the Barremian, after which Barremian-Cenomanian Orbitolina and rudist platform carbonates (Afaghi and Salek, 1977) were deposited. The block was folded toward the end of Cretaceous, and subsequently unconformably overlain by Paleocene siliciclastics (the Kerman Conglomerate) (Stöcklin, 1968). The volcanics of the Urumieh-Dokhtar Magmatic Belt cover the Tabas Block in the south and the sedimentary record is completed with Neogene to

Quaternary continental sediments that were deposited either in the Tabas Basin (north) or in the Abdoughi Basin (south) (Konon et al., 2016, Fig. 7).

3.7.4 The Lut Block

Finally, the Lut Block forms the easternmost part of the Central-East Iranian Microcontinent (CEIM), bounded by Tabas Block in the west along the Nayband fault and from the Sabzevar ophiolites by the sinistral Doruneh Fault in the north (Stöcklin, 1968, 1974a, Fig. 2). To the east, the Lut block borders the Sistan suture zone (Tirrul et al., 1983).

Pan-African basement is exposed in the middle and northern parts of the Lut Block (Fig. 7) (Mahmoudi et al., 2010). The Paleozoic cover consists of Devonian limestones and shales, and Upper Devonian-Permian sands, shales, marls, limestones, and dolomites (Ghorbani, 2019; Yarahmadzahi et al., 2012), scarcer, but overall similar to the other CEIM blocks (Fig. 3). Lower Triassic dolomites (the Shotori Formation) are unconformably overlain by the Upper Triassic-Middle Jurassic Shemshak Formation (Amirhassankhani et al., 2014). Subsequent Jurassic shale and sandstones are either covered by the Cretaceous Orbitolina limestone or by the Paleogene volcanics. At the end of the Cretaceous, the region became emergent, and terrestrial conditions remained until the Present (Stöcklin, 1968).

The eastern and southeastern margin of the Lut block was intruded in the middle Jurassic by plutons (the Shah-Kuh pluton, with 168 Ma K-Ar ages, (Esmaeily et al., 2004, as cited in Esmaeily et al., 2005), gneisses of the Deh-Salm metamorphic Complex with a 166-163 Ma U-Pb zircon age (Mahmoudi et al., 2010), and migmatitic gneisses from the Anjul complex (presumably Jurassic magmatic protolith with a Cretaceous metamorphic overprint, ~110 Ma U-Pb zircon age (Bröcker et al., 2013, Fig. 7). These rocks have calc-alkaline or high-K calc-alkaline compositions interpreted as subduction-related (Karimpour et al., 2011b; Mazhari and Safari, 2013). No late Jurassic-early Cretaceous magmatism is known from the Lut Block. Sparse late Cretaceous magmatism has been documented from the Bajestan granite-granodiorite (79-76 Ma; K-Ar) in the north, the Bazman granodiorite (83-72 Ma; U-Pb dating on zircon and titanite) in the south, and the Gazu granodiorite (75-60 Ma) in the west (Berberian et al., 1982; Karimpour et al., 2011b; Ghodsi et al., 2016; Mahdavi et al., 2016; Ahmadirouhani et al., 2017) (Fig. 7). In the Paleocene to the Oligocene, with an Eocene peak,

magmatism is widespread and characterized by intermediate to felsic volcanic and sub-volcanic rocks including granodiorites, diorites, andesites, monzonite and pyroclastics. It is followed by alkali olivine basalts with a primitive asthenospheric signature from the Miocene to the Quaternary (Pang et al., 2012; Saadat et al., 2010). Much of the Lut block is at present covered by sandy desert formations of Quaternary age (Figs. 1 and 7).

3.7.5 Fault Systems in and around the Central-East Iranian Microcontinent

The 900 km long, sinistral **Doruneh fault,** or Great Kavir fault that bounds the CEIM in the north and northwest (Fig. 2) extends from the Iranian border in the east to the southern edge of the Great Kavir desert in the west (Wellman, 1966; Fattahi et al., 2007; Farbod et al., 2011; Walpersdorf et al., 2014; Javadi et al., 2015). The names of the fault are used interchangeably, although the eastern, transpressional portion of the fault zone is called Doruneh, and the near-linear NE-SW trending, purely sinistral western portion is called Great Kavir Fault (Stöcklin, 1968; Fattahi et al., 2007; Farbod et al., 2011; Pezzo et al., 2012; Javadi et al., 2013; Walpersdorf et al., 2014; Bagheri et al., 2016). The transpressional nature of the Doruneh segment results from its more E-W trend, and is associated with reverse faulting (Farbod, 2012; Cifelli et al., 2013; Tadayon et al., 2019). Neogene to Quaternary deposits thrust onto Holocene deposits along NE-dipping reverse faults shows that reverse faulting continues today (Farbod, 2012). Structural analysis on the pre-Pliocene units and drainage systems indicates a former dextral displacement (Javadi et al., 2013, 2015; Tadayon et al., 2019).

The ~400 km long NW trending dextral **Dehshir Fault** delimits the CEIM in the southwest and cuts through the Nain-Baft ophiolitic belt and the UDMA. Based on map view offsets, we estimate a displacement of Eocene-Oligocene volcanics of the UDMA by ~50 km (Fig. 6).

Transpressional movement along the dextral **Nayband fault** was mainly accommodated in the middle part of the Tabas Block, by E-W oriented imbricated thrust faults that get younger towards the north (Fig. 7). The total strike-slip displacement is not well known, only a Quaternary offset of 3 km dextral offset along the Lower Pleistocene basalts (Walker et al., 2009). The Nayband fault connects to the dextral **Gowk Fault** in the south with a change in its strike from ~175˚to 155˚and a 12 km dextral displacement since the Pliocene (Walker and Jackson, 2002).

The East and West Neh faults (the Neh Fault Zone in Fig. 7) are two subparallel faults within the Sistan suture zone. The Neh fault system, which comprises a series of faults anastomosing between two main N-NE-trending trending strike-slip faults, have several tens of kilometres of cumulative dextral displacement (Table 3). Southward, the Neh Fault Zone connects to the Nosrat-Abad and Kahurak faults along the eastern Lut margin (Figure 7; Stöcklin, 1968; Walker and Jackson, 2004). The Neh fault system together with the Hari-Rud fault represent the easternmost part of the shearing system that accommodates the displacement between Afghan and Iranian units (Berberian, 1981; Walker and Jackson, 2004).

Table 3: Types and amount of tectonic displacement documented in and around the Central-East Iranian Microcontinent from published studies.

Region	Fault Name	Type of discplacement	Amount of displacement	Since	Method	Reference
West of the Yazd Block	Deh Shir Fault	Dextral	50 km		offset in Eocene-Oligocene volcanics	1
			65± 15 km	40-25 Ma	offset of the Nain-Baft suture	2
Yazd Block	Anar Fault	Dextral	20 km		offset in Lower Cretaceous shales	1
West of the Posht-e Badam Block	Chapedony fault	Extension	2 km vertical displacement	30 Ma	E-W to NE-SW exhumation of Chapedony complex	1, 3
West of the Tabas Block	Kuh Banan Fault	Dextral	5-7 km		length of pull-apart basins	4

West of the Lut Block	Nayband Fault	Dextral	3.2 km	2 Ma	offset in basalts	1
NW Tabas Block	Shotori Mountains	Shortening	25%	late Neogene-Quaternary		5
Southwest of the Lut Block	Gowk Fault	Dextral	12 km	5 Ma	geomorphologic indices	6
	Sabzevaran	Dextral	6 km			7, 8
The Lut Block	Shahdad thrust belt	Shortening	4-7km	late Pliocene-Quaternary	restored cross sections	9
N-NE of the CEIM	Doruneh Fault	Sinistral	1.33 km	late Quaternary	offset in alluvial fans	10
Lut-Afghanistan	Dasht-e-Lut	Dextral	75 Km	5 Ma		1
			105 km	7 Ma		1
Sistan Suture	Zahedan	Dextral	13km		offset in Cretaceous to Eocene mudstones and phyllites	1
	East Neh Fault	Dextral	50 km		offset in late Cretaceous peridotite and Tertiary turbidites and phyllites	1

	East Neh Fault	Dextral	65 km		total offset in the Neh complex	11
	West Neh Fault	Dextral	10 km		offset in Jurassic phyllites and Cretaceous ophiolitic material	1
Central Iran	Dehu, Anar, Deh Shir, Kashan, Ab-Shirin-Shurab, Kousht Nousrat, Qom, Bid Hand, Indes, Soltanieh and Takab faults	Dextral	250 km (total offset)		offset of geological and geomorphic markers	12
the Central Basin		Shortening	40-50 km	10 Ma	restoration of cross sections	13
1: Walker and Jackson (2004); **2**: Meyer et al. (2006); **3**: Kargaranbafghi et al. (2011); **4**: Walker and Allen (2012); **5**: Berberian (1981); **6**: Walker and Jackson (2002); **7**:Regard et al. (2005); **8**: Rashidi et al. (2020); **9**: Mohajjel (2009); **10**: Farbod et al. (2011); **11**: Tirrul et al. (1983); **12**: Allen et al. 2011; **13**: Morley et al. (2009)						

3.8. The Sabzevar Zone

To the south of the Kopet Dagh mountain range and north of the Central-East Iranian Microcontinent, between the Jovain fault in the north and the Doruneh fault in the south, is

a belt of dismembered ophiolitic and OPS rocks known as the Sabzevar Zone (Lensch and Davoudzadeh, 1982; Ohnenstetter, 1983; Baroz et al., 1984; Omrani et al., 2018) (Fig. 4). The Sabzevar Zone hosts complete ophiolitic sequences that appear as imbricated massifs (Ohnenstetter, 1983; Omrani et al., 2013; Bröcker et al., 2021). Lensch and Davoudzadeh (1982) subdivided the Sabzevar Zone in 3 groups: a) the Sabzevar ophiolite, with a well-developed Penrose-sequence (harzburgite, lherzolite, cumulate gabbro, diabase dikes, pillow lavas and well-bedded micritic limestones, see also Khalatbari Jafari et al. (2013)), b) ocean plate stratigraphy of Oryan-Bardaskan which contain thrusted sequences of massive lava, siliceous shale, radiolarite and pyroclastics, and c) the coloured mélange of Torbat-e-Heydarieh (dismembered harzburgite, gabbro and sheeted diabase mixed in a serpentinite matrix).

The Sabzevar ophiolite is divided into two based on their geochemical characteristics. A depleted mantle source indicating a supra-subduction zone (SSZ) setting, with U/Pb zircon ages of gabbros and plagiogranites clustering between 100 and 90 Ma (Khalatbari-Jafari et al., 2013; Shafaii Moghadam et al., 2014; Omrani et al., 2018; Kazemi et al., 2019) (Table 4) and a MORB-type precursor with a sheeted dyke complex of island arc tholeiitic affinity thought to represent formation in a back-arc basin (Stöcklin, 1974a; Shojaat et al., 2003; Rossetti et al., 2010; Nasrabady et al., 2011; Shafaii Moghadam et al., 2014; Rezaei et al., 2018). *Globotruncana*-bearing limestones were deposited between the pillow lavas of the SSZ series of Sabzevar indicating Upper Campanian to Lower Maastrichtian ages (Baroz et al., 1984; Shafaii Moghadam et al., 2014; Khalatbari-Jafari et al., 2016). K/Ar radiometric ages of pillow lavas and diabases in Sabzevar range from 81±4 Ma to 77±4 Ma (Lensch and Davoudzadeh, 1982).

Table 4: Radiometric data from the Sabzevar Zone

Region	Unit/Massif	Sample Number	Lithology	Dated mineral	Dating Method	Age	Error	Reference
The Sabzevar Zone	Sabzevar Ophiolite	IRN.78.154	Diorite in ophiolitic series	Amp	K/Ar	85.5	11	1
		IRN.78.172				84	22	

			Amphibolite			52.5	2.5	
			Nodular gneiss			50.5	1.6	
			Granoblastic lens			48	12.3	
		8059	Blueschist	WR	Rb-Sr	56.52	0.32	2
		8060				57.2	0.32	
		8063				55.12	0.33	
		SZ11-28	Tonalitic dike	Zr	U-Pb	99.9	0.12	3
		SZ10-72	Plagiogranite			98.4		
		SZ11-44				90.2	0.12	
	Torbat-e-Heydarieh Ophiolite	TH12-20				77.8	0.28	
		TH12-20	Plagiogranitic dike	Zr	U-Pb	99.32	0.72	4
		TH11-82B				91.9	0.33	
		TH11-12	Gabbroic dike			96.7	2.1	
	Oryan-Bardaskan Ophiolite	K-2	Diorite			75.78	0.29	5
Amp: Amphibole, WR: Whole Rock, Zr: Zircon.								
1: Baroz et al. (1984); **2**: Bröcker et al. (2020); **3**: Shafaii Moghadam et al. (2014); **4**: Shafaii Moghadam et al. (2019); **5**: Kazemi et al. (2019)								

Lower Cretaceous deep marine sediments in the OPS sequences indicate that oceanic crust of the inferred back-arc basin had formed by that time, and extension is thought to have started

in the late Jurassic (Lindenberg et al., 1984). Dismembered NW-SE striking tectonic slivers of mafic granulites crop out to the northwest of Sabzevar city and early Cretaceous (107 Ma c.) peak metamorphism may record subduction initiation (Rossetti et al., 2010). Lawsonite-bearing blueschists (Baroz, 1984; Bröcker et al., 2020, Table 4) along with amphibolite and greenschist were reported from the northern part of the accretionary complexes (Omrani et al., 2018) (Fig. 4). Bröcker et al. (2020) reported 57-55 Ma Rb-Sr ages (Table 4) from blueschists and interpreted ongoing burial or exhumation in the Sabzevar region around this time (Fig. 4).

South of the Sabzevar Zone, metamorphic core complexes with continental basement. The Taknar metamorphic core complex crop out (Malekpour-Alamdari, 2017). These include Precambrian metamorphic rocks are intruded by Neoproterozoic-Cambrian granites, diorites and gabbros (metarhyolite 550±6 Ma, U-Pb zircon dating) and overlying Paleozoic continental sediments (Shafaii Moghadam et al., 2017; Abasnia et al., 2019). The Fariman metamorphic complex crops out to the east of the Torbat-e-Heydarieh ophiolite and consists of amphibolite facies Precambrian rocks (Ranjbarmoghadam et al. 2019). These units likely represent the obducted margin of the back-arc basin, connected to equivalents in the Kopet Dagh mountains to the north. The Sabzevar ophiolite complex is unconformably covered by Lutetian nummulitic limestones and Eocene calc-alkaline basaltic, andesitic, and dacitic lavas and pyroclastics (Shafaii Moghadam et al., 2014). Towards the west, the Sabzevar Zone disappears beneath the young deposits of the Central Basin. In the east, it is truncated by the N-S trending Hari-Rud fault and beyond this fault the Band-e Turkestan mountain range (Paropamisus), the representative of the Eurasian continental margin (the Turan Platform) and units of Central Afghanistan (Ulmishek, 2004).

3.9 The Sistan Suture Zone

Between the Lut block of the CEIM in the west and the Farah Rud block and Sistan Basin of Afghanistan in the east, lies a N-S trending belt of ocean-derived, partly metamorphosed rocks overlain by ophiolites and a volcano-sedimentary cover, collectively known as the Sistan Suture zone (Tirrul et al., 1983; Berberian et al., 2000, Fig. 7). The highest structural units in the Sistan Suture zone, exposed in the east, are non-metamorphosed ophiolites with supra-subduction zone geochemical signatures (e.g., the Siahjangal, Nosrat-Abad, Tchehel-Kureh, and Nehbandan ophiolites (Fig. 7) (Delaloye and Desmons, 1980; Saccani et al., 2010;

Moslempour et al., 2012; Karimzadeh et al., 2020). The boundary of the ophiolites with the Helmand Block is covered by alluvium and cannot be directly observed, but is widely assumed to have been reactivated by the Neogene Hari Rud Fault, to the east of which no ophiolites and underlying OPS units are known and to the west of which no continental basement is exposed (Stöcklin, 1989; Shahraki et al., 2022). Direct age constraints on the SZZ ophiolites are sparse. Delaloye and Desmons (1980) reported a 92 ± 3 Ma K-Ar age from the Tchehel-Kureh ophiolite, the oldest overlying sediments are Turonian in age (Tirrul et al., 1983), and the intruding Mahi Rud complex that was recently interpreted based on geochemistry as an arc-related sequence (Keshtgar et al., 2019) that yielded a U/Pb zircon age of 103.9 ± 2.9 Ma (Bagheri and Gol, 2020). The ophiolites are thus thought to have formed during late Cretaceous spreading above a nascent subduction zone (Saccani et al., 2010), adjacent to the Helmand block along the (modern) eastern margin of the suture zone (Saccani et al., 2010; Zarrinkoub et al., 2012; Angiboust et al., 2013; Delavari et al., 2014).

Structurally below the ophiolites is a series of accreted OPS units, with westward younging ages of accretion as inferred from the youngest trench-fill clastic deposits. The oldest, eastern units (the Ratuk Complex) include HP-LT metamorphic blocks in a serpentinite-dominated matrix, whereas the western units (the Neh complex) are mostly unmetamorphosed and have a sediment-hosted matrix (Tirrul et al., 1983). The Ratuk Complex consists of metamorphosed elements of OPS sequences, including metabasalt, metachert, and quartzites and phyllites interpreted as trench fill, metamorphosed at blueschist, amphibolite, or eclogite facies (Fotoohi Rad et al., 2005, 2009; Kurzawa et al., 2017; Bonnet et al., 2018). The age of metamorphism is estimated from U/Pb dating of zircon in eclogite, and by Rb/Sr and $^{40}Ar/^{39}Ar$ ages of high-pressure rocks, and ranges from 86-75 Ma (Bröcker et al., 2013; Kurzawa et al., 2017; Bonnet et al., 2018). Protolith ages of the Ratuk complex are at least Cenomanian-Campanian in age based on biostratigraphy of radiolarian cherts (Babazadeh and De Wever, 2004a, b).

The mostly non-metamorphic Neh complex contains OPS sequences that include mafic and ultramafic rocks with MORB geochemical signatures (Delaloye and Desmons, 1980; Desmons and Beccaluva, 1983; Biabangard et al., 2020), of which the most prominent is the ‘Birjand Ophiolite’ (Zarrinkoub et al., 2010). From that ophiolite, U/Pb zircon ages in gabbros of 113-107 Ma were reported (Zarrinkoub et al., 2012). Radiolarian cherts in the Neh complex have

ages of Aptian-Albian (Ozsvárt et al., 2020) and hemipelagic series with turbidites with Upper Cretaceous to Lower Eocene ages are interpreted as trench-fill sediments (Tirrul et al., 1983). Rare low-grade metamorphic rocks in the Neh complex yielded K-Ar ages of 65-68 Ma (Delaloye and Desmons, 1980).

The suture zone complex is overlain by a sedimentary series of up to 8 kilometers thick, known as the Sefidabeh basin (Fig. 7) (Camp and Griffis, 1982; Tirrul et al., 1983). This is an Upper Cretaceous to Lower Eocene marine clastic sedimentary succession with the oldest rock units overlying the ophiolites and the younger units progressively covering the accretionary complexes to the west. It consists of intercalating shallow-marine limestones and arc volcanic rocks (Camp and Griffis, 1982; Tirrul et al., 1980). The clastic sediments contain erosion products of ophiolite and arc sequences and are overlain by Paleocene to Lower Eocene reefal limestones (Tirrul et al., 1980). The Sefidabeh basin is interpreted as a forearc basin that formed above an east-dipping (in modern coordinates) subduction zone from the late Cretaceous to the middle Eocene (Tirrul et al., 1983; Saccani et al., 2010; Zarrinkoub et al., 2012; Angiboust et al., 2013; Delavari et al., 2014).

The sequence was folded and subsequently unconformably covered by continental clastic rocks of Middle Eocene age, Upper Eocene nummulitic limestones, and Oligo-Miocene terrestrial continental clastics and basaltic volcanics that are also known from the neighboring Lut and Helmand Blocks (Fauvelet and Eftekhar-Nezhad, 1990; Eftekhar-Nezhad and Stöcklin, 1992; Pang et al., 2012, 2013). This unconformity is interpreted as the age of collision (Babazadeh, 2013) and it coincides with the age of the oldest rocks of the E-W trending Makran accretionary prism that seals the Sistan Suture Zone in the south (McCall and Kidd, 1982; Fruehn et al., 1997) (see section 4.12). The Upper Eocene and younger sequence are folded and may have accommodated an additional 30–50 km of shortening after the final closure (Jentzer et al., 2022).

Towards the north, the Sistan Suture zone and its widespread oceanic units abruptly end in the curvilinear Madar Kuh thrust that exposes Mesozoic shallow marine limestones and younger volcanic rocks in the hanging wall (Tirrul et al., 1983; Bagheri and Gol, 2020; Rojhani et al., 2026). Rojhani et al. (2026) recently showed that the curvilinear nature of the Madar Kuh thrust is the result of post-middle Eocene refolding of an originally ~E-W trending fault that accommodated thrust motion earlier in the Eocene. Because the Sistan Suture zone does

not continue to the north of this fault, and the fault strikes-perpendicular to the suture zone, they inferred that it likely reactivates a subduction transform edge propagator (STEP) fault (Govers and Wortel, 2005) that formed the northern termination of the Sistan subduction zone during its activity from the Cretaceous to early Eocene. The Madar Kuh fault is cut and dextrally offset by the Hari Rud fault, and Rojhani et al. (2026) interpreted that it may continue along faults parallel to the Waser suture zone of Afghanistan, such as the Helmand Fault (see next section).

3.10 Central Afghanistan

The geology of Central Afghanistan is not extensively described in the literature, and mostly relies on geological mapping from the before the 1970's. At first order, it may be subdivided into the southern margin of Eurasia in the north (the Turan Platform, and to the east units known as Band-e Turkestan, Hindu Kush, and North Pamir (Girardeau et al., 1989), bounded by the Paleo-Tethys suture in the south from 'Cimmerian continental fragments. The northernmost of these is the Band-e Bayan Block, overlain by the Farah Rud basin to the south. These two zones are separated by the Hari Rud Fault in the west from the Kopet Dagh, Sabzevar, and Lut Block of Iran. To the south, the Farah Rud basin is bounded by the Waser Suture from the Helmand Block to the southeast. The Helmand block is bounded by the Sistan Suture in the west, and the Chaman Fault in the east that separates it from Indian Plate-derived units. The South, the Helmand block is bounded by the Makran accretionary complex (Fig. 2). This overall collage is cut by major faults many of which are active today (Wellman, 1966; Shnizai, 2020).

3.10.1 The Farah Rud Zone and the Waser Suture

South of the Herat fault is a deformed belt dominated by Mesozoic sedimentary rocks known as the Farah Rud Zone (Girardeau et al., 1989). In map view, the zone shows a wedge shape with its narrow edge pointing to the east where it is truncated by the Kabul Block (Figs. 2 and 9). The Farah Rud Zone is separated from the Band-e Turkestan Zone in the north by the Paleo-Tethys Suture or by the still-active Herat Fault. In the west, it is bounded by the Sistan suture and the Hari Rud Fault separating it from the Cimmerian continental units of NE Iran. From

north to south the Farah Rud Zone consists of the Band-e Bayan Block in the north and the Farah Basin in the south. To the southeast, it is separated from the Helmand Block by the Waser Suture zone and the young Helmand Fault (Abdullah and Chmyriov 2008; Siehl 2017) (Figs 9 and 10).

The Band-e Bayan Block exposes pre-Triassic rocks and is separated, e.g. in the Ghorband region, from the Turan Platform by a belt of ophiolitic rocks and associated Paleozoic-Triassic sedimentary and volcanic rocks that are interpreted as the Paleo-Tethys suture (Tapponnier et al., 1981; Stöcklin, 1989) (Figs. 2 and 9). The Band-e Bayan Block consists of supposedly Middle Proterozoic, amphibolite to greenschist facies metasedimentary and -volcanic rocks (Abdullah and Chmyriov, 2008; Montenat, 2009). A Paleozoic sequence unconformably overlies the metamorphic basement, starting with Lower Paleozoic shallow-water sediments, Lower Devonian evaporites overlain by red continental sandstones, and Upper Devonian to Permian platform carbonates (Boulin, 1988). Lower Triassic bauxites and Upper Triassic plant-bearing continental deposits indicate on and off emergence of the region (Montenat, 2009). Jurassic marine sedimentation formed reefal limestones and marls, which are discontinuous and highly deformed. The sequence deepens towards the south. The Band-e Bayan sequence alternates with Triassic-Cretaceous volcanics with a tholeiitic and/or calc-alkaline affinity interpreted as a volcanic arc (Debon et al., 1987; Montenat, 2009). Cenozoic volcanism is seen on the both sides of the Herat fault and shows a calc-alkaline to sub-alkaline character (Debon et al., 1987).

The Band-e Bayan Block is bounded in the south by the north-dipping Garghanaw (Qarganaw) Fault (Treloar and Izatt, 1983; Siehl, 2017) that thrusts the block over Triassic and younger, marine clastic sedimentary rocks and volcanics of the Farah Basin. In the north, near Kerman, the basement of the Farah Basin is exposed, consisting of gneisses and schists of (presumed?) Precambrian age overlain by dolomites, sandstones, and volcanics of presumed, but undated, Vendian to Cambrian age (Schreiber et al., 1972; Abdullah and Chmyriov, 2008). In the northwest and southeast of Farah Rud Zone, Carboniferous-Lower Permian continental clastics with fusulinids have been reported (Fig. 9, Leven 1997; Abdullah and Chmyriov 2008). In the southeast, Upper Permian-Carnian reefal limestones and intermediate to mafic volcanics crop out (Fig. 9, Abdullah and Chmyriov, 2008). The Late Permian-Carnian interval represents a shallow marine environment with deposition of reefal limestones and

intermediate-to basic volcanics. These sequences are comparable to those of the Band-e Bayan Block (Montenat, 2009). During late Triassic to early Jurassic time, following the closure of the Paleo-Tethys suture, the Farah Basin subsided and an up to 2000 m thick marine clastic sequence was deposited (the Karajangal series) (Abdullah and Chmyriov, 2008; Montenat 2009) (Fig.3).

In latest Jurassic- early Cretaceous the Farah Basin became filled with a turbiditic series known as the 'Panjaw flysch' (Siehl, 2017). The Panjaw flysch contains plant, ammonite, and belemnite fragments that are also found on the Band-e Bayan Block (Montenat, 2009; Siehl, 2017). The Lower Cretaceous rocks are typical terrestrial clastic series ('molasse') that crops out discontinuously in the east but in the west become thousands of meters thick (Girardeau et al., 1989). The Panjaw Flysch is folded due to N-S shortening, and unconformably covered by Senonian Orbitolina and rudist-bearing neritic limestones (Girardeau et al., 1989), by a thick, Paleogene felsic to intermediate volcaniclastic sequence (Montenat, 2009) (Fig. 10). From late Cretaceous to Eocene-Oligocene, the emplacement of subalkaline and alkaline magmatic rocks as well as basalts occurred: sparse K-Ar ages range from 103-42 Ma and basaltic to andesitic rocks as young as Oligocene are reported (31.5 Ma, Debon et al., 1987). Deformed and steeply folded clastics of Oligocene age indicates that also in the Cenozoic, N-S significant shortening occurred, but the exact timing and magnitude are unknown (Treloar and Izatt, 1993).

The Farah Rud Zone has been interpreted either as a continental fragment between the Waser suture in the south and the Paleo-Tethys Suture in the north (Tapponnier et al., 1981) or as an oceanic basin between these two ophiolitic belts (Bassoulet et al., 1980). In the west, Hari-Rud fault forms a lithological divider and the Farah Basin units and the structures that deform it do not continue into Iran. In the east, the Kabul Block interferes and a direct connection to the units to the east is lost. Although the direct link is not visible, the Farah Rud Zone is usually correlated with the Rushan-Pshart Series in the Pamirs based on their similar lithology (Tapponnier, 1981; Burtman, 1994).

The Farah Basin is bounded in the south by a steeply dipping, narrow band of ophiolitic mélange is situated between the Band-e Bayan and Helmand blocks (Tapponnier et al., 1981) (Fig. 10). The mélange consists of a thick Upper Triassic to Upper Jurassic trench-fill clastic series (the Waras Flysch), which tectonically intercalates with lenses of ultramafic-mafic rock

and Permo-Triassic limestone blocks (Tapponnier, 1981; Girardeau et al., 1989, Treloar and Izatt, 1993; Wittekindt et al., 1997; Fig. 10). The ophiolitic section contains spilites, pillow lavas and tuffs, radiolarite, dismembered gabbro and serpentinized peridotite with unknown age (Stöcklin, 1989) that reflect OPS sequences.

Both the Waras Flysch and the ophiolitic mélange have undergone metamorphism from greenschist to garnet-amphibolite facies. The series is unconformably overlain by red detrital continental sediments and overlying Barremian-Aptian marine orbitolinids limestones. The timing of suturing is constrained as pre-Mid-Cretaceous based on these overlying sediments (Tapponnier, 1981; Şengör et al., 1991). The Senonian deposits that unconformably overlie the Farah Basin also unconformably cover the Waras Flysch (Girardeau et al., 1989). The Waser Suture is interpreted as the relict of a subduction zone that existed from the late Triassic closure of the Paleo-Tethys Suture until the early Cretaceous, with the Farah Basin as a forearc basin in front of an arc in the Band-e Bayan Block.

3.10.2 The Helmand Block

The Helmand Block is separated from the Farah Basin by the Waser Suture in the northwest, by the Chaman Fault from the Kabul Block and the Katawaz Basin in the east, and from the Lut Block by the Sistan Suture in the west. Geographically, the Helmand Block hosts the Central Mountains of Afghanistan (Figs. 2 and 9).

The basement of the Helmand Block consists of metavolcanics and metasediments of Middle and Upper Proterozoic age that were intruded by Cambro-Ordovician granitoids (Montenat et al., 1981). It is overlain by a thick and continuous sedimentary Paleozoic sequence (Boulin, 1988; Shroder et al., 2021) (Fig. 3). The sedimentation began with Vendian-Cambrian basal conglomerates, followed by siliciclastics, limestones and dolomites and the Ordovician-Devonian interval is characterized by limestones and siliciclastic rocks deposited under marine platform conditions. The Carboniferous and Lower Permian is a discontinuous series of sandstones, shales, and siltstones containing cold-water bivalves and brachiopods and glacial sediments (e.g., Abdullah and Chmyriov, 2008) suggesting proximity to Gondwana-Land that underwent glaciations at that time (Termier and Termier, 1974; Wolfart and Wittekindt, 1980). Upper Permian rocks unconformably rest on the Lower Permian and older formations with traces of erosion (Abdullah and Chmyriov, 2008) (Fig. 3).

From late Permian to late Triassic, marine platform conditions dominated as demonstrated by the accumulation of limestones, dolomites, and marls (Siehl, 2017). Abundance of typical tidal-flat environment stromatolite and algal mats in the west and presence of pelagic ammonites and radiolaria in the east indicate sedimentation on an easterly-dipping basin (in modern coordinates) (Siehl, 2017). Norian megalodon-bearing limestones were reported from the Central Mountains (Abdullah and Chmyriov, 2008), indicating regression. This Triassic regression led around the turn to the Jurassic to deposition of a terrigenous clastic sequence (Fig.3). During the early and middle Jurassic, the platform reinitiated on an easterly-dipping (modern coordinates) carbonate ramp that resulted in emergence and erosion of western regions while the eastern parts subsided. Cretaceous terrigenous deposits overlie the Jurassic strata, either disconformably or with angular unconformity (Montenat, 2009). A major phase of folding took place during the late Aptian, around 115 Ma, and resulted in emergence of the Helmand Block. This shortening correlates the transition from marine to terrestrial environments in the Farah Basin (Abdullah and Chmyriov, 2008).

In the late Jurassic and Cretaceous, the southeastern margin of the Helmand Block was intruded by granodiorites and overlain by calc-alkaline volcanics, in the Kandahar arc (Tapponnier et al., 1981). The arc contains calc-alkaline volcanic breccia and rhyolites, tuffs, dacites and intercalations of Kimmeridgian neritic limestones and it is intruded by granites, diorites and mafic dykes in the Tertiary (Kazmi and Qasim Jan, 1997; Siehl, 2017). Sparse K-Ar ages of the plutons range from 158 (?) to 140 Ma and from 110-79 Ma (Blaise et al. 1972; Debon et al., 1987; Siehl, 2017). Magmatism also occurred in the Cenozoic. Volcanogenic rocks of the Eocene-Oligocene Tangai Series (Abdullah and Chmyriov, 2008) were intruded by Oligocene granitoids (e.g., the Arghandab batholith) (Figs 9 and 10).

The southern half of the Helmand Block is covered by the sandy desert of the Sistan Basin (Fig. 9). This basin is a depression that formed in the Neogene by uplift of the eastern regions and was filled with fluvial and eolian continental clastic eroded from uplifted surrounding mountain ranges (Abdullah and Chmyriov, 2008).

In the south of the Sistan desert, the Chagai and Raskoh arcs are exposed. The Chagai arc lies along the Afghanistan-Pakistan border, and it is separated from the Raskoh arc by the sediment-filled Dalbandin through (Siddiqui, 2012). The magmatic complexes are bounded by the Chaman fault in the east and by the Sistan Basin desert in the west. The Chagai arc consists

of a ~2.5 km thick sequence of Upper Cretaceous basalt-andesite lavas intercalated with volcaniclastics, siltstone, and sandstones. (Siehl, 2017). Maastrichtian limestones seal a Cretaceous magmatic history, after which volcanism resumed in the Eocene with andesitic to dacitic lavas, continuing to the Pleistocene (Doebrich et al., 2007; Perelló et al., 2008). The total thickness of the Chagai arc exceeds 10 kilometres (Abdullah and Chmyriov, 2008). The Raskoh arc hosts an ophiolitic mélange that contains radiolarites and limestones of Lower to Upper Jurassic age (Siddiqui, 2012; Siehl, 2017). Available $^{40}Ar/^{39}Ar$ ages (Gnos et al., 2000) demonstrate that the metamorphic soles of the southeastern part of the ophiolitic massif formed at ca. 110 Ma. This complex is followed by Cretaceous volcanic group similar to the Chagai arc (Siddiqui, 2012). The Chagai arc is interpreted as a magmatic arc on the southern margin of the Helmand Block (Debon et al., 1987), and the Raskoh arc formed on an oceanic basement (Khan et al., 2010) that may have been part of the Helmand.

3.10.3 Fault Systems in and around Central Afghanistan

Afghanistan is cut by a series of major faults that fan from an E-W trend of the Herat Fault in the north to a NE-SW trend of the Chaman Fault in the southeast. These faults become buried below the desert of the Sistan Basin in the southwest (Figure 9).

The dextral Herat strike-slip fault runs from the north of the Kabul Block to the Iranian border, over a length of ~1200 km (Wellman, 1966, Fig. 9). The eastern part of the fault, beyond the Kabul Block is known as the Panjshir Fault. In the west, it becomes difficult to trace towards the Hari Rud Fault, but it may have connected to the Doruneh/Great Kavir Fault System, stepping right ~ 50 km along the Hari Rud fault (Fig. 2). Formation of transtensional basins along the fault with Oligo-Miocene fluvial-eolian sediments and accompanying alkaline volcanism show that it has been active since at least this time the Oligocene-Miocene interval (Tapponnier et al., 1981; Shroder et al., 2021) and the fault is still seismically active (Zhao et al., 2025). Because the fault runs more or less parallel to the Paleo-Tethys suture zone (Ahmadi and Rahmani, 2018), the displacement along the fault, or the onset of its activity, are unknown.

The Chaman fault is a well-defined, major sinistral fault that forms the western boundary of rock units accreted from the Indian plate (Wellman, 1966). To the southwest, the Chaman fault curves south-westward and connects to the subduction zone of the Makran accretionary complex. To the northeast, it and splits into two branches around the Kabul

Block. It merges with the Moqor Fault along the western side of the block and continues to the northeast where it meets the Herat Fault, ~70 km north of the Kabul (Whitney, 2006) (Fig. 9). The eastern side of the Kabul Block is delimited by the Gardez Fault that accommodated that the Kabul Block was wedged into the southern Eurasian units of the NE Afghanistan and Nuristan regions (Treloar and Izatt, 1983). The subparallel faults within Central Afghanistan include the Farah Rud fault between the Panjaw and Waras flysches that left-laterally displaced streams by about 80 kilometres (Auden, 1974) (Table 5). Due to the harsh morphological conditions and political conflict, the active fault maps of Afghanistan relied heavily on satellite imagery, and the other major faults, such as the Helmand Fault (Fig. 9) that are prominent in satellite imagery may have significant displacements, but little of that has been mapped in the field (Yeats, 2012).

Table 5: Types and amount of tectonic displacement documented in Farah Rud Zone and Helmand Block from published studies.

Region	Fault Name	Type of displacement	Amount of displacement	Since	Method	Reference
North of Band-e Bayan	Andarab Fault	Dextral	40 km	Pliocene-Quaternary	geomorphologic indices	1
North of Farah Rud	Herat Fault	Dextral	0.7-0.8 km		offset in drainage pattern	2
South of Farah Rud	Farah Fault	Dextral	80 km	Eocene	offset in dike swarms	2
Southeast of Helmand Block	Chaman Fault	Sinistral	~ 300 km	Eocene		2
			min. 155 km	Tertiary	offset of geological markers	3

			~60-80 km	2 Ma	offset in a 2 Ma old volcanic unit	4
			200-400km	late Oligocene or early Miocene		5
			460 ± 10 km	25-20 Ma	offset of geological markers	6
1: Abdullah and Chmyriov (2008); **2**: Auden (1974); **3**: Lawrence and Yeats (1979) [as cited in Ahmad et al. (2018)]; **4**: Beun et al. 1(979) [as cited in Ul-Hadi (2012)]; **5**: Lawrence et al. (1981); **6**: Lawrence et al. (1992) [as cited in Ul-Hadi (2012)]						

3.11 The Nuristan Block and the Pamir-Hindu Kush-Kohistan region

To the east, beyond the Kabul Block, is the Nuristan Block (also known as Nurestan, Nooristan or Nouristan) that is separated from the Helmand Block by the Kabul Block, bounded in the west by the northward continuation of the Chaman Fault, and to the east by the Altimur Fault (Fig. 9). Along these two faults, the Kabul Block, as part of the Indian plate, indented into the Asian collage during Cenozoic India-Asia collision (Treloar and Izatt, 1993). Consequently, prior to Kabul Block indentation the Nuristan Block was the northeastern continuation of the Helmand. This is exemplified by a similar overall stratigraphy, with Lower Proterozoic metamorphic rocks at the base (Abdullah and Chmyriov, 2008; Cocker, 2011; Siehl, 2017), overlain by Paleozoic-Triassic platform (Schreiber et al., 1972; Abdullah and Chmyriov, 2008). In the late Triassic (Noria-Rhaetian), the block uplifted and siltstone, sandstone, shale, and conglomerate rest conformably on the Upper Permian-Carnian units (Abdullah and Chmyriov, 2008), after which the block remained emergent from the Jurassic to the Paleogene (Schreiber et al., 1972). The Lower Cretaceous Nilaw igneous complex (gabbro, monzonite, diorite and granodiorite) and the Oligocene Laghman granitoid complex intrude into the Lower Proterozoic and Triassic units (Abdullah and Chmyriov, 2008).

In the tectonic unit subdivision that is widely used for the Pamir-Hindu Kush orocline, the Nuristan Block is part of the Southern Pamirs, which is correlated eastwards into Tibet as the Qiangtang Block (Robinson, 2015; Yin and Harrison, 2000) (Fig. 12). The Central Pamir is bounded to the north by the Rushan-Pshart Zone, a suture zone with trench-fill clastics that are Triassic in age in the east, towards Tibet (Wang et al., 2020), and these are consequently correlated to the Songpan Ganzi accretionary prism of Tibet that has the same age (Yin and Harrison, 2000). However, in west of the Pamir, the Rushan-Pshart Suture is thought to have closed in late Jurassic-early Cretaceous time (Yogibekov et al., 2023), i.e. with a similar age as the Waser Suture. To the north is the Central Pamir, which is bounded by a Triassic suture interpreted as the Paleo-Tethys Suture from the North Pamir (Robinson, 2015). The Central Pamir is thus interpreted as part of the Cimmerides, correlating westwards to the Farah Rud Zone and eastwards to the Western Kunlun. The North Pamir is interpreted as the southern margin of Eurasia, from which it was separated by lithosphere that subducted southwards to form the modern Pamir Slab (Negredo et al., 2007). The nature of this lithosphere is unknown, because it left barely an accreted record, but it may have been a back-arc basin of unknown age, similar in age and setting to the South Caspian Sea (Jackson et al., 2002; van Hinsbergen et al., 2011).

To the south, the Nuristan-South Pamir is bounded by the Karakoram, which is separated by a narrow rift that closed in Triassic time (Robinson, 2015) - the Karakoram and South Pamir may thus collectively be represented by the Qiangtang Block, which has also been subdivided into a northern and southern part (e.g., Kapp and DeCelles, 2019, and references therein). To the south, there may be a narrow sliver that may be the western termination of the Lhasa of southern Tibet (Schwab et al., 2004) and that has no equivalent in Afghanistan (Fig. 12).

Finally, the southernmost zone that separates the Pamirs from the Indian plate-derived Himalayas is the Kohistan-Ladakh arc (Fig. 12). The Kohistan arc is built on oceanic crust and developed as an intra-oceanic subduction zone from the early Cretaceous until the Eocene (Treloar et al., 1996; Jagoutz and Schmidt, 2012). The Ladakh arc to the east is built on either continental (Lakhan et al., 2020) or oceanic crust (Jagoutz et al., 2019) and is similar early Cretaceous to Eocene age. The arcs are separated by the Shyok Suture Zone from the Pamirs to the north. The age of this suture is debated: sediments on the Ladakh arc of late Cretaceous age (~85 Ma) show provenance of Tibetan terranes suggesting proximity of the arc to Tibet at

that time (Borneman et al., 2015), but arc magmatism north of the Shyok Suture, and accretion in the suture may have occurred until as young as 40 Ma (Bouilhol et al., 2013). Recent paleomagnetic data yielded a low paleolatitude of the Ladakh arc of ~8°N in the late Cretaceous that would suggest the presence of an ocean basin between the Kohistan-Ladakh arc at this time (Martin et al., 2020), whereas recent paleomagnetic data from a Cretaceous forearc that appears continuous from south of the Kohistan-Ladakh arc to southern Tibet shows paleolatitudes adjacent to southern Tibet around the same time (Xu et al., 2025). These observations may be reconciled by the opening of a back-arc basin between the Kohistan-Ladakh arc and the Pamirs in the late Cretaceous and its subsequent closure in the Paleogene (Rolland, 2002; Xu et al., 2025; Martin et al., 2025).

3.12 India and Arabia-derived thrust belts

The Cimmerian blocks of the Iran-Afghan system are surrounded in the east, south, and west by accretionary fold-thrust belts derived from underthrusted/subducted portions of the Arabian and Indian plate that we here that summarize in a 'southern domain' (Stöcklin, 1977). These consist of the Arabian continental margin-derived Zagros fold-thrust belt, off scraped clastic sedimentary deposits of the oceanic lithosphere of the Gulf of Oman (the Makran accretionary prism), and the western Indian margin-derived Katawaz Basin, Kabul Block, and Sulaiman Ranges (Figs. 1 and 2).

Indian plate-derived accreted rock units are located to the east of the Chaman Fault (Fig. 2). The west Indian margin is overthrust by the Sulaiman fold-thrust belt that consists of deformed Mesozoic and Cenozoic Indian passive margin sedimentary rocks (Mahmood et al., 1995). The southern and central Sulaiman Ranges were overthrust until early Eocene time by the uppermost Cretaceous Bela and Muslim Bagh supra-subduction zone ophiolites (Mahmood et al. 1995; Gnos et al., 1997; Ahmed and Ernst, 1999; Kassi et al., 2009). Obduction occurred in an intra-oceanic, subduction zone during oblique India-Arabia convergence between 65 and 50 Ma, i.e. long before the west Indian margin collided with the Helmand Block (Gnos et al., 1997; Gaina et al., 2015). This latter collision is reflected by the evolution of the Katawaz foreland basin that unconformably overlies the obducted and deformed west Indian margin to the west. Sedimentation in the Katawaz basin started in the

Paleogene and it underwent major shortening during the early Miocene collision of the west Indian margin with the Helmand Block (Treloar and Izatt, 1993).

To the north, the history is more complex. There, the Sulaiman ranges were overthrusted in late Cretaceous time by the Waziristan-Khost ophiolites during closure of an early Cretaceous ocean basin that separated the Kabul Block from India (Robinson et al., 2000; Gaina et al. 2015). The continental Kabul Block has a Proterozoic basement similar to that of the Indian Craton (Tapponnier et al., 1981; Faryad et al., 2016) and a discontinuous cover of Upper Permian to Cretaceous platform sediments (Badshah et al., 2000; Abdullah and Chmyriov, 2008; Montenat, 2009). It is thought to have formed a microcontinent that became separated from Arabia and India during a series of ridge jumps in the late Jurassic to early Cretaceous and recollided with India upon late Cretaceous closure of the Waziristan-Khost Ocean (Tapponnier et al., 1981; Faryad et al., 2016; Gaina et al., 2015). In latest Cretaceous to Eocene time, the Kabul Block was obducted by the Kabul-Altimur ophiolites. These contain Jurassic MORB crust thought to derive from the west Indian passive margin, but they were emplaced at the same time and in the same direction as the Bela and Muslim Bagh ophiolites (Beck et al., 1996; Badshah et al., 2000; Gaina et al., 2015). The detailed reconstruction of the deformation history of the Kabul Block, Waziristan-Khost suture, and Sulaiman Ranges relative to India are not of key importance for our study. We here adopt the reconstruction of Gaina et al. (2015) and van Hinsbergen et al. (2019) and refer to those papers for further details.

Towards the south, the Chaman fault connects to the E-W trending, ~1000 km long and 350 km wide Makran accretionary complex that is exposed north of the Gulf of Oman (Jacob and Quittmeyer, 1979; Burg, 2018) (Fig. 2). The Makran accretionary complex widens towards the east and grew by foreland propagated accretion, i.e. southward and oceanward, since the Oligocene (McCall and Kidd, 1982; McCormick, 1989).

The Makran accretionary complex includes Eocene-recent flysch turbidite sequences and constitutes the largest active sub-areal accretionary prism in the world (e.g., McCall and Kidd, 1982; Fruehn et al., 1997). At the onset of its formation by the end of the Eocene, the Makran was a simple north-dipping subduction zone that evolved on the southern margin of the Helmand and Lut Blocks, just after the closure of the Sistan Suture. Since then, it steadily accreted vast amounts of deep-marine clastic deposits that formed from the Indus fan (McCormick, 1989; Clift et al., 2001), which first dewatered through the Katawaz Basin, and

later through the Sulaiman foreland (Carter et al., 2010). The Makran accretionary prism also contains fragments of accreted oceanic crust. Gabbros from the Kahnuj complex (K–Ar ages on amphibole) and the Haji-Abad (Esfandagheh) massif (U–Pb zircon ages) yielded crystallization ages of 156–139 Ma and 173 Ma, respectively, likely representing Neotethyan ocean floor ages (Kananian et al., 2001; Shafaii Moghadam et al., 2016) (Table 6). At present, edifices of a volcanic arc are subducting below the Makran prism that are likely of late Cretaceous age, related to subduction below intra-oceanic subduction that emplaced ophiolites over the Arabian margin in Oman (Ninkabou et al., 2021).

The west-east striking Makran accretionary prism is separated by the dextral transpressional Minab-Zendan fault system (Regard et al., 2005) from the 2000 km long the Zagros fold-and thrust belt (ZFTB) (Fig. 7). The frontal thrust of the Zagros belt represents the active plate boundary with the underthrusting Arabian plate. The northern boundary of the Zagros fold-thrust belt, adjacent to the Sanandaj-Sirjan Zone, is a chaotic zone with ocean-derived mélanges, in places metamorphosed to high-pressure, low-temperature metamorphic conditions, and isolated remains of non-metamorphosed SSZ ophiolites (Stöcklin, 1968, 1974a; Agard et al., 2005, 2006, 2011). This chaotic zone is widely interpreted as the Neo-Tethys suture (e.g., Agard et al., 2011).

The ophiolites of the Zagros fold-thrust belt include, from NW to SE, the Piranshahr-Serow, Kermanshah-Kurdistan, Neyriz, and Haji-Abad ophiolites, also referred to as the Outer Zagros Ophiolites (as opposed to the Nain-Baft Ophiolitic belt also known as the Inner Zagros ophiolites north of the Sanandaj-Sirjan Zone). These form the highest structural units south of the Main Zagros Fault (Figs. 6 and 7). Most ophiolites have late Cretaceous (~92 Ma) crustal ages (Table 6), and where associated with a metamorphic sole, similar cooling ages of late Cretaceous are found (Lanphere and Adib 1983, as cited in Babaie et al., 2006, Babaie et al., 2005). These ophiolites are part of a belt of ophiolites with similar ages (~96 Ma in Oman (Rioux et al., 2013) and ~92 Ma in Anatolia, Cyprus, and Syria (e.g., Parlak et al., 2004) that were emplaced onto the Arabian continental margin in the late Cretaceous (Berberian and King, 1981; Agard et al., 2011; Homke et al., 2009). In the Zagros mountains, the Arabian margin including overlying ophiolites became in Miocene time thrusted and folded during Arabian underthrusting below Iran. To the east, in Oman, and west, in southeastern Turkey and Syria, however, the ophiolites obducted in late Cretaceous time over the Arabian margin

remain in their original obducted position by uppermost Cretaceous sedimentary rocks (e.g., Robertson, 1987; Searle and Cox, 1999; Al-Riyami et al., 2002; Kaymakçı et al., 2010). These Cretaceous ophiolites formed as part of an intra-oceanic subduction system that is not of direct relevance to the tectonic evolution of Iran and Afghanistan, and we refer for reconstructions and discussions to Maffione et al. (2017) and van Hinsbergen et al. (2020, 2021). An exception may be the Kermanshah Ophiolite, which also has younger ages up to ~35 Ma, and may represent a remnant of the forearc adjacent to the Sanandaj-Sirjan Zone above the Neo-Tethyan subduction zone (Ao et al., 2016).

Finally, the east Anatolian Plateau to the west of the Iranian Cimmerides is the locus of a late Cretaceous to Neogene accretionary fold-thrust belt that formed during subduction in the eastern Mediterranean system. We refer to the reader to detailed reconstructions and descriptions of orogenic architecture in van Hinsbergen et al. (2020, 2024) and Nikogosian et al. (2023).

Table 6: Radiometric data from the Zagros fold-thrust belt

Region	Unit/Massif	Lithology	Dated mineral	Dating Method	Age (Ma)	Reference	Interpretation
Khoy-Maku Ophiolite		metagabbro	Amp	K-Ar	197-181	1	metamorphism
		metagabbro			160-155		ductile deformations in shear fault zones
		amphibolite			121-102		
		Plagioclase vein in gabbro	Plg		101		crystallization
		isotropic gabbro			72		
		porphyritic diabasic dike			65		
		gabbros and amphibolites	Hbl	Ar-Ar	111-108	2	crystallization

Piranshahr-Serow Ophiolite	Hasanbag igneous complex	Diorite dike, kaersutite	Hbl	Ar-Ar	106-92	3	crystallization
Kermanshah Ophiolite	Sahneh	leucodiorite	WR	K-Ar	86	4	crystallization
		diabase	Amp	K-Ar	81		
	Harsin	gabbro	Zr	U-Pb	79.3	5	crystallization
	Sahneh	foliated gabbro			37.06		
		plagiogranite			35.7		
	Kamyaran	gabbro			39-36		
		plagiogranite			38		
Neyriz Ophiolite	Tang-e Hana	plagiogranite	Hbl	Ar-Ar	93-92	6	crystallization
		pargasite schist	Amp	Ar-Ar	94.9	7	shearing and amphibolitization along the sole detachment
		diabase tholeiitic sheeted dikes	Hbl	Ar-Ar	85.9		crystallization
	Qori metamorphic complex	trondhjemite	Zr	SHRIMP	147.4	8	arc related regional metamorphic event
	Chah Gaz	plagiogranite, isotropic gabbro	Zr	U-Pb	101-93	9	crystallization
Esfandagheh Ophiolite	Sikhoran ultramafic/	diabase	WR	K-Ar	159-134	10	crystallization
		amphibolite	Amp	K-Ar	164		

	mafic complex	pegmatoid			222.6			
		pargasitic hornblende-bearing pegmatoid gabbros			253			
					255.6			
	Haji-Abad	plagiogranite	Zr	U-Pb	186	11	crystallization	
		gabbro			174.9			
	Soghan Complex	isotropic gabbro	Amp	K-Ar	182	12	crystallization	
					186			
		diabasic dykes			76			
	Esfandagheh	amphibole schist	Mus		98	4	crystallization	
Kahnuj Ophiolite	Dare Anar complex	gabbro	Amp	K-Ar	156-139	13	crystallization	
		potassic granites		K-Ar	93-89			
	Band-e Zeyarat/ Dar Anar			Ar-Ar	143-140	14	crystallization	
Amp: Amphibole, Hbl: Hornblende, Mus: Muscovite, Plg: Plagiogranite, WR: Whole Rock, Zr: Zircon.								
1: Khalatbari-Jafari et al. (2003); **2**: Ghazi et al. (2003); **3**: Ali et al. (2012); **4**: Delaloye and Desmons (1980); **5**: Ao et al. (2016); **6**: Babaie et al. (2006); **7**: Lanphere and Adib (1983), as cited in Babaie et al. (2006); **8**: Fazlnia et al. (2009); **9**: Monsef et al. (2018); **10**: Ghasemi et al. (2002); **11**: Shafaii Moghadam et al. (2017); **12**: Ahmadipour et al. (2003); **13**: Kananian et al. (2001); **14:** Ghazi et al. (2004)								

4. Reconstruction

Embedded in the Arabia–Nubia–North America–Eurasia plate circuit and the constraints on deformation in the Iran and Afghanistan regions as summarized in the previous section. In our reconstruction, we also use the paleomagnetic database from the tectonic blocks of the

Iranian-Afghan region (Table S1 and Fig. 11) to complement and guide our reconstruction, although we do not use paleomagnetism as key ingredient for the reconstructions. The exception is the ~90° counterclockwise rotation of the Central-East Iranian Microcontinent in the Cretaceous, which we have aligned with the paleomagnetic findings. We developed a geometrically and kinematically consistent restoration using GPlates plate reconstruction software (Müller et al., 2018). All reconstruction files are provided in the Supplementary Information 2. We present our reconstruction of the Central Tethysides in 6 time-slices on the scale of the orogen in a Eurasia-fixed reference frame from the present back to the Early Jurassic, and then zoom out for a reconstruction back to the Permian in a paleomagnetic reference frame to display a larger and less detailed paleogeographic and plate tectonic scale, displaying its context within the Tethyan and Mongol-Okhotsk oceans and surrounding continents. These time slices are chosen to illustrate times of important changes in the tectonic evolution of the region.

4.1 Late Oligocene (25Ma)

The latest Oligocene time slice (Fig. 13) has been restored for N-S shortening that dominated the Central Tethysides since after that time. Northward subduction continues in eastern Turkey and in the Makran, whilst the Zagros and Katawaz Basin-Sulaiman Ranges are in the early stages of collision with the Central Tethysides. The Zagros fold-thrust belt is restored according to the estimates of McQuarrie and van Hinsbergen (2013) and covers the Arabian passive margin, still overlain by Cretaceous obducted ophiolites.

The 25 Ma tectonic map shows the situation of the **Alborz Mountains** corrected for post-7 Ma southward convex oroclinal bending associated with evolution of the Kopet Dagh (Cifelli et al., 2015; Rashid, 2016) (Fig. 11), and ~50 km of shortening is reconstructed that occurred since 12 Ma (Guest et al., 2006a; Cifelli et al., 2015). In addition, much of the Talesh-Caucasus orocline is restored (van der Boon et al., 2018). The **Kopet Dagh** is restored for N-S shortening and northward convex oroclinal bending that reactivated Mesozoic extensional faults (Hollingsworth et al., 2006; Mattei et al., 2019; Ruh et al., 2019). This restores the Kopet Dagh Basin into its pre-shortened configuration as the continuation of the Caspian Sea basin, but with eastward decreasing, continental extension. This reconstruction moved the Paleo-Tethys suture 65-75 km south relative to stable Eurasia and makes the Alborz Mountains contiguous

with the Kopet Dagh and Talesh zones (Fig. 13) as previously suggested based on paleomagnetic data (Mattei et al., 2017).

To the south, the restoration of the Kopet Dagh shortening restores the Central-East Iranian Micro Continent and parts of the Sistan Suture (CEIM) southwards along the Hari Rud and Neh Fault systems. This strike-slip motion transfers the shortening in Kopet Dagh to the Makran region, and in northern Afghanistan no Neogene N-S shortening is reconstructed. Restoration of sinistral strike-slip displacements along e.g., the Main Kopet Dagh Fault and Doruneh Fault (Table 1) restored the CEIM and Afghan segment eastward. Within the CEIM, we restored the positions of the Yazd, Posht-e Badam, Tabas, and Lut blocks using the displacements along the dextral faults within CEIM (Anar, Kuh Banan, Nayband, Gowk, Sabzevaran faults) (Figs 6 and 7, Table 3). To avoid spatial gaps, we modified the shape of the blocks, representing the widespread but unquantified thrusting and normal faulting that affected these blocks in the Neogene (Berberian, 1976; Arfania and Hamedani, 2008).

The northern side of **the Central Basin** follows the trend of the Alborz Mountain ranges, and with the unbending of the Alborz ranges, it becomes more linear in the reconstruction (Fig. 13). The N-S width in the late Oligocene reconstruction is wider than today due to restoration of ~40 km of post-10 Ma shortening (Morley et al., 2009). We restore shortening in Central Iran parallel to the Arabia-Eurasia convergence direction, which given the NW-SE strike of Iran includes an overall dextral component of shear. One fault where we restored Miocene strike-slip deformation is the dextral Deh Shir Fault that displaces Eocene-Oligocene volcanics in the Urumiyeh-Dokhtar Zone ~50 km, displacing **the Sanandaj-Sirjan Zone** relative to the Central Basin (Table 3). Restoration of lateral motion along the Sabzevaran Fault (Fig. 7) firmly connects the Durkan Complex to the Sanandaj-Sirjan Zone. We did not reconstruct the displacement of all other individual faults but included a ~250 km overall strike-slip component distributed over the Central Basin, Sanandaj-Sirjan, and Zagros zones, consistent with estimates of cumulative Neogene shear based on fault analysis and block rotations of Allen et al. (2011).

The 25 Ma reconstruction restored ~70 km of right-lateral motion between Eurasia and **Central Afghanistan**, e.g. along the Herat Fault (Table 5). This motion is accommodated to the east by restoring the Kabul Block with the Indian Plate following Gaina et al. (2015) and van Hinsbergen et al. (2019). This allows for the eastward reconstruction of Afghanistan relative

to the Pamir units and restores a contiguous lateral connection between the Nuristan/southern Pamir unit and the Helmand Block.

4.2 Middle Eocene (40Ma)

Between 25 and 40 Ma, ~400-600 km of Arabia-Eurasia convergence occurred at the position of the NW and SE Iranian Tethysides, respectively. Because all major shortening in the Zagros and the Iranian upper plate post-date 25 Ma, and subduction around the CEIM predates 40 Ma, this convergence must have been accommodated by wholesale subduction of Arabian plate lithosphere. We consequently infer that this consumed oceanic Neo-Tethyan lithosphere and our reconstruction at 40 Ma displays a northward Neo-Tethys subduction along the Sanandaj-Sirjan and southern Helmand margin. The Outer Zagros ophiolites (perhaps excluding the Kermanshah Ophiolite) were at this time located on the African/Arabian plate margin, and the ophiolites on the Sulaiman ranges and Kabul block were located on the Indian plate margin (Fig. 14).

The Kopet Dagh Basin is restored to its full original width, restoring the minor shortening and rotation that occurred between late Eocene and late Oligocene time (VahdatiRad et al., 2016; Aghababaei et al., 2022). The Alborz Mountains are restored as an almost E–W linear belt, as also the Oligocene part of the Caucasus oroclinal bending is now restored. The South Caspian Basin is reconstructed to its maximum original extent, connected to the Greater Caucasus Basin in the west and the Kopet Dagh Basin in the east (Kaz`min and Verzhitskii, 2011). At 40 Ma, the Doruneh-Great Kavir Fault was active (Omrani et al., 2018), rotating the Central-East Iranian Microcontinent westwards, which we infer was accommodated by shortening within the continent and perhaps by thrusting of the Nain Baft suture zone rocks over the Sanandaj-Sirjan Zone (Fig. 14). Part of this motion was partitioned north of the Sabzevar ophiolites at the Jovain Fault.

Restoration of dextral slip along the Hari-Rud Fault links the Herat Fault with the Doruneh-Great Kavir Fault, allowing these structures to function as a continuous, throughgoing fault system that accommodates the westward translation of the **Central-East Iranian Microcontinent** and the Farah-Rud Block. As an estimate to reconstruct how the total amount of lateral motion of >500 km along the Doruneh-Great Kavir Fault that displaced the Paleo-

Tethys into central Iran was partitioned over time, and the position of the CEIM and Farah Rud Block may thus have been already farther west or still farther east.

Our reconstruction at 40 Ma reconstructs the ~110-150 km of ~E-W post-collisional shortening estimated by Jentzer et al. (2022) for the **Sistan** region reflected by the deformation of the Eocene deposits that unconformably overly the suture and the Sefidabeh Basin (Babazadeh, 2013). The Makran accretionary complex only started to form around 40 Ma and consequently does not exist yet. In the **Sanandaj-Sirjan Zone**, we restored ~30-40 NE-SW shortening. In addition, we reconstructed Oligocene core complex exhumation in Central Basin, compatible with the clockwise rotation of the Urumiyeh-Dokhtar Magmatic Belt that developed on the Sanandaj-Sirjan Zone (Malekpour-Alamdari, 2017; Song et al., 2023).

4.3 Earliest Paleocene (65Ma)

At 65 Ma, the Iranian Neo-Tethys was 900-1200 km wide and was subducting below the Central Tethysides, both along the Sanandaj-Sirjan Zone creating the Urumieh-Dokhtar Arc and along the southern Helmand Block creating the Raskoh-Chagai Hills arc (Fig. 15). The northern Central Tethysides were formed by the Greater Caucasus-South Caspian-Kopet Dagh Basin that was in its post-rift stage a its maximum areal extent.

By 65 Ma, the oceanic basin of the **Nain-Baft** zone was likely in its final stages of closure (Stöcklin, 1977; Shafaii Moghadam et al., 2009; Shafaii Moghadam and Stern, 2015), whereas the blueschists of the Govain Mountain (10 km southeast of Soltanabad, Fig. 4) record late Paleocene to early Eocene high-pressure metamorphism in the Sabzevar zone indicating the subduction in the **Sabzevar Ocean** continued into the early Cenozoic (Fig. 15, Bröcker et al., 2020).

At 65 Ma, the **Central-East Iranian Microcontinent** underwent its counter-clockwise rotation accommodated by westward translation along the curved Doruneh-Great Kavir Fault. To account for this rotation within the spatial constraints given by the Sanandaj-Sirjan and Sabzevar regions, we reconstruct book-shelf-style transform motion between the blocks that together make up the CEIM. We also restore a speculative 20% of shortening between these blocks to account for documented folding (Stöcklin, 1968; Haghipour, 1974; Wilmsen et al., 2015). Field geological evidence shows that the Sanandaj-Sirjan Zone was undergoing

transpression around this time. Around this time, much of the forearc southwest of the Sanandaj-Sirjan Zone, possibly represented by the Kermanshah Ophiolite (Ao et al., 2016), in which case it consisted of oceanic crust, may have been lost due to tectonic processes, explaining the northward shift in the magmatic arc from the Sanandaj-Sirjan Zone to the UMDA. Lei et al. (2025) speculated that this missing forearc may be represented by ophiolites that are exposed below the thick volcanic cover of the east Anatolian Plateau. Our reconstruction does not explicitly reconstruct these motions and infers that this forearc may have been lost to subduction erosion instead. We here follow the subduction and accretion history in eastern Anatolia is from van Hinsbergen et al. (2020), but we note that detailed mapping around the Kagizman-Khoy suture zone in eastern Anatolia may require to update our view in the future.

The westward displacement of Paleo-Tethys remnants into Central Iran along the Doruneh-Great-Kavir Fault, albeit long recognized (Bagheri and Stampfli, 2008) has not previously been kinematically reconstructed and requires a much greater internal mobility within the Iranian and Afghan blocks that inferred in earlier reconstructions (e.g., Stampfli and Borel, 2002; Golonka, 2004; Stern et al., 2021). The major westward motion of the CEIM-Farah Rud Block, over 100s of km, closing a **Sabzevar-Nain Baft** oceanic basin by eastward subduction below the western CEIM, in the east requires extrusion from the Pamir Hindu-Kush region. Moreover, also the **Sistan Ocean,** as a separate oceanic basin between the Lut and Helmand Blocks, was in the process of subducting at 65 Ma, requiring that the Helmand Block extruded faster than the CEIM/Farah Rud Block (see also Bagheri and Gol, 2020). Bagheri and Gol inferred that this extrusion of Helmand was accommodated by formation of a bi-vergent, northward convex orocline in the Sistan Suture. Based on the west-southwest younging of accretionary complex and southeasterly vergence of the folds and thrusts, and arc magmas intruded into the Nehbandan ophiolite at 58.6 ± 2.1 Ma (Delavari et al., 2014), we prefer a scenario of a single, eastward subduction polarity (e.g., Angiboust et al. 2013). In our model, the northern tip of the **Sistan Ocean** connects to the **Waser Suture** through a sinistral fault system (Rojhani et al., 2026), which may have been the Helmand Fault, which accommodated the faster westward extrusion of the Helmand Block than the Farah Rud Block.

Restoring the extrusion of the Helmand and Farah Rud blocks places these blocks between the terranes that now constitute the Pamir orogen. The Helmand Block connects eastwards

with the Nuristan Block and South Pamir, which are the continuation of the Qiangtang Block of Tibet. Taking the reconstruction of shortening in Tibet into account using the reconstruction of (van Hinsbergen et al., 2011), we reconstruct the Helmand Block as the northwestern part of the Qiangtang/South Pamir, the Farah Rud as part of the Central Pamirs, and the Waser Suture as part of the (western) Rushan-Pshart Zone (Fig. 15).

4.4 Late Cretaceous (90Ma)

At 90 Ma, the restored width of the Neo-Tethys exceeds 2000 km, and the Neo-Tethys Ocean subducted below the Cimmerian units. At this time, a second, intra-oceanic subduction zone existed within the Neo-Tethys ocean (e.g., Agard et al., 2011; our reconstruction follows van Hinsbergen et al., 2021) that placed the ophiolites of the Zagros (e.g., Neyriz) over the Arabian margin by the end of the Cretaceous.

With subduction of the Cretaceous Nain-Baft-Sabzevar and Sistan ocean basins, and hence the extrusion of the Helmand and CEIM-Farah Rud blocks, having started around 100 Ma, this time slice restores these ocean basins close to their maximum width. To this end, we have restored the Paleo-Tethys suture remains of Central Iran (Anarak and Bayazeh complexes (Bagheri and Stampfli, 2008)) to a position equivalent to modern NW Afghanistan, such that the Nain-Baft Ocean is located between the Kopet Dagh and Sanandaj-Sirjan Zone. We restore an eastward widening basin, oceanic in the east and extended continental in the west below the Central Basin. This basin is separated from the Caspian-Kopet Dagh Basin to the north by the Alborz-Kopet Dagh block, but the two basins may have opened simultaneously (Golonka, 2004; Jentzer et al., 2022). The Caspian basin pinched out eastwards, whereas the Sabzevar-Nain-Baft basin pinched out westwards. We thus infer that they partitioned late Jurassic-early Cretaceous back-arc extension, with the Kopet Dagh-Alborz ranges acting as mega-relay ramp.

The Sistan and Sabzevar oceanic basins are reconstructed as two separate ocean basins. We reconstruct the counter-clockwise rotation of the Lut, Tabas, Posht-e Badam, and Yazd blocks (Fig. 11), combined with lateral motions between them, positioning them along the southern Eurasian margin of what is now northern Afghanistan. This differs from most previous reconstructions that connected the Sistan and Sabzevar oceans (Şengör, 1991; Rosetti et al., 2010; Bröcker et al., 2021).

At 90 Ma, subduction of the Sistan Ocean was also already ongoing SSZ ophiolitic crust had already formed in the forearc of the western Helmand Block (Delaloye and Desmons, 1980; Bröcker et al., 2013; Bonnet et al., 2018; Bagheri and Gol, 2020). Therefore, we reconstruct the Sistan Ocean at almost its widest form by the Turonian reaching some 500 km in the south. Reconstructing the rotation of the CEIM leads to a triangular shape of the Sistan Ocean, pinching out northwards (see also Stern et al., 2021), at the connection to the Waser Suture. The Sistan subduction zone connects to the transform that accommodated the westward extrusion of the Helmand Block. The Farah Rud Block and Waser Suture are reconstructed to a position fully within the Pamir orogenic collage. The reconstruction of the extrusion of the Helmand Block brings the Chagai-Raskoh arc in the upper plate of the Shyok subduction zone, north of the Kohistan-Ladakh arc.

4.5 Early Cretaceous (140Ma); Late Triassic (220 Ma); Permian (300 Ma)

At 140 Ma, A north-dipping subduction zone existed along the Cimmerian margin, consuming Neo-Tethyan ocean floor. Within the Neo-Tethys, mid-ocean ridge spreading was likely still active in the Neo-Tethys Ocean as suggested by the ages of the Kahnuj and Haji-Abad oceanic crustal rocks accreted in the Makran accretionary prism (Kananian et al., 2001; Shafaii Moghadam et al., 2016). In the upper plate of the Neo-Tethyan subduction zone, and behind the Sanandaj-Sirjan arc, the Central Tethysides of Iran we reconstructed back-arc extension that opened the South Caspian-Kopet Dagh basin to the north, and the Central Basin-Sabzevar-Nain Baft Basin to the south. Figure 17 illustrates the distribution of this extension, with the oceanic Caspian Sea Basin forming north of the continental rift of the Central Basin, and the oceanic Sabzevar-Nain Baft basin forming south of the continental rift of the Kopet Dagh Basin. This reconstruction placed the Sanandaj–Sirjan Zone against the Kopet Dagh zone before extension.

The 140 Ma slice shows the fully restored position of the Central-East Iranian Microcontinent, with the full paleomagnetic rotation accounted for (Davoudzadeh and Schmidt 1984; Soffel et al., 1996). The Permian–Triassic metamorphic units and Paleo-Tethys suture zone units of Central Iran are restored as part of the Paleo-Tethys suture zone in modern northern Afghanistan.

The Afghan sector, restored within the Pamir orogen, faces the complication that by the early Cretaceous, the Waser Ocean was likely in the final processes of closure (Girardeau et al., 1989; Treloar et al., 1993; Montenat, 2009). This means that a subduction plate boundary was present in this area, between the northwestern Qiangtang Terrane and the Central Kunlun/Farah Rud Zone, whose development must somehow have been linked to the evolution of the Sistan Ocean, which was likely opening at this time given the OPS ages in the Sistan Suture Zone (e.g., Babazadeh and De Wever 2004a, b).

We illustrate the possible context of the Waser suture in a zoom-out of our reconstruction and combined it with reconstructions of the Tibetan segment (Figure 18a, b). The Waser Suture requires that a subduction existed between the northwestern Qiangtang Block (i.e., the Helmand Block) and Eurasia until the early Cretaceous. Our reconstruction tentatively connects this subduction zone to a hypothetical plate boundary to the northeast recently postulated by Wang et al. (2025), the rationale for which we will return to in the Discussion section.

Finally, Figure 18c-f illustrates the pre-late Jurassic history of the Central Tethysides, with a late Triassic collision of the Iranian, north Afghan, and Central Pamir blocks with Eurasia, closing the Paleo-Tethys. We made no attempt to reconstruct the Paleo-Tethys ocean in detail in this paper, but we illustrate our version of the tectonic reconstruction in Figure 18. This follows the widely-held views (e.g., Şengör et al., 1991; Stampfli and Borel, 2002), with a coherent Cimmerian terrane, separated with transform systems from the eastern Mediterranean and Tibetan Tethyan systems. These transforms date back at least to the early Permian, by which time the Central Tethyan Cimmerides are restored at the Arabian margin.

5. Discussion

Reconstructing continental regions remains one of the most complex tasks in tectonics because the geological record is almost always incomplete, extensively reworked, and commonly overprinted by multiple phases of deformation. This challenge is especially pronounced in the Tethyan domain, where the Cimmerian Continent underwent successive episodes of rifting, subduction, collision, lateral extrusion, and strike-slip partitioning. From

west to east, the Tethyan system exhibits pronounced strain partitioning, dividing the region into Mediterranean, Iranian–Afghan, and Indian segments.

The tectonic reconstruction presented here offers new insights into the evolution of the Iranian–Afghan segment of the Cimmerian Continent and challenges several long-standing assumptions about deformation patterns in the Central Tethyan domain. In this section, we place these findings in a broader geodynamic context, examine the evidence supporting our proposed configuration, and address the limitations inherent to reconstructing a region where the geological record is incomplete, variably overprinted, and in the case of many areas in Iran and especially Afghanistan, far from completely mapped and studied in the field. These general shortcomings notwithstanding, we believe that our reconstructions identify three elements whose implications may be worth discussing: the drivers of major lateral extrusion from western Tibet/Pamir in the light of ongoing discussions on the tectonic history of the Kohistan-Ladakh arc, and future directions on reconstructing the triple junction region between the Tethyan and Mongol-Okhotsk-related subduction zones.

5.1 Drivers of lateral extrusion from western Tibet/Pamir

Extrusion of the Helmand Block from western Tibet has previously been suggested based on the fault patterns of Afghanistan (Tapponnier et al., 1981), and the realization that the closure of the Sistan Ocean requires a major component of E-W convergence in the upper plate of an overall northward subducting ocean (Bagheri and Gol, 2020; Şengör et al., 2023). Such extrusion systems are well known from subduction-related orogenic belts (e.g., Whitney et al., 2025). Famous examples are found to the west of the Central Tethysides in Anatolia, which has been extruded westwards towards the Aegean subduction zone over ~85 km since ~11 Ma (Şengör et al., 2005; Whitney et al., 2023), and to the east where Indochina was extruded from eastern Tibet some 600-700 km between ~50 and 8 Ma (Tapponnier et al., 1982; Leloup et al., 1995; Schoenbohm et al., 2006; Li et al., 2017). Those extruding systems are driven by upper plate shortening during the underthrusting of one continent below another and are accommodated on the extruding side by subduction zones. In the case of Iran and Afghanistan, extrusion is accommodated by two subduction zones: Sabzevar-Nain-Baft and Sistan. We estimate that the amount of extrusion is likely even larger than in eastern Tibet, exceeding

1000 km, between ~100 and 45 Ma. This must have been driven, at least initially, by shortening in western Tibet.

Shortening in Tibet in the Cretaceous is well-documented (Murphy et al., 1997; Kapp et al., 2007; van Hinsbergen et al., 2011) and is thought to represent Andean-style orogenesis in the upper plate of an oceanic subduction zone (Kapp and DeCelles, 2019). This makes extrusion in the west towards 'free' oceanic boundaries formed by the previously opened oceanic Sabzevar-Nain-Baft and Sistan Oceans in principle feasible. However, a history of continued upper plate shortening throughout the extrusion history may be challenged by recent interpretations of the tectonic history of the Kohistan-Ladakh arc (Figure 12, 15, 16).

Our reconstructions display the Kohistan-Ladakh arc as a westward oceanic continuation of an arc built on southern Tibet (the Gangdese Arc). This is a simplest-case scenario used in van Hinsbergen et al. (2019), but recent data may challenge this view. As mentioned previously, recent paleomagnetic (Martin et al., 2020; Xu et al., 2025), structural geological (Martin et al., 2025), and sediment provenance data (Borneman et al., 2015) were used to propose that the Kohistan-Ladakh arc was located adjacent to the Tibetan/Pamir upper plate around 85 Ma, but then rifted off opening a back-arc basin that subsequently closed between ~70 and 40 Ma (Xu et al., 2025). If correct, extrusion of the Iran-Afghan units between 85 and 70 Ma cannot have been driven by N-S shortening in the Pamir region. Detailed field observations in the Afghan, Pakistan, and Indian parts of this system are needed to reconstruct this history with confidence, but at this point we speculate that extension was triggered by upper plate shortening between 100 and 90 Ma, and initiated subduction in the Sistan and Sabzevar-Nain-Baft back-arc basins of Iran. By 90-85 Ma, these new subduction zones were rolling back, as shown by the development of supra-subduction zone spreading centers generating the SSZ ophiolites in these systems. We propose that the extrusion in the 85-70 Ma interval was driven by this roll-back rather than upper plate shortening in the Pamir. Following the onset of closure of the back-arc basin behind the Kohistan arc at the Shyok subduction zone, upper plate shortening could have contributed to extrusion again.

5.2 The Helmand Block and Waser and Sistan sutures: the missing triple junction between the Tethyan and Mongol-Okhotsk ocean basin systems?

Our reconstruction identified that the early Cretaceous Waser suture must have separated the northwestern Qiangtang Block from Eurasia (Fig. 18a, b). By very nature, suture zone represents former plate boundaries, which must surround plates and end in triple junctions. Thus, the Waser suture must have connected to other plate boundaries that were active until the early Cretaceous. We postulate that this suture may form a missing link in the understanding of the final amalgamation of the Asian continent.

The suture zone that is well-known from Tibet to the north of the Qiangtang Block is the Songpan Ganzi accretionary complex (Yin and Harrison, 2000). However, this cannot be the lateral equivalent of the Waser Suture, because it is a Triassic suture that separates the Qiangtang Block from the eastern Kunlun/Qaidam terrane that has been connected to the North China Block since the Paleozoic. However, paleomagnetic data have long demonstrated that the China Blocks moved 1000s of km northward towards Siberia until the early Cretaceous (Kravchinsky et al., 2002; Cogné et al., 2005; van der Voo et al., 2015; Wu et al., 2017). From this it follows that a plate boundary must have existed until the early Cretaceous somewhere between the China-Tibetan blocks in the east and the western part of the Tarim Basin that collided with Eurasia in the Tien Shan in the Permian (Wang, 2025).

The location of this plate boundary is unknown, and it is surprisingly difficult to find any geological record of it. There is a clear geological record of early Cretaceous closure of the Mongol-Okhotsk Ocean, with a suture in Mongolia and far-east Russia (Kravchinsky et al., 2002; Zhu et al., 2023), but how that plate boundary connected to the Tethyan systems is unknown. Wang et al. (2025) speculated that it may be buried below the Tarim Basin, or below NW Tibet. We postulate that the Waser Suture form the southwestern end of this last intra-Asian suture. It is located along the northwestern Helmand margin of the Qiangtang Block, but it cannot connect eastwards to the Songpan Ganzi accretionary complex that is the Paleo-Tethys suture of Tibet (Fig. 18), which is Triassic. It thus stands to reason to connect it north-eastwards to the enigmatic pre-early Cretaceous China-Eurasia plate boundary postulated by Wang et al. (2025).

This solution also offers a mechanism to open the triangular Sistan Ocean. If that ocean opened simultaneously with the final closure of the Waser suture, the connection between

these two was the rotation pole between the plate carrying the China terranes and the Eurasian plate. To the southwest of that pole, the Sistan ocean opened, and to the northeast, the Waser suture closed. This is equivalent to the modern situation in the southeastern the Philippine Sea Plate that has a rotation pole with the Pacific Plate around Palau: to the north is the Marianas-Izu Bonin subduction zone, to the south the Ayu spreading ridge (van de Lagemaat et al., 2024). We postulate that the Sistan Ocean may have formed part of the original Suture zone, and that the Jurassic arc plutons in the Lut Block (Esmaeily et al., 2004; Mahmoudi et al., 2010) were part of an active margin arc connected to the Sanandaj-Sirjan arc until Qiangtang/Helmand collision. A subsequent northward shift of the rotation pole would then have opened the Sistan Ocean (see e.g., van Hinsbergen et al., 2025, for an equivalent history in the Pyrenees).

The Waser Suture may thus have played a pivotal role in the final amalgamation of Asia and provide a lead to trace the last intra-Asian suture towards the known Mongol-Okhotsk suture in Mongolia. The only equivalent that may have been identified to date is located in the Rushan-Pshart suture of the Pamir, although these have been assigned two ages. Based on the youngest detrital zircon ages with Northeast Pamir affinity in the eastern Rushan-Pshart accretionary complex and high pressure metamorphic rocks, a late Triassic-early Jurassic closure and collision of the South Pamir and the Central Pamir has been proposed, i.e. an age equivalent to the Songpan Ganzi accretionary complex (Burtman, 2010; Angiolini et al., 2013; Yogibekov et al. 2020). In contrast, the presence of 124-118 Ma S-type post-collisional granites and assuming a typical lag time between continent-continent collision and the onset of post-collisional magmatism, suggests that the final closure of the western Rushan–Pshart Ocean occurred in the late Jurassic–early Cretaceous (Shvol'man, 1978; Pashkov and Shvol'man, 1979; Burtman and Molnar, 1993; Schwab et al., 2004; Yogibekov et al. 2023). It will require detailed field study to identify which parts of that suture may relate to Waser and which to the Songpan Ganzi. We foresee that there are two possible locations where the Waser suture may connect northeastward to buried equivalents: either to the west of the Western Kunlun. This may be favored by the reported east Rushan-Pshart ages. In that case, the Western Kunlun is equivalent to the eastern Kunlun zone. Alternatively, the Waser Suture may connect to a structure coinciding with the modern Altyn Tagh fault. This would connect the Western Kunlun Fault to the Central Pamir and the Central Tethysides and make it independent from

the eastern Kunlun terrane. If that scenario is valid, a corollary is that the estimates of Altyn Tagh fault displacement, which is in part based on the assumption that the western and eastern Kunlun were originally a single unit (Cowgill et al., 2003) must be revisited. Summarizing, we foresee that detailed mapping of the Kunlun, Central Pamir, Rushan-Pshart, and of course Afghanistan is necessary, and worthwhile, to further the debate on the plate tectonic configuration of east Asia prior to the final, early Cretaceous collision between the China Blocks and Eurasia.

6. Conclusions

In this paper, we review and restore orogenesis and the underlying plate tectonic history of the Central Tethysides, the Iranian and Afghan section of the Alpine-Himalayan mountain belt. This segment has a distinct tectonic history from the adjacent Mediterranean and Tibetan segments. This history is characterized by an early drift history of a 'Cimmerian' continental fragment that now constitutes much of Iran and Afghanistan from the Gondwana-Land margin of Arabia to Eurasia in the Permian to late Triassic closing the Paleo-Tethys and opening the Neo-Tethys in its wake. Subsequently, oceanic basins opened in the upper plate of the Neo-Tethyan subduction zones that we kinematically reconstruct in detail in this paper.

Our main conclusions are the following:

1) Taking the detailed constraints on shortening in the upper Iranian plate of the Neo-Tethyan subduction zone, and the reconstructions of the Zagros fold-thrust belt into account, Arabia-Eurasia collision must have occurred in the late Oligocene, as previously concluded.

2) The closure of the ocean basins that opened within the Iranian Cimmerides was associated with major extrusion from the western Tibet/Pamir orogen. The Sabzevar-Nain-Baft ocean basin closed by westward to south-westward motion of the Central-Eastern Iranian Microcontinent (CEIM, including the Lut Block) and its eastern continuation, the Farah Rud Block of Afghanistan, along the Doruneh-Great Kavir Fault that connected eastwards to the Herat Fault of Afghanistan. Superimposed on this, the Helmand Block of Afghanistan extruded faster, closing the Sistan Ocean between the Lut Block of the CEIM and

the Helmand Block. This extrusion was accommodated along a fault parallel to the Waser Suture, which may have been the Helmand Fault, and the Chaman Fault that is the modern India-Asia plate boundary.

3) Opening of the Sabzevar-Nain-Baft oceanic basin occurred in the late Jurassic to early Cretaceous as a back-arc basin in the upper plate of the Neo-Tethys subduction zone below the Sanandaj-Sirjan Zone. Extension magnitude decreased westwards into the continental Central Basin of west Iran. To the north, a second set of extensional basins with opposite trend in extension magnitude: in the west, the oceanic South Caspian basin opened, whereas decreasing extension eastwards led to the continental Kopet Dagh basin. The Alborz-Kopet Dagh block formed a rotating relay ramp in between these extensional systems.

4) Reconstructing the extrusion of the Helmand Block, Waser Suture, and Farah Rud blocks of Afghanistan places these units within the Pamir/west Tibetan orogen. The Helmand Block restores as the northwestern part of the Southern Pamir/Qiangtang Block, the early Cretaceous Waser suture is likely equivalent to the western Rushan-Pshart zone of the Pamir of which a similar closure age has been interpreted, and the Farah Rud zone is equivalent to the Central Pamir.

5) The early Cretaceous closure of the Waser Suture shows that the NW part of the Qiangtang Block was not part of Eurasia until this time. The Waser Suture cannot connect to the suture that is north of the Qiangtang Block in the Tibetan Plateau (i.e., the Songpan Ganzi accretionary complex), because it is Triassic in age. We infer that this suture instead may connect through a suture whose location has been postulated to be hidden below the Tarim Basin that accommodated the plate motion of the China Blocks relative to Eurasia until the early Cretaceous. This motion is well-documented by paleomagnetism and in the Mongol-Okhotsk suture zone of Mongolia, but its connection to the Tethyan systems remained enigmatic: the Waser Suture may be part of that missing link.

6) We infer that the Sistan ocean reactivated a suture that formed in late Jurassic time between the Helmand/Qiangtang of the China blocks collage, and the Iranian Cimmerides, when the rotation pole between the two shifted northwards to the junction with the Waser Suture. Counterclockwise rotation of the China blocks relative to Eurasia closed the system

from the Waser Suture to the Mongol-Okhotsk suture, while opening the Sistan Ocean to the south of the pole.

7) Our reconstruction of the Central Tethysides identifies a history with tectonic elements that are known from the widely studied and reconstructed Mediterranean and Tibetan neighbours, but that were not previously restored. The Iranian and Afghan geology may contain spectacular examples of back-arc opening and closure, tectonic extrusion, and associated magmatism and mineralization, but decades of detailed mapping are ahead to unlock the full potential in this monumental part of the Tethyan orogenic belt.

Acknowledgements
This work was supported by the Netherlands Organization for Scientific Research (NWO Vici Grant 865.17.001) to DJJvH. We are indebted to many colleagues for discussions on Iranian and Afghan and surrounding geology during the many years that it took to build this reconstruction, including but not limited to Federico Rossetti, Emad Rohjani, Abdul Qayyum, Celal Şengör and Boris A. Natal`in.

References

Abasnia, H., Karimpour, M.H. and Malekzadeh Shafaroudi, A., 2019. Petrology, geochemistry, Zircon dating and Sr-Nd isotopes of metamorphic and igneous rocks in Kabodan area, Northern Bardaskan, Khorasan Razavi province. Scientific Quarterly Journal of Geosciences, 29(113), pp.189-198. (in Persian with abstract in English)

Abdullah, Sh and Chmyriov, V.,M. (editors in chief), 2008. Geology and Mineral Resources of Afghanistan. Book 1 Geology. British Geological Survey Occasional Publication No.15., ix+488 p.

Advokaat, E.L. and van Hinsbergen, D.J.J. 2024. Finding Argoland: reconstructing a microcontinental archipelago from the SE Asian accretionary orogen. Gondwana Research, 128, 161-263.

Afaghi, A. and Salek, M.M., 1977. Geological Map of Sheet No.2 North-Central Iran 1:1.000.000. National Iranian Oil Company, Tehran.

Afaghi, A., Salek, M.M. and Moazami, J. (Eds), 1977. Geological Cross Sections North-West Iran 1:500.000. National Iranian Oil Company, Tehran.

Agard, P., Omrani, J., Jolivet, L. and Mouthereau, F. 2005. Convergence history across Zagros (Iran): constraints from collisional and earlier deformation. International Journal of Earth Sciences, 94, 401-419, https://doi.org/10.1007/s00531-005-0481-4.

Agard, P., Monié, P., Gerber, W., Omrani, J., Molinaro, M., Meyer, B., Labrousse, L., Vrielynck, B., Jolivet, L. and Yamato, P., 2006. Transient, synobduction exhumation of Zagros blueschists inferred from P-T, deformation, time, and kinematic constraints: Implications for Neotethyan wedge dynamics. Journal of Geophysical Research: Solid Earth, 111(B11)., doi:10.1029/2005JB004103.

Agard, P., Omrani, J., Jolivet, L., Whitechurch, H., Vrielynck, B., Spakman, W., Monié, P., Meyer, B. and Wortel, R., 2011. Zagros orogeny: a subduction-dominated process. Geological Magazine, 148(5-6): 692-725.

Aghababaei, A., Adollahie-Fard, I., Martins-Ferreira, M.A.C., Ghaemi, F., Rahimi, B. and Moussavi-Harami, R., 2022. Influence of rift geometry over successive post-rift sedimentation: Tectonostratigraphy of the eastern Kopeh Dagh Belt (NE Iran). Marine and Petroleum Geology, 142, p.105729.

Ahadnejad, V., Valizadeh, M.V., Deevsalar, R. and Rezaei-Kahkhaei, M., 2011. Age and geotectonic position of the Malayer granitoids: Implication for plutonism in the Sanandaj-Sirjan Zone, W Iran. Neues Jahrbuch Fur Geologie Und Palaontologie-Abhandlungen, 261(1), p.61.

Ahmad, S., Hassan, S., Mehnood, K. and Maqsood, T., 2018. Role of Chaman transform boundary fault in the deformation of Eastern Kharan Fore-Arc Basin. Journal of Himalayan Earth Science, 51(1).

Ahmadi, H. and Rahmani, A.B., 2018. Study on The Mineral Anomalies of Muqur-Chaman Fault and Its Comparison with Harirud (Herat) Fault (Afghanistan) Using Geophysical and Remote Sensing (Aster-Hymap) Data. Геология и охрана недр, (1), pp.28-38 (Abstract in Russian and Kazakh).

Ahmadi Khalaji, A., Esmaeily, D., Valizadeh, M.V. and Rahimpour-Bonab, H., 2007. Petrology and geochemistry of the granitoid complex of Boroujerd, Sanandaj-Sirjan Zone, Western Iran. Journal of Asian Earth Sciences, 29(5-6), pp.859-877.

Ahmadipour, H., Sabzehei, M., Emami, M., Whitechurch, H. and Rastad, E., 2003. Soghan complex as an evidence for paleospreading center and mantle diapirism in Sanandaj-Sirjan zone (south-east Iran). Journal of Sciences, Volume:14, Issue:2 Page(s): 157-1,72

Ahmadirouhani, R., Karimpour, M.H., Rahimi, B., Malekzadeh Shafaroudi, A., Klotzli, U. and Santos, J.F., 2017. Petrology, geochronology, geochemistry and petrogenesis of Bajestan granitoids, North of Ferdows, Khorasan Razvi Province. Journal of Economic Geology, 8(2), pp.525-552.

Ahmed, Z. and Ernst, W.G., 1999. Island arc–related, back-arc basinal, and oceanic-island components of the Bela Ophiolite-Mélange Complex, Pakistan. International geology review, 41(8), pp.739-763.

Al-Riyami, K., Robertson, A., Dixon, J. and Xenophontos, C., 2002. Origin and emplacement of the Late Cretaceous Baer–Bassit ophiolite and its metamorphic sole in NW Syria. Lithos, 65(1-2), pp.225-260.

Alavi, M., 1991. Sedimentary and structural characteristics of the Paleo-Tethys remnants in northeastern Iran. Geological Society of America Bulletin, 103(8), pp.983-992.

Alavi, M., 1992. Thrust tectonics of the Binalood region, NE Iran. Tectonics, 11(2), pp.360-370.

Alavi, M., 1996. Tectonostratigraphic synthesis and structural style of the Alborz mountain system in northern Iran. Journal of Geodynamics, 21(1), pp.1-33.

Alavi, M., Vaziri, H., Seyed-Emami, K. and Lasemi, Y., 1997. The Triassic and associated rocks of the Nakhlak and Aghdarband areas in central and northeastern Iran as remnants of the southern Turanian active continental margin. Geological Society of America Bulletin, 109(12), pp.1563-1575.

Ali, S.A., Buckman, S., Aswad, K.J., Jones, B.G., Ismail, S.A. and Nutman, A.P., 2012. Recognition of Late Cretaceous Hasanbag ophiolite-arc rocks in the Kurdistan Region of the

Iraqi Zagros suture zone: A missing link in the paleogeography of the closing Neo-Tethys Ocean. Lithosphere, 4(5), pp.395-410.

Allen, M.B., Ghassemi, M.R., Shahrabi, M. and Qorashi, M., 2003a. Accommodation of late Cenozoic oblique shortening in the Alborz range, northern Iran. Journal of structural geology, 25(5), pp.659-672.

Allen, M.B., Kheirkhah, M., Emami, M.H. and Jones, S.J., 2011. Right-lateral shear across Iran and kinematic change in the Arabia—Eurasia collision zone. Geophysical Journal International, 184(2), pp.555-574.

Allen, M.B., Vincent, S.J., Alsop, G.I., Ismail-zadeh, A. and Flecker, R., 2003b. Late Cenozoic deformation in the South Caspian region: effects of a rigid basement block within a collision zone. Tectonophysics, 366(3-4), pp.223-239.

Amirhassankhani, F., Senowbari-Daryan, B. and Rashidi, K., 2014. Upper Triassic (Norian-Rhaetian) hypercalcified sponges from the Lut Block, east central Iran. In: Rivista Italiana di Paleontologia e Stratigrafia, 120, pp.287-315.

Angiboust, S., Agard, P., De Hoog, J.C.M., Omrani, J. and Plunder, A., 2013. Insights on deep, accretionary subduction processes from the Sistan ophiolitic “mélange”(Eastern Iran). Lithos, 156, pp.139-158.

Angiolini, L., Zanchi, A., Zanchetta, S., Nicora, A. and Vezzoli, G., 2013. The Cimmerian geopuzzle: new data from South Pamir. Terra Nova, 25(5), pp.352-360.

Ao, S., Xiao, W., Jafari, M.K., Talebian, M., Chen, L., Wan, B., Ji, W. and Zhang, Z., 2016. U–Pb zircon ages, field geology and geochemistry of the Kermanshah ophiolite (Iran): from continental rifting at 79 Ma to oceanic core complex at ca. 36 Ma in the southern Neo-Tethys. Gondwana Research, 31: 305-38.

Arefifard, S. and Isaacson, P.E., 2011. Permian Sequence stratigraphy in east-central Iran: Microplate records of Peri-Tethyan and Peri-Gondwanan events. Stratigraphy, 8(1), p.61.

Arfania, R. and Hamedani, A., 2008. Geometrical analysis of folding in Kalut area (NE of Ardakan). Geotechnical Geology, 4(1), pp.1-11.

Arian, M. and Noroozpour, H., 2015. Tectonic Geomorphology of Iran’s Salt Structures. Open Journal of Geology, Vol.05 No.02 doi: 10.4236/ojg.2015.52006

Auden, J.B., 1974. Afghanistan-West Pakistan. Geological Society, London, Special Publications, 4(1), pp.235-253.

Azizi, H. and Stern, R.J., 2019. Jurassic igneous rocks of the central Sanandaj–Sirjan zone (Iran) mark a propagating continental rift, not a magmatic arc. Terra Nova, 31(5), pp.415-423.

Azizi, H., Kazemi, T. and Asahara, Y., 2017. A-type granitoid in Hasansalaran complex, northwestern Iran: Evidence for extensional tectonic regime in northern Gondwana in the Late Paleozoic. Journal of Geodynamics, 108, pp.56-72.

Azizi, H., Nouri, F., Stern, R.J., Azizi, M., Lucci, F., Asahara, Y., Zarinkoub, M.H. and Chung, S.L., 2020. New evidence for Jurassic continental rifting in the northern Sanandaj Sirjan Zone, western Iran: the Ghalaylan seamount, southwest Ghorveh. International Geology Review, 6 (13-14), pp.1635-1657.

Babaei, A., Babaie, H.A. and Arvin, M., 2005. Tectonic evolution of the Neyriz ophiolite, Iran: an accretionary prism model. Ofioliti, 30(2), pp.65-74.

Babaie, H.A., Babaei, A., Ghazi, A.M. and Arvin, M., 2006. Geochemical, 40Ar/39Ar age, and isotopic data for crustal rocks of the Neyriz ophiolite, Iran. Canadian Journal of Earth Sciences, 43(1), pp.57-70.

Babazadeh, S.A., 2013. A note on stratigraphic data and geodynamic evolution of Sistan Suture Zone (Neo-Tethyan margin) in Eastern Iran. Geodynamics Research International Bulletin (GRIB), 1(1), pp.1-7.

Babazadeh, S.A. and De Wever, P., 2004a. Early Cretaceous radiolarian assemblages from radiolarites in the Sistan Suture (eastern Iran). Geodiversitas, 26(2), pp.185-206.

Babazadeh, S.A. and De Wever, P., 2004b. Radiolarian Cretaceous age of Soulabest radiolarites in ophiolite suite of eastern Iran. Bulletin de la Société géologique de France, 175(2), pp.121-129.

Badr, A., Davoudian, A.R., Shabanian, N., Azizi, H., Asahara, Y., Neubauer, F., Dong, Y. and Yamamoto, K., 2018. A-and I-type metagranites from the North Shahrekord Metamorphic Complex, Iran: Evidence for Early Paleozoic post-collisional magmatism. Lithos, 300, pp.86-104.

Badshah, M.S., Gnos, E., Jan, M.Q., and Afridi, M.I., 2000. Stratigraphic and tectonic evolution of the northwestern Indian plate and Kabul Block, *in* Tectonics of the Nanga Parbat Syntaxis and the Western Himalaya. Khan, M. A., Treloar, P. J., Searle, M. P. & Jan, M. Q. (eds). Geological Society, London, Special Publications, 170,461-475.

Bagheri, S. and Gol, S.D., 2020. The eastern iranian orocline. Earth-Science Reviews, 210, p.103322.

Bagheri, S. and Stampfli, G.M., 2008. The Anarak, Jandaq and Posht-e-Badam metamorphic complexes in central Iran: new geological data, relationships and tectonic implications. Tectonophysics, 451(1-4), pp.123-155.

Bagheri, S., Madhanifard, R., and Zahabi, F., 2016, Kinematics of the Great Kavir fault inferred from a structural analysis of the Pees Kuh Complex, Jandaq area, central Iran, in Sorkhabi, R., ed., Tectonic Evolution, Collision, and Seismicity of Southwest Asia: In Honor of Manuel Berberian's Forty-Five Years of Research Contributions: Geological Society of America Special Paper 525, p. 213–227, doi:10.1130/2016.2525(06).

Balini, M., Nicora, A., Berra, F., Garzanti, E., Levera, M., Mattei, M., Muttoni, G., Zanchi, A., Bollati, I., Larghi, C. and Zanchetta, S., 2009. The Triassic stratigraphic succession of Nakhlak (Central Iran), a record from an active margin. Geological Society, London, Special Publications, 312(1), pp.287-321.

Balini, M., Nicora, A., Zanchetta, S., Zanchi, A., Marchesi, R., Vuolo, I., Hosseiniyoon, M., Norouzi, M. and Soleimani, S., 2019. Olenekian to Early Ladinian stratigraphy of the western part of the Aghdarband window (Kopeh-Dag, NE Iran). Rivista Italiana di Paleontologia e Stratigrafia, 125(1), pp.283-315.

Baroz, F., Macaudiere, J., Montigny, R., Noghreyan, M., Ohnenstetter, M. and Rocci, G., 1984. Ophiolites and related formations in the central part of the Sabzevar range (Iran) and possible geotectonic reconstructions. Neues Jahrbuch für Geologie und Paläontologie-Abhandlungen, pp.358-388.

Barrier, E., Vrielynck, B., Brouillet, J.F. and Brunet, M.F., 2018. Paleotectonic Reconstruction of the Central Tethyan Realm. Tectonono-Sedimentary-Palinspastic Maps from Late Permian to Pliocene.

Bassoulet, J., Boulin, J., Colchen, M., Montenat, C., Marcoux, J. and Mascle, G., 1980. The Evolution of the Tethyan Domains Around the Indian Shield, Form Carboniferous to Cretaceous Times. Congres Geologique International. 26/1980/Paris; Fra; Orleans: B.R.G.M.; Vol. 3; Pp. 1382

Baud, A. and Stämpfli, G.M., 1989. Tectonogenesis & evolution of a segment of the Cimmerides: the volcano-sedimentary Triassic of Aghdarband (Kopet-Dagh, North-East Iran). In Tectonic evolution of the Tethyan region (ed. A.M.C Şengör), Series C: Mathematical and Physical Sciences, vol. 259, pp.265-275.

Bazhenov, M.L., 1987. Paleomagnetism of Cretaceous and Paleogene sedimentary rocks from the Kopet-Dagh and its tectonic implications. Tectonophysics, 136(3-4), pp.223-235.

Bazhenov, M.L. and Burtman, V.S., 1986. Tectonics and paleomagnetism of structural arcs of the Pamir-Punjab syntaxis. Journal of geodynamics, 5(3-4), pp.383-396.

Bea, F., Mazhari, A., Montero, P., Amini, S. and Ghalamghash, J., 2011. Zircon dating, Sr and Nd isotopes, and element geochemistry of the Khalifan pluton, NW Iran: Evidence for Variscan magmatism in a supposedly Cimmerian superterrane. Journal of Asian Earth Sciences, 40(1), pp.172-179.

Beck, R.A., Burbank, D.W., Sercombe, W.J., Khan, A.M. and Lawrence, R.D., 1996. Late Cretaceous ophiolite obduction and Paleocene India-Asia collision in the westernmost Himalaya. Geodinamica Acta, 9(2-3), pp.114-144.

Berberian, F. and Berberian, M., 1981. Tectono-plutonic episodes in Iran. Zagros Hindu Kush Himalaya Geodynamic Evolution, 3, pp.5-32.

Berberian, F., Muir, I.D., Pankhurst, R.J. and Berberian, M., 1982. Late Cretaceous and early Miocene Andean-type plutonic activity in northern Makran and Central Iran. Journal of the Geological Society, 139(5), pp.605-614.

Berberian, M., 1976. Pre-quaternary faults in Iran. Geological Survey of Iran, 39, pp.259-269.

Berberian, M., 1981. Active faulting and tectonics of Iran. Zagros Hindu Kush Himalaya Geodynamic Evolution, 3, pp.33-69.

Berberian, M., 1983. The southern Caspian: a compressional depression floored by a trapped, modified oceanic crust. Canadian Journal of Earth Sciences, 20(2), pp.163-183.

Berberian, M., 2014. Active Tectonics and Geologic Setting of the Iranian Plateau. Developments in Earth Surface Processes, Volume 17, pp. 151-171.

Berberian, M. and King, G.C.P. 1981. Towards a palaeogeography and tectonic evolution of Iran. Canadian Journal of Earth Sciences, 18, 210-65.

Berberian, M., Jackson, J.A., Qorashi, M., Talebian, M., Khatib, M. and Priestley, K., 2000. The 1994 Sefidabeh earthquakes in eastern Iran: blind thrusting and bedding-plane slip on a growing anticline, and active tectonics of the Sistan suture zone. Geophysical Journal International, 142(2), pp.283-299.

Besse, J., Torcq, F., Gallet, Y., Ricou, L.E., Krystyn, L. and Saidi, A., 1998. Late Permian to Late Triassic palaeomagnetic data from Iran: constraints on the migration of the Iranian block through the Tethyan Ocean and initial destruction of Pangaea. Geophysical Journal International, 135(1), pp.77-92.

Biabangard, H., Baghari, S. and Vysinasab, S., 2020. Petrology, geochemistry and origin of Mirabad dacitoid dykes, south of Zahedan (Southeast of Iran). Petrological Journal, 10(4), pp.67-82 (in Persian with English abstract).

Bin, Z. and Meiyin, D., 2010, March. Geological setting of Garmsar block, Iran. In 2010 International Conference on Challenges in Environmental Science and Computer Engineering, Vol. 2, pp. 433-437.

Bina, M.M., Bucur, I., Prevot, M., Meyerfeld, Y., Daly, L., Cantagrel, J.M. and Mergoil, J., 1986. Palaeomagnetism, petrology and geochronology of tertiary magmatic and sedimentary units from Iran. Tectonophysics, 121(2-4), pp.303-329.

Blaise, J., Bordet, P., Carbonnel, J.P. and Montenat, C., 1978. Flyschs et ophiolites dans la region de Panjaw; une suture neocimmerienne en Afghanistan central. Bulletin de la Société Géologique de France, 7(5), pp.795-798 (with English abstract).

Bonnet, G., Agard, P., Angiboust, S., Monie, P., Jentzer, M., Omrani, J., Whitechurch, H. and Fournier, M., 2018. Tectonic slicing and mixing processes along the subduction interface: The Sistan example (Eastern Iran). Lithos, 310, pp.269-287.

Borneman, N.L., Hodges, K.V., Van Soest, M.C., Bohon, W., Wartho, J.A., Cronk, S.S. and Ahmad, T. 2015. Age and structure of the Shyok suture in the Ladakh region of northwestern India: implications for slip on the Karakoram fault system. Tectonics, 34, 2011-2033.

Boulin, J., 1988. Hercynian and Eocimmerian events in Afghanistan and adjoining regions. Tectonophysics, 148, 253-278.

Bouilhol, P., Jagoutz, O., Hanchar, J.M. and Dudas, F.O. 2013. Dating the India–Eurasia collision through arc magmatic records. Earth and Planetary Science Letters, 366, 163-175.

Boyden, J.A., Müller, R.D., Gurnis, M., Torsvik, T.H., Clark, J.A., Turner, M., Ivey-Law, H., Watson, R.J. and Cannon, J.S., 2011. Next-generation plate-tectonic reconstructions using GPlates. In: Geoinformatics: Cyberinfrastructure for the Solid Earth Sciences. Cambridge University Press, Cambridge, pp. 95-113.

Bröcker, M., Omrani, H., Berndt, J. and Moslempour, M.E., 2021. Unravelling metamorphic ages of suture zone rocks from the Sabzevar and Makran areas (Iran): Robust age constraints for the larger Arabia–Eurasian collision zone. Journal of Metamorphic Geology, 39(9), pp.1099-1129.

Bröcker, M., Rad, G.F., Burgess, R., Theunissen, S., Paderin, I., Rodionov, N. and Salimi, Z., 2013. New age constraints for the geodynamic evolution of the Sistan Suture Zone, eastern Iran. Lithos, 170, pp.17-34.

Buchs, D.M., Bagheri, S., Martin, L., Hermann, J. and Arculus, R., 2013. Paleozoic to Triassic ocean opening and closure preserved in Central Iran: constraints from the geochemistry of meta-igneous rocks of the Anarak area. Lithos, 172, pp.267-287.

Burg, J.P., 2018. Geology of the onshore Makran accretionary wedge: Synthesis and tectonic interpretation. Earth-Science Reviews, 185, pp.1210-1231.

Burtman, V.S., Molnar, P., 1993. Geological and geophysical evidence for deep subduction of continental crust beneath the Pamir. Geological Society of America Special Paper 281, 1 – 76.

Burtman, V.S., 1994. Meso-Tethyan oceanic sutures and their deformation. Tectonophysics, 234(4), pp.305-327.

Cai, F., Ding, L., Wang, H., Laskowski, A.K., Zhang, L., Zhang, B., Mohammadi, A., Li, J., Song, P. and Li, Z., 2021. Configuration and timing of collision between Arabia and Eurasia in the Zagros collision zone, Fars, southern Iran. Tectonics, 40(8): e2021TC006762

Camp V. E., and R. J. Griffis, 1982. Character, genesis and tectonic setting of igneous rocks in the Sistan suture zone, eastern Iran, Lithos, 15(3), 221–239.

Carter, A., Najman, Y., Bahroudi, A., Bown, P., Garzanti, E. and Lawrence, R.D. 2010. Locating earliest records of orogenesis in western Himalaya: Evidence from Paleogene sediments in the Iranian Makran region and Pakistan Katawaz basin. Geology, 38, 807-810, https://doi.org/10.1130/g31087.1.

Chiu, H.Y., Chung, S.L., Zarrinkoub, M.H., Mohammadi, S.S., Khatib, M.M. and Iizuka, Y., 2013. Zircon U–Pb age constraints from Iran on the magmatic evolution related to Neotethyan subduction and Zagros orogeny. Lithos, 162, pp.70-87.

Chiu, H.Y., Chung, S.L., Zarrinkoub, M.H., Melkonyan, R., Pang, K.N., Lee, H.Y., Wang, K.L., Mohammadi, S.S. and Khatib, M.M., 2017. Zircon Hf isotopic constraints on magmatic and tectonic evolution in Iran: Implications for crustal growth in the Tethyan orogenic belt. Journal of Asian Earth Sciences, 145, pp.652-669.

Cifelli, F., Ballato, P., Alimohammadian, H., Sabouri, J. and Mattei, M., 2015. Tectonic magnetic lineation and oroclinal bending of the Alborz range: Implications on the Iran-Southern Caspian geodynamics, Tectonics, 34, 116–132, doi:10.1002/2014TC003626

Cifelli, F., Mattei, M., Rashid, H. and Ghalamghash, J., 2013. Right-lateral transpressional tectonics along the boundary between Lut and Tabas blocks (Central Iran). Geophysical Journal International, 193(3), pp.1153-1165.

Clift, P.D., Shimizu, N., Layne, G., Blusztajn, J., Gaedicke, C., Schluter, H.-U., Clark, M. and Amjad, S. 2001. Development of the Indus Fan and its significance for the erosional history of the Western Himalaya and Karakoram. Geological Society of America Bulletin, 113, 1039-1051.

Cocker, M., 2011. Summary for the Mineral Information Package for the Nuristan Rare-Metal Pegmatite Area of Interest.". Summaries of Important Areas in Mineral Investment and Production Opportunities of Nonfuel Minerals in Afghanistan, pp.2011-1204.

Cogné, J.-P., Kravchinsky, V.A., Halim, N. and Hankard, F. 2005. Late Jurassic-Early Cretaceous closure of the Mongol-Okhotsk Ocean demonstrated by new Mesozoic palaeomagnetic results from the Trans-Baïkal area (SE Siberia). Geophysical Journal International, 163, 813-832, https://doi.org/10.1111/j.1365-246X.2005.02782.x.

Conrad, G., Montigny, R., Thuizat, R. and Westphal, M., 1981. Tertiary and Quaternary geodynamics of southern Lut (Iran) as deduced from palaeomagnetic, isotopic and structural data. Tectonophysics, 75(3-4), pp.T11-T17.

Cowgill, E., Forte, A.M., Niemi, N., Avdeev, B., Tye, A., Trexler, C., Javakhishvili, Z., Elashvili, M. and Godoladze, T., 2016. Relict basin closure and crustal shortening budgets during continental collision: An example from Caucasus sediment provenance. Tectonics, 35(12), pp.2918-2947.

Cowgill, E., Yin, A.N., Harrison, T.M. and Xiao-Feng, W., 2003. Reconstruction of the Altyn Tagh fault based on U-Pb geochronology: Role of back thrusts, mantle sutures, and heterogeneous crustal strength in forming the Tibetan Plateau. Journal of Geophysical Research: Solid Earth, 108(B7).

Crawford, A.R., 1977. A Summary of Isotopic Age Data for Iran Pakistan and India. Mem. h. Ser. Soc. geol. France, 8, 251-260.

Dastanpour, 1996. The Devonian System in Iran: a review. Geological Magazine, 133(02), 159. doi:10.1017/s0016756800008670

Davies R. G., Jones C. R., Hamzepour B. and Clark G. G., 1972. Geology of the Masuleh sheet, 1:100,000. NW Iran: Geological Survey of Iran, Report No. 24, pp. 110.

Davoudian, A.R., Genser, J., Neubauer, F. and Shabanian, N., 2016. 40Ar/39Ar mineral ages of eclogites from North Shahrekord in the Sanandaj–Sirjan Zone, Iran: implications for the tectonic evolution of Zagros orogen. Gondwana Research, 37, pp.216-240.

Davoudzadeh, M. and Schmidt, K., 1982. Zur Trias des Iran. Geologische Rundschau, 71, pp.1021-1039.

Davoudzadeh, M. and Schmidt, K., 1984. A review of the Mesozoic paleogeography and paleotectonic evolution of Iran. Neues Jahrbuch für Geologie und Palaeontologie-Abhandlungen, pp.182-207.

Davoudzadeh, M., Lammerer, B. and Weber-Diefenbach, K., 1997. Paleogeography, stratigraphy, and tectonics of the tertiary of Iran. Neues Jahrbuch für Geologie und Palaontologie Abhandlungen, 205, pp.33-67.

Davoudzadeh, M., Seyed-Emami, K. and Amidi, M., 1969. Preliminary note on a newly discovered Triassic Section northeast of Anarak (central Iran), with some remarks on the age of the Metamorphism on the Anarak Region. Geological Survey of Iran, Note, 5, pp.1-23.

Davydov, V. I., and Arerifard, S., 2007. Permian fusulinid fauna of peri-Gondwanan affinity from the Kalmard region, East-Central Iran and its significance for tectonics and paleogeography. Palaeotologia Electronica, 10, 2, 1-40.

Delaloye, M. and Desmons, J., 1980. Ophiolites and mélange terranes in Iran: a geochronological study and its paleotectonic implications. Tectonophysics, 68(1-2), pp.83-111.

Delavari, M., Amini, S., Schmitt, A.K., McKeegan, K.D. and Harrison, T.M., 2014. U–Pb geochronology and geochemistry of Bibi-Maryam pluton, eastern Iran: Implication for the late stage of the tectonic evolution of the Sistan Ocean. Lithos, 200, pp.197-211.

Derakhshi, M. and Ghasemi, H., 2015. Soltan Maidan Complex (SMC) in the eastern Alborz structural zone, northern Iran: magmatic evidence for Paleotethys development. Arabian Journal of Geosciences, 8(2), pp.849-866.

Debon, F., Afzali, H., Le Fort, P. and Sonet, J., 1987. Major intrusive stages in Afghanistan: typology, age and geodynamic setting. Geologische Rundschau, 76(1), pp.245-264.

Deevsalar, R., Shinjo, R., Ghaderi, M., Murata, M., Hoskin, P.W.O., Oshiro, S., Wang, K.L., Lee, H.Y. and Neill, I., 2017. Mesozoic–Cenozoic mafic magmatism in Sanandaj–Sirjan zone, Zagros Orogen (Western Iran): geochemical and isotopic inferences from middle Jurassic and late Eocene gabbros. Lithos, 284, pp.588-607.

Dercourt, J., Gaetani, M., Vrielynck, B., Barrier, E., Biju-Duval, B., Brunet, M.F., Cadet, J.P., Crasquin, S. and Sandulescu, M., 2000. Peri-Tethys palaeogeographical atlas 2000. Université Pierre et Marie Curie, Paris.

Desmons, J. and Beccaluva, L., 1983. Mid-ocean ridge and island-arc affinities in ophiolites from Iran: palaeographic implications: complementary reference. Chemical Geology, 39(1-2), pp.39-63.

Dewey, J. and Şengör, A.M.C., 1979. Aegean and surrounding regions: complex multiplate and continuum tectonics in a convergent zone. Geological Society of America Bulletin, 90(1): 84-92.

Djamour, Y., Vernant, P., Bayer, R., Nankali, H.R., Ritz, J.F., Hinderer, J., Hatam, Y., Luck, B., Le Moigne, N., Sedighi, M. and Khorrami, F., 2010. GPS and gravity constraints on continental deformation in the Alborz mountain range, Iran. Geophysical Journal International, 183(3), pp.1287-1301.

Doebrich, J.L. and Wahl, R.R., 2006. Geologic and mineral resource map of Afghanistan (USGS open file report No. 2006-1038 version 2). Geological Survey (US).

Doebrich, J., Ludington, S., Peters, S., Finn, C., Mars, J., Rowan, L., Stoeser, D., King, T., Eppinger, R. and Wasy, A. 2007. Porphyry copper potential of Tethyan magmatic arcs of Afghanistan. Irish Association for Economic Geology, 1, 129-132.

Dorani, M., Arvin, M., Oberhänsli, R. and Dargahi, S., 2017. PT evolution of metapelites from the Bajgan complex in the Makran accretionary prism, south eastern Iran. Geochemistry, 77(3), pp.459-475.

Eftekharnezhad, J. and Behroozi, A., 1991. Geodynamic significance of recent discoveries of ophiolites and Late Paleozoic rocks in NE Iran (including Kopet Dagh). Abhandlungen der Geologischen Bundesanstalt, 38, pp.89-100.

Eftekhar-Nezhad, J. and Stöcklin, J., 1992. Geological map of Iran sheet K8 (Birjand), scale 1: 250,000. Geological Survey of Iran, Tehran.

Ehteshami-Moinabadi, M., 2016. Possible basement transverse faults in the western Alborz, northern Iran. Journal of Sciences, Islamic Republic of Iran, 27(4), pp.329-342.

Ehteshami-Moinabadi, M., Yassaghi, A. and Amini, A., 2012. Mesozoic basin inversion in Central Alborz, evidence from the evolution of Taleqan-Gajereh-Lar paleograben. JGeope 2 (2), pp. 43-63.

Esmaeily, D., Nédélec, A., Valizadeh, M.V., Moore, F. and Cotten, J., 2005. Petrology of the Jurassic Shah-Kuh granite (eastern Iran), with reference to tin mineralization. Journal of Asian Earth Sciences, 25(6), pp.961-980.

Esna-Ashari, A., Tiepolo, M., Valizadeh, M.V., Hassanzadeh, J. and Sepahi, A.A., 2012. Geochemistry and zircon U–Pb geochronology of Aligoodarz granitoid complex, Sanandaj-Sirjan zone, Iran. Journal of Asian Earth Sciences, 43(1), pp.11-22.

Etemad-Saeed, N., Hosseini-Barzi, M., Adabi, M.H., Sadeghi, A. and Houshmandzadeh, A., 2015. Provenance of Neoproterozoic sedimentary basement of northern Iran, Kahar Formation. Journal of African Earth Sciences, 111, pp.54-75.

Farbod, Y., 2012. Active tectonics of the Doruneh Fault: seismogenic behavior and geodynamic role Doctoral dissertation, Aix-Marseille. 174 p.

Farbod, Y., Bellier, O., Shabanian, E. and Abbassi, M.R., 2011. Geomorphic and structural variations along the Doruneh Fault System (central Iran). Tectonics, 30(6). doi:10.1029/2011TC002889.

Faryad, S.W., Collett, S., Finger, F., Sergeev, S.A., Čopjaková, R. and Siman, P., 2016. The Kabul Block (Afghanistan), a segment of the Columbia Supercontinent, with a Neoproterozoic metamorphic overprint. Gondwana Research, 34, pp.221-240.

Fattahi, M., Walker, R.T., Khatib, M.M., Dolati, A. and Bahroudi, A., 2007. Slip-rate estimate and past earthquakes on the Doruneh fault, eastern Iran. Geophysical Journal International, 168(2), pp.691-709.

Fauvelet, E., Eftekhar-Nezhad, j., 1990, Explanatory Text of the Taybad Quadrangle Map1:250000, Geological Survey of Iran.

Fazlnia, A., Schenk, V., Appel, P. and Alizade, A., 2013. Petrology, geochemistry, and geochronology of the Chah-Bazargan gabbroic intrusions in the south Sanandaj–Sirjan zone, Neyriz, Iran. International Journal of Earth Sciences, 102, pp.1403-1426.

Fazlnia, A., Schenk, V., van der Straaten, F. and Mirmohammadi, M., 2009. Petrology, geochemistry, and geochronology of trondhjemites from the Qori Complex, Neyriz, Iran. Lithos, 112(3-4), pp.413-433.

Forte, A.M., Gutterman, K.R., van Soest, M.C. and Gallagher, K. 2022. Building a Young Mountain Range: Insight into the growth of the Greater Caucasus mountains from detrital zircon (U-Th)/He thermochronology and 10Be erosion rates. Tectonics, 41, e2021TC006900.

Fotoohi Rad, G.R., Droop, G.T.R., Amini,S. and Moazzen, M., 2005. Eclogites and blueschists of the Sistan Suture Zone, eastern Iran: A comparison of P-T histories from a subduction melange. Lithos 84, 1–24.

Fotoohi Rad, G.R., Droop, G.T.R. and Burgess, R., 2009. Early Cretaceous exhumation of high-pressure metamorphic rocks of the Sistan Suture Zone, eastern Iran. Geological Journal 44, 104–16.

Fourcade, E., Azéma, J., Bassoullet, J.P., Cecca, F., Dercourt, J., Enay, R. and Guiraud, R., 1995. Paleogeography and paleoenvironment of the Tethyan realm during the Jurassic breakup of Pangea. In The Tethys Ocean (pp. 191-214). Springer, Boston, MA.

Fruehn, J., White, R.S. and Minshull, T.A., 1997. Internal deformation and compaction of the Makran accretionary wedge. Terra nova, 9(3), pp.101-104.

Fürsich, F.T., Wilmsen, M., Seyed-Emami, K. and Majidifard, M.R., 2009a. The Mid-Cimmerian tectonic event (Bajocian) in the Alborz Mountains, Northern Iran: evidence of the break-up unconformity of the South Caspian Basin. Geological Society, London, Special Publications, 312(1), pp.189-203.

Fürsich, F.T., Wilmsen, M., Seyed-Emami, K. and Majidifard, M.R., 2009b. Lithostratigraphy of the Upper Triassic–Middle Jurassic Shemshak Group of Northern Iran. Geological Society, London, Special Publications, 312(1) pp.129-160.

Fürsich, F.T., Pan, Y., Wilmsen, M. and Majidifard, M.R., 2016. Biofacies, taphonomy, and paleobiogeography of the Kamar-e-Mehdi Formation of east-central Iran, a Middle to Upper Jurassic shelf lagoon deposit. Facies, 62(1), pp.1-23.

Gaina, C., Van Hinsbergen, D.J. and Spakman, W., 2015. Tectonic interactions between India and Arabia since the Jurassic reconstructed from marine geophysics, ophiolite geology, and seismic tomography. Tectonics, 34(5), pp.875-906.

Ghasemi, H., Juteau, T., Bellon, H., Sabzehei, M., Whitechurch, H. and Ricou, L.E., 2002. The mafic–ultramafic complex of Sikhoran (central Iran): a polygenetic ophiolite complex. Comptes Rendus Geoscience, 334(6), pp.431-438.

Ghazi, A.M., and Hassanipak, A.A., 2000, Petrology and geochemistry of the Shahr-Babak ophiolite, central Iran, in Dilek, Y., Moores, E.M., Elthon, D., and Nicolas, A., eds., Ophiolites and Oceanic Crust: New Insights from Field Studies and the Ocean Drilling Program: Boulder, Colorado, Geological Society of America Special Paper 349, p. 485–497.

Ghazi, A.M., Hassanipak, A.A., Mahoney, J.J. and Duncan, R.A., 2004. Geochemical characteristics, 40Ar–39Ar ages and original tectonic setting of the Band-e-Zeyarat/Dar Anar ophiolite, Makran accretionary prism, SE Iran. Tectonophysics, 393(1-4), pp.175-196.

Ghazi, A.M., Hassanipak, A.A., Tucker, P.J., Mobasher, K. and Duncan, R.A., 2001, December. Geochemistry and 40Ar-39Ar ages of the Mashhad Ophiolite, NE Iran: a rare occurrence of a 300 Ma (Paleo-Tethys) Oceanic Crust. In AGU Fall Meeting Abstracts (Vol. 2001, pp. V12C-0993).

Ghazi, A.M., Pessagno, E.A., Hassanipak, A.A., Kariminia, S.M., Duncan, R.A. and Babaie, H.A., 2003. Biostratigraphic zonation and 40Ar–39Ar ages for the Neotethyan Khoy ophiolite of NW Iran. Palaeogeography, Palaeoclimatology, Palaeoecology, 193(2), pp.311-323.

Ghazi, J.M., Moazzen, M., Rahgoshay, M. and Moghadam, H.S., 2012. Geochemical characteristics of basaltic rocks from the Nain ophiolite (Central Iran); constraints on mantle wedge source evolution in an oceanic back arc basin and a geodynamical model. Tectonophysics, 574, pp.92-104.

Ghodsi, M.R., Boomeri, M., Bagheri, S., Ishiyama, D. and Corfu, F., 2016. Geochemistry, zircon U-Pb age, and tectonic constraints on the Bazman granitoid complex, southeast Iran. Turkish Journal of Earth Sciences, 25(4), pp.311-340.

Ghorbani, M., 2019. Lithostratigraphy of Iran. Springer, xiv+296p. https://doi.org/10.1007/978-3-030-04963-8

Girardeau, J., Marcoux, J. and Montenat, C., 1989. The Neo-Cimmerian ophiolite belt in Afghanistan and Tibet: comparison and evolution. In Tectonic Evolution of the Tethyan region (ed. A.M.C. Şengör) pp. 477-504. Springer, Dordrecht.

Gnos, E., Immenhauser, A. and Peters, T.J., 1997. Late Cretaceous/early Tertiary convergence between the Indian and Arabian plates recorded in ophiolites and related sediments. Tectonophysics, 271(1-2), pp.1-19.

Gnos, E., Khan, M., Mahmood, K., Villa, I.M., Khan, A.S., 2000. Age and tectonic setting

of the Raskoh ophiolites. Pakistan. Acta Mineral. Pakistanica 11, 105–117.

Golonka, J., 2004. Plate tectonic evolution of the southern margin of Eurasia in the Mesozoic and Cenozoic. Tectonophysics, 381(1-4), pp.235-273.

Govers, R. and Wortel, M.J.R., 2005. Lithosphere tearing at STEP faults: Response to edges of subduction zones. Earth and Planetary Science Letters, 236(1-2), pp.505-523.

Guest, B., Axen, G.J., Lam, P.S. and Hassanzadeh, J., 2006a. Late Cenozoic shortening in the west-central Alborz Mountains, northern Iran, by combined conjugate strike-slip and thin-skinned deformation. Geosphere, 2(1), pp.35-52.

Guest, B., Stockli, D.F., Grove, M., Axen, G.J., Lam, P.S. and Hassanzadeh, J., 2006b. Thermal histories from the central Alborz Mountains, northern Iran: implications for the spatial and temporal distribution of deformation in northern Iran. Geological Society of America Bulletin

118(11-12), pp.1507-1521.

Haghipour, A., 1974. Etude géologique de la région de Biabanak-Bafq (Iran central): Pétrologie et tectonique du socle précambrien et de sa couverture (Doctoral dissertation, Université Scientifique et Médicale de Grenoble).

Hassanzadeh, J. and Wernicke, B.P., 2016. The Neotethyan Sanandaj-Sirjan zone of Iran as an archetype for passive margin-arc transitions. Tectonics, 35(3): 586-621

Hassanzadeh, J., Stockli, D.F., Horton, B.K., Axen, G.J., Stockli, L.D., Grove, M., Schmitt, A.K. and Walker, J.D., 2008. U-Pb zircon geochronology of late Neoproterozoic–Early Cambrian granitoids in Iran: Implications for paleogeography, magmatism, and exhumation history of Iranian basement. Tectonophysics, 451(1-4), pp.71-96.

Hollingsworth, J., Fattahi, M., Walker, R., Talebian, M., Bahroudi, A., Bolourchi, M.J., Jackson, J. and Copley, A., 2010. Oroclinal bending, distributed thrust and strike-slip faulting, and the accommodation of Arabia–Eurasia convergence in NE Iran since the Oligocene. Geophysical Journal International, 181(3), pp.1214-1246.

Hollingsworth, J., Jackson, J., Walker, R., Reza Gheitanchi, M. and Javad Bolourchi, M., 2006. Strike-slip faulting, rotation, and along-strike elongation in the Kopeh Dagh mountains,

NE Iran. Geophysical Journal International, 166(3), pp.1161-1177.

Homke, S., Vergés, J., Serra-Kiel, J., Bernaola, G., Sharp, I., Garcés, M., Montero-Verdú, I., Karpuz, R. and Goodarzi, M.H., 2009. Late Cretaceous–Paleocene formation of the proto–Zagros foreland basin, Lurestan Province, SW Iran. Geological Society of America Bulletin, 121(7-8), pp.963-978.

Honarmand, M., Nabatian, G., Aflaki, M., Ebrahimi, M., 2020. Zircon U-Pb dating and geochemistry of the Moghanlou mylonite gneiss and granite intrusions, west of Zanjan. Scientific Quarterly Journal of Geosciences, Volume 29, Serial Number 116 (in Persian with English abstract) https://doi.org/10.22071/gsj.2019.112509.1361

Honarmand, M., Omran, N.R., Corfu, F., Emami, M.H. and Nabatian, G., 2013. Geochronology and magmatic history of a calc-alkaline plutonic complex in the Urumieh-Dokhtar Magmatic Belt, Central Iran: Zircon ages as evidence for two major plutonic episodes. Neues Jahrbuch für Mineralogie-Abhandlungen, 190/1pp.67-77.

Hsü, K.J., 1977. Tectonic Evolution of the Mediterranean Basins. In: Nairn, A.E.M., Kanes, W.H., Stehli, F.G. (eds) The Ocean Basins and Margins. Springer, Boston, MA. https://doi.org/10.1007/978-1-4684-3036-3_2

Huber, H., 1977. Geological Cross Sections North-West Iran. 1:500.000 scale. National Iranian Oil Company.

Hunziker, D., Burg, J.P., Bouilhol, P. and von Quadt, A., 2015. Jurassic rifting at the Eurasian Tethys margin: Geochemical and geochronological constraints from granitoids of North Makran, southeastern Iran. Tectonics, 34(3), pp.571-593.I

Isozaki, Y., Maruyama, S. and Furuoka, F., 1990. Accreted oceanic materials in Japan. Tectonophysics, 181(1-4), pp.179-205.

Jackson, J., Priestley, K., Allen, M. and Berberian, M., 2002. Active tectonics of the south Caspian basin. Geophysical Journal International, 148(2), pp.214-245.

Jackson, M.P.A., Cornelius, R.R., Craig, C.H., Gansser, A., Stöcklin, J., Talbot, C.J., 1990. Salt Diapirs of the Great Kavir, Central Iran. Geol. Soc. America Memoirs 177, 139.

Jacob, K.H. and Quitmeyer, R., 1979. The Makran region of Pakistan and Iran: Trench-arc system with active plate subduction. In Aul Farah and Kees A. DeJong, eds., Geodynamics of Pakistan, Geological Survey of Pakistan, pp.305-317.

Jagoutz, O. and Schmidt, M.W. 2012. The formation and bulk composition of modern juvenile continental crust: The Kohistan arc. Chemical Geology, 298, 79-96.

Jagoutz, O., Bouilhol, P., Schaltegger, U. and Müntener, O. 2019. The isotopic evolution of the Kohistan Ladakh arc from subduction initiation to continent arc collision. Geological Society, London, Special Publications, 483, 165-182.

Jamaliashtiani, R., Scherer, E.E., Schmitt, A.K., Hassanzadeh, J. and Hertwig, A.T., 2024. Lu-Hf and U-Pb dating of the Zayanderud eclogites: Implications for Jurassic subduction initiation along the Neotethys margin in Iran. Lithos, 482, p.107742.

Jamei, S., Ghorbani, M., Jafari, A., Williams, I.S. and Moayyed, M., 2021a. Geochronology and tectonic significance of A-type granite from Misho, NW Iran: Implications for the detachment of Cimmeria from Gondwana and the opening of Neo-Tethys. Geological Journal, 56(10), pp.5275-5289.

Jamei, S., Ghorbani, M., Williams, I.S. and Moayyed, M., 2021b. Tethyan oceans reconstructions with emphasis on the Early Carboniferous Pir-Eshagh A- type rhyolite and the Late Palaeozoic magmatism in Iran. International Geology Review, 63(11), pp.1389-1405.

Javadi, H.R., Esterabi Ashtiani, M., Guest, B., Yassaghi, A., Ghassemi, M.R., Shahpasandzadeh, M. and Naeimi, A., 2015. Tectonic reversal of the western Doruneh fault system: implications for Central Asian tectonics. Tectonics, 34(10), pp.2034-2051.

Javadi, H.R., Ghassemi, M.R., Shahpasandzadeh, M., Guest, B., Ashtiani, M.E., Yassaghi, A.L.I. and Kouhpeyma, M., 2013. History of faulting on the Doruneh Fault System: implications for the kinematic changes of the Central Iranian Microplate. Geological Magazin, 150(4), pp.651-672.

Jentzer, M., Agard, P., Bonnet, G., Monié, P., Fournier, M., Whitechurch, H., Omrani, J., Zarrinkoub, M.H., Khatib, M.M., Kohansal, R. and Do Couto, D., 2022. The North Sistan orogen (Eastern Iran): Tectono-metamorphic evolution and significance within the Tethyan realm. Gondwana Research, 109, pp.460-492.

Jentzer, M., Fournier, M., Agard, P., Omrani, J., Khatib, M.M. and Whitechurch, H., 2017. Neogene to Present paleostress field in Eastern Iran (Sistan belt) and implications for regional geodynamics. Tectonics, 36(2), pp.321-339.

Kadirov, F.A., 2000. Application of the Hartley transform for interpretation of gravity anomalies in the Shamakhy–Gobustan and Absheron oil-and gas-bearing regions, Azerbaijan. Journal of applied geophysics, 45(1), pp.49-61.

Kafshdouz, M.M., 1997. Structure and tectonic evolution of palaeozoic-mesozoic rocks: Sanandaj-Sirjan Zone, Werstern Iran. Doctor of Philosophy thesis, School of Geosciences, University of Wollongong, xiv+224+2+2 plates

Kananian, A., Juteau, T., Bellon, H., Darvishzadeh, A., Sabzehi, M., Whitechurch, H. and Ricou, L.E., 2001. The ophiolite massif of Kahnuj (western Makran, southern Iran): new geological and geochronological data. Comptes Rendus de l'Académie des Sciences-Series IIA-Earth and Planetary Science, 332(9), pp.543-552.

Kapp, P., DeCelles, P.G., Gehrels, G.E., Heizler, M. and Ding, L. 2007. Geological records of the Lhasa-Qiangtang and Indo-Asian collisions in the Nima area of central Tibet. Geological Society of America Bulletin, 119, 917-933, https://doi.org/10.1130/b26033.1.

Kapp, P. and DeCelles, P.G. 2019. Mesozoic–Cenozoic geological evolution of the Himalayan-Tibetan orogen and working tectonic hypotheses. American Journal of Science, 319, 159-254.

Kargaranbafghi, F., Neubauer, F. and Genser, J., 2011. Cenozoic kinematic evolution of southwestern Central Iran: Strain partitioning and accommodation of Arabia–Eurasia convergence. Tectonophysics, 502(1-2), pp.221-243.

Karimpour, M.H., Stern, C.R. and Farmer, G.L., 2010. Zircon U–Pb geochronology, Sr–Nd isotope analyses, and petrogenetic study of the Dehnow diorite and Kuhsangi granodiorite (Paleo-Tethys), NE Iran. Journal of Asian Earth Sciences, 37(4), pp.384-393.

Karimpour, M.H., Farmer, G.L. and Stern, C.R., 2011a. Rb–Sr and Sm–Nd Isotopic Compositions, U-Pb Age and Petrogenesis of Khajeh Mourad Paleo-Tethys Leucogranite, Mashhad, Iran. Journal of Geoscience, 20(80), pp.171-182. 10.22071/GSJ.2011.55249

Karimpour, M.H., Stern, C., Farmer, L. and Saadat, S., 2011b. Review of age, Rb-Sr geochemistry and petrogenesis of Jurassic to Quaternary igneous rocks in Lut Block, Eastern Iran. Geopersia, 1(1), pp.19-54.

Karimzadeh, H., Rahgoshay, M. and Monsef, I., 2020. Mineralogy, Geochemistry and Petrogenesis of Mantle Peridotites of Nehbandan Ophiolitic Complex, East of Iran. Journal of Economic Geology, 12(2), pp.157-176.

Kassi, A.M., Kelling, G., Kasi, A.K., Umar, M. and Khan, A.S., 2009. Contrasting Late Cretaceous–Palaeocene lithostratigraphic successions across the Bibai Thrust, western Sulaiman Fold–Thrust Belt, Pakistan: Their significance in deciphering the early-collisional history of the NW Indian Plate margin. Journal of Asian Earth Sciences, 35(5), pp.435-444.

Kaymakci, N. Inceöz, M., Ertepinar, P. and Koç, A., 2010. Late Cretaceous to recent kinematics of SE Anatolia (Turkey). Geological Society, London, Special Publications, 340(1), pp.409-435.

Kaz'min, V.G., and Verzhbitskii, E.V., 2011. Age and origin of the South Caspian Basin. Oceanology 51, 131–140. https://doi.org/10.1134/S0001437011010073

Kazemi, Z., Ghasemi, H., Tilhac, R., Griffin, W., Moghadam, H.S., O'Reilly, S. and Mousivand, F., 2019. Late Cretaceous subduction-related magmatism on the southern edge of Sabzevar basin, NE Iran. Journal of the Geological Society, 176(3), pp.530-552.

Kazmi, A.H. and Qasim Jan, M., 1997. Geology and Tectonics of Pakistan; Graphic Publishers: Karachi, Pakistan, xiv, 554 p.

Keshtgar, S., Bagheri, S., Boomeri, M., 2019. Tectonic setting of Mahirud Volcano-plutonic complex: different insight into the geodynamic history of East Iran. Scientific Quarterly Journal of Geosciences, 113, 131–144 (in Persian with an English abstract).

Khalatbari Jafari, M., Babaie, H.A., and Moslempour, M.E., 2016, Mid-ocean-ridge to suprasubduction geochemical transition in the hypabyssal and extrusive sequences of major Upper Cretaceous ophiolites of Iran, in Sorkhabi, R., ed., Tectonic Evolution, Collision, and Seismicity of Southwest Asia: In Honor of Manuel Berberian's Forty-Five Years of Research Contributions: Geological Society of America Special Paper 525, p. 229–289, doi:10.1130/2016.2525(07).

Khalatbari-Jafari, M., Juteau, T., Bellon, H. and Emami, H., 2003. Discovery of two ophiolite complexes of different ages in the Khoy area (NW Iran). Comptes Rendus Geoscience, 335(12), pp.917-929. https://doi.org/10.22071/gsj.2013.53594 (in Persian with English abstract)

Khalatbari Jafari, M., Mirzaie, M., Jannessary, M.R., 2013. Study of the Ophiolitic Plutonic Crustal Sequence of Garagoli- Bagjar, North East Sabzevar. Scientific Quarterly Journal of Geosciences, Vol.23, No.89.

Khain, V.Ye., Bogdanov, N.A., (eds.) 2005. International Tectonic Map of the Caspian Sea Region, Scale 1:2 500 000 Explanatory Notes. 129+11p.

Khalili, K., Torabi, G. and Arai, S., 2016. Metamorphism of peridotites from Posht-e-Badam Paleozoic ophiolite (Yazd Province, Central Iran). Neues Jahrbuch für Geologie und Paläontologie-Abhandlungen, pp.59-77.

Khan, M.A., Siddiqui, R.H. and Jan, M.Q., 2010, Temporal evolution of Cretaceous to Pleistocene magmatism in the Chagai Arc, Balochistan, Pakistan, in Leech, M.L., and others, eds., Proceedings for the 25th Himalaya-Karakoram-Tibet Workshop: U.S. Geological Survey, Open-File Report 2010-1099, 2 p. http://pubs.usgs.gov/of/2010/1099/khan/].

Konon, A., Nadimi, A., Koprianiuk, M., Wysocka, A., Szaniawski, R., Wyglądała, M., Słaby, E., Beygi, S. and Barski, M., 2016. Formation of intracontinental basins in the opposite corners of the Tabas block as coeval structures controlled by transpressional faulting, Iran. Bulletin, 128(11-12), pp.1593-1617.

Koshnaw, R.I., Stockli, D.F. and Schlunegger, F., 2019. Timing of the Arabia-Eurasia continental collision—Evidence from detrital zircon U-Pb geochronology of the Red Bed Series strata of the northwest Zagros hinterland, Kurdistan region of Iraq. Geology, 47(1): 47-50.

Kravchinsky, V.A., Cogné, J.-P., Harbert, W.P. and Kuzmin, M.I. 2002. Evolution of the Mongol-Okhotsk Ocean as constrained by new palaeomagnetic data from the Mongol-Okhotsk suture zone, Siberia. Geophysical Journal International, 148, 34-57.

Kurzawa, T., Bröcker, M., Rad, G.F., Berndt, J. and Lisker, F., 2017. Cretaceous high-pressure metamorphism and low pressure overprint in the Sistan Suture Zone, eastern Iran:

Additional temperature estimates for eclogites, geological significance of U-Pb zircon ages and Rb-Sr constraints on the timing of exhumation. Journal of Asian Earth Sciences, 147, pp.332-344.

Lakhan, N., Singh, A.K., Singh, B.P., Sen, K., Singh, M.R., Khogenkumar, S., Singhal, S. and Oinam, G. 2020. Zircon U–Pb geochronology, mineral and whole-rock geochemistry of the Khardung volcanics, Ladakh Himalaya, India: Implications for Late Cretaceous to Palaeogene continental arc magmatism. Geological Journal, 55, 3297-3320.

Lam, P.S., 2002. Geology, geochronology, and thermochronology, of the Alam Kuh Area, Central Alborz Mountains, Northern Iran (Doctoral dissertation, University of California, Los Angeles).

Lasemi, Y., Ghomashi, M., Amin-Rasouli, H, Kheradmand A., 2008. The Lower Triassic Sorkh Shale Formation of the Tabas block, east central Iran: Succession of a failed-rift basin at the paleotethys margin. Carbonates Evaporites 23, 21–38 (2008). https://doi.org/10.1007/BF03176249

Lawrence, R.D., Yeats, R.S., Khan, S.H., Farah, A. and DeJong, K.A., 1981. Thrust and strike slip fault interaction along the Chaman transform zone, Pakistan. Geological Society, London, Special Publications, 9(1), pp.363-370.

Lei, Y., Chu, Y., Allen, M.B., Lin, W., Wan, B., Chen, L., Talebian, M., Xin, G., Liu, T. and Guo, Y., 2025. Restoring the missing Late Cretaceous arc of Iran. Geochemistry, Geophysics, Geosystems, 26, e2025GC012657.

Leloup, P.H., Lacassin, R., Tapponnier, P., Schärer, U., Zhong, D., Liu, X., Zhang, L., Ji, S. and Trinh, P.T., 1995. The Ailao Shan-Red river shear zone (Yunnan, China), tertiary transform boundary of Indochina. Tectonophysics, 251(1-4): 3-84.

Lensch, G. and Davoudzadeh, M., 1982. Ophiolites in Iran. Neues Jahrbuch für Geologie und Paläontologie-Monatshefte, pp.306-320.

Li, Z., Ding, L., Lippert, P.C., Song, P., Yue, Y. and van Hinsbergen, D.J.J. 2016. Paleomagnetic constraints on the Mesozoic drift of the Lhasa terrane (Tibet) from Gondwana to Eurasia. Geology, 44, 727-730, https://doi.org/10.1130/g38030.1.

Li, S., Advokaat, E.L., van Hinsbergen, D.J.J., Koymans, M., Deng, C. and Zhu, R., 2017. Paleomagnetic constraints on the Mesozoic-Cenozoic paleolatitudinal and rotational history of Indochina and South China: Review and updated kinematic reconstruction. Earth-Science Reviews, 171: 58-77.

Lindenberg, H.G., Görler, K., Jacobshagen, V. and Ibbeken, H., 1984. Postpaleozoic stratigraphy, structure and orogenetic evolution of the southern Sabzewar zone and the Taknar block (Khorassan, NE Iran). Neues Jahrbuch für Geologie und Paläontologie-Abhandlungen, pp.287-326.

Lybéris, N. and Manby, G., 1999. Oblique to orthogonal convergence across the Turan block in the post-Miocene. AAPG bulletin, 83(7), pp.1135-1160.

Lybéris, N., Manby, G., Poli, J.T., Kalougin, V., Yousouphocaev, H. and Ashirov, T., 1998. Post-Triassic evolution of the southern margin of the Turan plate. Comptes Rendus de l'Académie des Sciences-Series IIA-Earth and Planetary Science, 326(2), pp.137-143.

Madanipour, S., Ehlers, T.A., Yassaghi, A. and Enkelmann, E., 2017. Accelerated middle Miocene exhumation of the Talesh Mountains constrained by U-Th/He thermochronometry: Evidence for the Arabia-Eurasia collision in the NW Iranian Plateau. Tectonics, 36(8), pp.1538-1561.

Madanipour, S., Ehlers, T.A., Yassaghi, A., Rezaeian, M., Enkelmann, E. and Bahroudi, A., 2013. Synchronous deformation on orogenic plateau margins: Insights from the Arabia–Eurasia collision. Tectonophysics, 608, pp.440-451.

Madanipour, S., Yassaghi, A., Ehlers, T.A. and Enkelmann, E., 2018. Tectonostratigraphy, structural geometry and kinematics of the NW Iranian Plateau margin: insights from the Talesh Mountains, Iran. American Journal of Science, 318(2), pp.208-245.

Maffione, M., van Hinsbergen, D.J., de Gelder, G.I., van der Goes, F.C. and Morris, A., 2017. Kinematics of Late Cretaceous subduction initiation in the Neo-Tethys Ocean reconstructed from ophiolites of Turkey, Cyprus, and Syria. Journal of Geophysical Research: Solid Earth, 122(5), pp.3953-3976.

Mahdavi, A., Karimpour, M.H., Mao, J., Shahri, M.R.H., Shafaroudi, A.M. and Li, H., 2016. Zircon U–Pb geochronology, Hf isotopes and geochemistry of intrusive rocks in the Gazu

copper deposit, Iran: Petrogenesis and geological implications. Ore Geology Reviews, 72, pp.818-837.

Mahmood, K., Boudier, F., Gnos, E., Monie, P. and Nicolas, A., 1995. 40Ar/39Ar dating of the emplacement of the Muslim Bagh ophiolite, Pakistan, Tectonophysics, 250, 169–181.

Mahmoudi, S., Masoudi, F., Corfu, F. and Mehrabi, B., 2010. Magmatic and metamorphic history of the Deh-Salm metamorphic Complex, Eastern Lut block, (Eastern Iran), from U–Pb geochronology. International Journal of Earth Sciences, 99(6), pp.1153-1165.

Malekpour-Alemdari, A., 2017. Regional Tectonic and Structural Significance of Late Cretaceous-Cenozoic Extension in Iran. New Mexico Institute of Mining and Technology. PhD Thesis. ix+157 p.

Martin, C.R., Jagoutz, O., Upadhyay, R., Royden, L.H., Eddy, M.P., Bailey, E., Nichols, C.I. and Weiss, B.P. 2020. Paleocene latitude of the Kohistan–Ladakh arc indicates multistage India–Eurasia collision. Proceedings of the National Academy of Sciences, 117, 29487-29494.

Martin, C., Van Buer, N., Matchette-Downes, H., Mueller, P., Cruz-Uribe, A., van Tongeren, J., Hanchar, J., Upadhyay, R. and Jagoutz, O. 2025. The geology of the Shyok suture zone: evidence for Cretaceous extension of the southern Eurasian margin and Eocene India–Eurasia collision. The Geological Society of London, jgs2024-2082.

Mattei, M., Cifelli, F., Alimohammadian, H., Rashid, H., Winkler, A. and Sagnotti, L., 2017. Oroclinal bending in the Alborz Mountains (Northern Iran): New constraints on the age of South Caspian subduction and extrusion tectonics. Gondwana Research, 42, pp.13-28.

Mattei, M., Cifelli, F., Muttoni, G. and Rashid, H., 2015. Post-Cimmerian (Jurassic–Cenozoic) paleogeography and vertical axis tectonic rotations of Central Iran and the Alborz Mountains. Journal of Asian Earth Sciences, 102, pp.92-101.

Mattei, M., Cifelli, F., Muttoni, G., Zanchi, A., Berra, F., Mossavvari, F. and Eshraghi, S.A., 2012. Neogene block rotation in central Iran: Evidence from paleomagnetic data. Bulletin, 124(5-6), pp.943-956.

Mattei, M., Muttoni, G. and Cifelli, F., 2014. A record of the Jurassic massive plate shift from the Garedu Formation of central Iran. Geology, 42(6), pp.555-558.

Mattei, M., Visconti, A.L., Cifelli, F., Nozaem, R., Winkler, A. and Sagnotti, L., 2019. Clockwise paleomagnetic rotations in northeastern Iran: Major implications on recent geodynamic evolution of outer sectors of the Arabia-Eurasia collision zone. Gondwana Research, 71, pp.194-209.

Mazhari, S.A. and Safari, M., 2013. High-K calc-alkaline plutonism in Zouzan, NE of Lut block, Eastern Iran: an evidence for arc related magmatism in Cenozoic. Journal of the Geological Society of India, 81(5), pp.698-708.

McCall, G.J., 2002. A summary of the geology of the Iranian Makran. Geological Society, London, Special Publications, 195(1), pp.147-204.

McCall, G.J.H. and Kidd, R.G.W., 1982. The Makran, Southeastern Iran: the anatomy of a convergent plate margin active from Cretaceous to Present. Geological Society, London, Special Publications, 10(1), pp.387-397.

McCann, T., Chalot-Prat, F. and Saintot, A., 2010. The Early Mesozoic evolution of the Western Greater Caucasus (Russia): Triassic–Jurassic sedimentary and magmatic history. Geological Society, London, Special Publications, 340(1): 181.

McCormick, G.R., 1989. Geology of the Baluchistan (Pakistan) Portion of the Southern Margin of the Tethys Sea. In Şengör A.M.C. (ed) Tectonic Evolution of the Tethyan Region. NATO ASI Series (Series C: Mathematical and Physical Sciences), vol 259, 277-288 Springer, Dordrecht

McQuarrie, N. and van Hinsbergen, D.J., 2013. Retrodeforming the Arabia-Eurasia collision zone: Age of collision versus magnitude of continental subduction. Geology, 41(3), pp.315-318.

Meyer, B., Mouthereau, F., Lacombe, O. and Agard, P., 2006. Evidence of Quaternary activity along the Deshir Fault: implication for the Tertiary tectonics of Central Iran. Geophysical Journal International, 164(1), pp.192-201.

Mirnejad, H., Lalonde, A.E., Obeid, M. and Hassanzadeh, J., 2013. Geochemistry and petrogenesis of Mashhad granitoids: An insight into the geodynamic history of the Paleo-Tethys in northeast of Iran. Lithos, 170, pp.105-116.

Mohajjel, M., 2009. Thin-skinned deformation near Shahdad, southeast Iran. Journal of Asian Earth Sciences, 36(2-3), pp.146-155.

Mollai, H., Dabiri, R., Torshizian, H.A., Pe-Piper, G. and Wang, W., 2019. Cadomian crust of Eastern Iran: evidence from the Tapeh Tagh granitic gneisses. International Geology Review, pp.1-21.

Mollai, H., Dabiri, R., Torshizian, H.A., Pe-Piper, G. and Wang, W.E., 2021. Upper Neoproterozoic garnet-bearing granites in the Zeber-Kuh region from east central Iran micro plate: Implications for the magmatic evolution in the northern margin of Gondwanaland. Geologica Carpathica, 72(6), pp.461-81.

Monfaredi, B., Hauzenberger, C., Neubauer, F., Schulz, B., Genser, J., Shakerardakani, F. and Halama, R., 2020. Deciphering the Jurassic–Cretaceous evolution of the Hamadan metamorphic complex during Neo-Tethys subduction, western Iran. International Journal of Earth Sciences, 109, pp.2135-2168.

Monsef, I., Monsef, R., Mata, J., Zhang, Z., Pirouz, M., Rezaeian, M., Esmaeili, R. and Xiao, W., 2018. Evidence for an early-MORB to fore-arc evolution within the Zagros suture zone: Constraints from zircon U-Pb geochronology and geochemistry of the Neyriz ophiolite (South Iran). Gondwana Research, 62, pp.287-305.

Montenat, C., Blaise, J., Bordet, P., Debon, F., Deutsch, S., Le Fort, P. and Sonet, J., 1981. Metamorphisme et plutonisme au Paleozoique ancien en domaine Gondwan. La marge nord-ouest des Montanes centrales d'Afghanistan. Bulletin de la Société Géologique de France, 7(1), pp.101-110.

Montenat, C., 2009. The mesozoic of Afghanistan. GeoArabia, 14(1), pp.147-210.

Morley, C.K., Kongwung, B., Julapour, A.A., Abdolghafourian, M., Hajian, M., Waples, D., Warren, J., Otterdoom, H., Srisuriyon, K. and Kazemi, H., 2009. Structural development of a major late Cenozoic basin and transpressional belt in central Iran: The Central Basin in the Qom-Saveh area. Geosphere, 5(4), pp.325-362.

Moslempour, M.E., Khalatbari-Jafari, M., Dabiri, R. and Shahdadi, S., 2012. Constraints on the Petrogenesis of Nosrat-Abad Ophiolite Extrusives, SE Iran. Iranian Journal of Earth Sciences, 4(2), pp.125-133.

Moussavi-Harami, R. and Brenner, R.L., 1992. Geohistory analysis and petroleum reservoir characteristics of Lower Cretaceous (Neocomian) sandstones, eastern Kopet-Dagh Basin, northeastern Iran. AAPG bulletin, 76(8), pp.1200-1208.

Mouthereau, F., 2011. Timing of uplift in the Zagros belt/Iranian plateau and accommodation of late Cenozoic Arabia–Eurasia convergence. Geological Magazine, 148(5-6): 726-738.

Müller, R.D., Cannon, J., Qin, X., Watson, R.J., Gurnis, M., Williams, S., Pfaffelmoser, T., Seton, M., Russell, S.H. and Zahirovic, S., 2018. GPlates: building a virtual Earth through deep time. Geochemistry, Geophysics, Geosystems, 19(7): 2243-2261.

Murphy, M.A., Yin, A., Harrison, T.M., Dürr, S.B., Z, C., Ryerson, F.J., Kidd, W.S.F., X, W. and X, Z. 1997. Did the Indo-Asian collision alone create the Tibetan plateau? Geology, 25, https://doi.org/10.1130/0091-7613(1997)025<0719:Dtiaca>2.3.Co;2.

Muttoni, G., Mattei, M., Balini, M., Zanchi, A., Gaetani, M. and Berra, F., 2009. The drift history of Iran from the Ordovician to the Triassic. Geological Society, London, Special Publications, 312(1): 7-29.

Nadimi, A., 2007. Evolution of the Central Iranian basement. Gondwana Research, 12(3), pp.324-333.

Nasrabady, M., Rossetti, F., Theye, T. and Vignaroli, G., 2011. Metamorphic history and geodynamic significance of the Early Cretaceous Sabzevar granulites (Sabzevar structural zone, NE Iran). Solid Earth, 2(2), pp.219-243.

Natal'in, B.A. and Şengör, A.M.C., 2005. Late Palaeozoic to Triassic evolution of the Turan and Scythian platforms: the pre-history of the Palaeo-Tethyan closure. Tectonophysics, 404(3-4), pp.175-202.

Negredo, A.M., Replumaz, A., Villaseñor, A. and Guillot, S. 2007. Modeling the evolution of continental subduction processes in the Pamir–Hindu Kush region. Earth and Planetary Science Letters, 259, 212-225, https://doi.org/10.1016/j.epsl.2007.04.043.

Nikogosian, I.K., Bracco Gartner, A.J., Mason, P.R., van Hinsbergen, D.J.J., Kuiper, K.F., Kirscher, U., Matveev, S., Grigoryan, A., Grigoryan, E. and Israyelyan, A. 2023. The South

Armenian Block: Gondwanan origin and Tethyan evolution in space and time. Gondwana Research, 121, 168-195.

Ninkabou, D., Agard, P., Nielsen, C., Smit, J., Gorini, C., Rodriguez, M., Haq, B., Chamot-Rooke, N., Weidle, C. and Ducassou, C., 2021. Structure of the offshore obducted Oman margin: emplacement of Semail ophiolite and role of tectonic inheritance. Journal of Geophysical Research: Solid Earth, 126(2), p.2020JB020187.

Nosouhian, N., Torabi, G. and Arai, S., 2019. Petrological aspects of the Bayazeh Paleozoic ophiolite (Central Iran); implications for Paleo-Tethys subduction. Periodico di Mineralogia, 88(2), pp.155-184.

Nouri, F., Davoudian, A.R., Allen, M.B., Azizi, H., Asahara, Y., Anma, R., Shabanian, N., Tsuboi, M. and Khodami, M., 2021. Early Cambrian highly fractionated granite, Central Iran: Evidence for drifting of northern Gondwana and the evolution of the Proto-Tethys Ocean. Precambrian Research, 362, p.106291.

Nouri, F., Davoudian, A.R., Shabanian, N., Allen, M.B., Asahara, Y., Azizi, H., Anma, R., Khodami, M. and Tsuboi, M., 2022. Tectonic transition from Ediacaran continental arc to early Cambrian rift in the NE Ardakan region, central Iran: Constraints from geochronology and geochemistry of magmatic rocks. Journal of Asian Earth Sciences, 224, p.105011.

Nutman, A.P., Mohajjel, M., Bennett, V.C. and Fergusson, C.L., 2014. Gondwanan Eoarchean–Neoproterozoic ancient crustal material in Iran and Turkey: zircon U–Pb–Hf isotopic evidence. Canadian Journal of Earth Sciences, 51(3), pp.272-285.

Ohnenstetter, M., 1983. The role of possible transverse faults in the development of the Sabzevar ophiolites, North-East Iran, with special reference to magma chamber tectonics. Sciences Géologiques, bulletins et mémoires, 36(1), pp.73-90.

Omrani, H., Moazzen, M. and Oberhänsli, R., 2018. Geodynamic evolution of the Sabzevar zone, northern central Iranian micro-continent. Mineralogy and Petrology, 112, pp.65-83.

Omrani, H., Moazzen, M., Oberhänsli, R., Altenberger, U. and Lange, M., 2013. The Sabzevar blueschists of the North-Central Iranian micro-continent as remnants of the Neo-Tethys-related oceanic crust subduction. International Journal of Earth Sciences, 102, pp.1491-1512.

Ozsvárt, P., Bahramnejad, E., Bagheri, S. and Sharifi, M., 2020. New Albian (Cretaceous) radiolarian age constraints for the Dumak ophiolitic mélange from the Shuru area, Eastern Iran. Cretaceous Research, 111, p.104451.

Pang, K.N., Chung, S.L., Zarrinkoub, M.H., Khatib, M.M., Mohammadi, S.S., Chiu, H.Y., Chu, C.H., Lee, H.Y. and Lo, C.H., 2013. Eocene–Oligocene post-collisional magmatism in the Lut–Sistan region, eastern Iran: Magma genesis and tectonic implications. Lithos, 180, pp.234-251.

Pang, K.N., Chung, S.L., Zarrinkoub, M.H., Mohammadi, S.S., Yang, H.M., Chu, C.H., Lee, H.Y. and Lo, C.H., 2012. Age, geochemical characteristics and petrogenesis of Late Cenozoic intraplate alkali basalts in the Lut–Sistan region, eastern Iran. Chemical Geology, 306, pp.40-53.

Parlak, O., Hock,V., Kozlu, H., and Delaloye, M., 2004. Oceanic crust generation in an island arc tectonic setting, SE Anatolian orogenic belt (Turkey), Geol. Mag., 141(5), 583–603, doi:10.1017/S0016756804009458

Pashkov, B.R. and Shvol'man, V.A., 1979. Riftogenic margins of Tethys in the Pamir. Geotektonika, 6, pp.42-57.

Pastor-Galán, D., López-Carmona, A., Rezaeian, M., Tsujimori, T., Gutiérrez-Alonso, G., Yi, K. and Langereis, C., 2025. From Rheic to Paleotethys: Subduction history of the Shanderman Eclogites (NW Iran). Geological Society of America Bulletin. https://doi.org/10.1130/B38187.1

Perelló, J., Razique, A. and Schloderer, J., 2008. The Chagai porphyry copper belt, Baluchistan province, Pakistan. Economic Geology, 103(8), pp.1583-1612.

Peyret, M., Djamour, Y., Hessami, K., Regard, V., Bellier, O., Vernant, P., Daignieres, M., Nankali, H., Van Gorp, S., Goudarzi, M. and Chery, J., 2009. Present-day strain distribution across the Minab-Zendan-Palami fault system from dense GPS transects. Geophysical Journal International, 179(2), pp.751-762.

Pezzo, G., Tolomei, C., Atzori, S., Salvi, S., Shabanian, E., Bellier, O. and Farbod, Y., 2012. New kinematic constraints of the western Doruneh fault, northeastern Iran, from interseismic deformation analysis. Geophysical Journal International, 190(1), pp.622-628.

Pirnia, T., Saccani, E., Torabi, G., Chiari, M., Goričan, Š. and Barbero, E., 2020. Cretaceous tectonic evolution of the Neo-Tethys in Central Iran: Evidence from petrology and age of the Nain-Ashin ophiolitic basalts. Geoscience Frontiers, 11(1), pp.57-81.

Popkov, V.I., 1992. Tektonika Zapada Turanskoy Plity. IGiRGI, Moscow.

Rachidnejad-Omran, N., Emami, M.H., Sabzehei, M., Rastad, E., Bellon, H. and Pique, A., 2002. Lithostratigraphy and Palaeozoic to Palaeocene history of some metamorphic complexes from Muteh area, Sanandaj-Sirjan zone (southern Iran). Comptes Rendus Geoscience, 334(16), pp.1185-1191.

Rahimpour-Bonab, H., Shariatinia, Z. and Siemann, M.G., 2007. Role of rifting in evaporite deposition in the Great Kavir Basin, central Iran. Geological Society, London, Special Publications, 285(1), pp.69-85.

Rahmani, F., Noghreyan, M. and Khalili, M., 2007. Geochemistry of sheeted dikes in the Nain ophiolite (Central Iran). Ofioliti, 32(2), pp.119-129.

Rahmati-Ilkhchi, M., Faryad, S.W., Holub, F.V., Košler, J. and Frank, W., 2011. Magmatic and metamorphic evolution of the Shotur Kuh metamorphic complex (Central Iran). International Journal of Earth Sciences, 100, pp.45-62.

Ramezani, J. and Tucker, R.D., 2003. The Saghand region, central Iran: U-Pb geochronology, petrogenesis and implications for Gondwana tectonics. American journal of science, 303(7), pp.622-665.

Ranjbar Moghadam, F., Masoudi, F., Corfu, F. and Homam, S.M., 2018. Ordovician mafic magmatism in an Ediacaran arc complex, Sibak, northeastern Iran: the eastern tip of the Rheic Ocean. Canadian Journal of Earth Sciences, 55(10), pp.1173-1182.

Ranjbar Moghadam, F., Masoudi, F., Homam, M. and Mohajel, M., 2019. Petrophabric and Microtectonic studies of the metamorphic rocks in southeast of Fariman in order to reconstruct the metamorphism evolution. Researches in Earth Sciences, 10(3), pp.108-123. 10.52547/esrj.10.3.108

Rashid, H., 2016. Cenozoic tectonic evolution and paleomagnetic rotation in Iran. Ph. D. Thesis. Universita' Degli Studi "Roma Tre". IX+103+22pp. Available at: https://arcadia.sba.uniroma3.it/handle/2307/5968 (Accessed: 27 December 2025).

Rashidi, A., Abbassi, M.R., Nilfouroushan, F., Shafiei, S., Derakhshani, R. and Nemati, M., 2020. Morphotectonic and earthquake data analysis of interactional faults in Sabzevaran Area, SE Iran. Journal of Structural Geology, 139, p.104147.

Regard, V., Bellier, O., Thomas, J.C., Bourlès, D., Bonnet, S., Abbassi, M.R., Braucher, R., Mercier, J., Shabanian, E., Soleymani, S. and Feghhi, K., 2005. Cumulative right-lateral fault slip rate across the Zagros—Makran transfer zone: role of the Minab—Zendan fault system in accommodating Arabia—Eurasia convergence in southeast Iran. Geophysical Journal International, 162(1), pp.177-203.

Rezaei, Z., Noghreyan, M. and Saccani, E., 2018. Petrology and geochemistry of sheeted dykes and pillow lavas from the Sabzevar Ophiolitic Mélange (Northeast Iran): new Constraints for the Late Cretaceous evolution of the Neo-Tethys Oceanic Basin between the Central Iranian Microcontinent and Eurasia. Ofioliti, 43(2), pp.147-172.

Rezaei, L., Timmerman, M.J., Altenberger, U., Moazzen, M., Wilke, F.D., Günter, C., Sudo, M. and Sláma, J., 2021, April. Ediacaran to Toarcian evolution of the Gasht Metamorphic Complex, Alborz Mountains, N Iran. In EGU General Assembly Conference Abstracts (pp. EGU21-9755).

Rezaeian, M., Carter, A., Hovius, N. and Allen, M.B., 2012. Cenozoic exhumation history of the Alborz Mountains, Iran: New constraints from low-temperature chronometry. Tectonics, 31(2).

Rezaeian, M., Kuijper, C.B., van der Boon, A., Pastor-Galán, D., Cotton, L.J., Langereis, C.G. and Krijgsman, W., 2020. Post-Eocene coupled oroclines in the Talesh (NW Iran): Paleomagnetic constraints. Tectonophysics, 786, p.228459.

Rioux, M., Bowring, S. A., Kelemen, P. B., Gordon, S., Miller, R., Dudás, F., 2013. Tectonic development of the Samail ophiolite: High-precision U-Pb zircon geochronology and Sm-Nd isotopic constraints on crustal growth and emplacement. Journal of Geophysical Research: Solid Earth, 118(5), 2085–2101. https://doi.org/10.1002/jgrb.50139

Ruh, J.B., Valero, L., Aghajari, L., Beamud, E. and Gharabeigli, G., 2019. Vertical-axis rotation in East Kopet Dagh, NE Iran, inferred from paleomagnetic data: oroclinal bending or complex local folding kinematics?. Swiss Journal of Geosciences, 112(2), pp.543-562.

Robert, A.M., Letouzey, J., Kavoosi, M.A., Sherkati, S., Müller, C., Vergés, J. and Aghababaei, A., 2014. Structural evolution of the Kopeh Dagh fold-and-thrust belt (NE Iran) and interactions with the South Caspian Sea Basin and Amu Darya Basin. Marine and Petroleum Geology, 57, pp.68-87.

Robertson, A., 1987. The transition from a passive margin to an Upper Cretaceous foreland basin related to ophiolite emplacement in the Oman Mountains. Geological Society of America Bulletin, 99(5), pp.633-653.

Robinson, A.C., 2015. Collaborative Research: Investigating Mesozoic Deformation in the Pamir: Implications for Crustal Thickening in the Pamir and the Evolution of the Tibetan Orogen. NSF Award Number 1450899. Directorate for Geosciences, 14(1450899), p.50899.

Robinson, J., Beck, R., Gnos, E. and Vincent, R.K. 2000. New structural and stratigraphic insights for northwestern Pakistan from field and Landsat Thematic Mapper data. Geological Society of America Bulletin, 112, 364-374, https://doi.org/10.1130/0016-7606(2000)112<364:Nsasif>2.0.Co;2.

Rojhani, E., Ghaemi, F., Bagheri, S., Li, S., Lom, N. and van Hinsbergen, D.J.J. 2026. Geology of the abrupt northern termination of the Sistan Suture Zone and the subduction zone configuration in eastern Iran since the late Cretaceous. Journal of Asian Earth Sciences, in press.

Rolland, Y. 2002. From intra-oceanic convergence to post-collisionnal evolution: the India-Asia convergence in NW Himalaya, from Cretaceous to present. Journal of the Virtual Explorer, 08, https://doi.org/10.3809/jvirtex.2002.00052.

Rossetti, F., Monié, P., Nasrabady, M., Theye, T., Lucci, F. and Saadat, M., 2017. Early Carboniferous subduction-zone metamorphism preserved within the Palaeo-Tethyan Rasht ophiolites (western Alborz, Iran). Journal of the Geological Society, 174(4), pp.741-758.

Rossetti, F., Nasrabady, M., Vignaroli, G., Theye, T., Gerdes, A., Razavi, M.H. and Vaziri, H.M., 2010. Early Cretaceous migmatitic mafic granulites from the Sabzevar range (NE Iran): implications for the closure of the Mesozoic peri-Tethyan oceans in central Iran. Terra Nova, 22(1), pp.26-34.

Rossetti, F., Nozaem, R., Lucci, F., Vignaroli, G., Gerdes, A., Nasrabadi, M. and Theye, T., 2015. Tectonic setting and geochronology of the Cadomian (Ediacaran-Cambrian) magmatism in central Iran, Kuh-e-Sarhangi region (NW Lut Block). Journal of Asian Earth Sciences, 102, pp.24-44.

Ruh, J.B., Valero, L., Aghajari, L., Beamud, E. and Gharabeigli, G., 2019. Vertical-axis rotation in East Kopet Dagh, NE Iran, inferred from paleomagnetic data: oroclinal bending or complex local folding kinematics?. Swiss Journal of Geosciences, 112(2), pp.543-562.

Ruttner, A.W., 1984. The pre-Liassic basement of the eastern Kopet Dagh Range. Neues Jahrbuch für Geologie und Paläontologie-Abhandlungen, pp.256-268.

Ruttner, A.W., 1993. Southern borderland of Triassic Laurasia in north-east Iran. Geologische Rundschau, 82, pp.110-120.

Ruttner A.W., Ruttner-Kolisko, A.E., 1972. Some Data on the Hydrology of the Tabas-Shirgest-Ozbak-kuh Area (East Iran). Jahrb. Geol. B.-A., Bd. 115, pp. 1-48

Ruttner, A.W., Brandner, R. and Kirchner, E., 1991. Geology of the Aghdarband area (Kopet Dagh, NE-Iran). Abhandlungen der Geologischen Bundesanstalt, 38, pp.7-79.

Saadat, S., Karimpour, M.H. and Stern, C., 2010. Petrochemical characteristics of Neogene and Quaternary alkali olivine basalts from the Western Margin of the Lut Block, Eastern Iran. Iranian Journal of Earth Sciences, 2(2), pp.87-106.

Saccani, E., Delavari, M., Beccaluva, L. and Amini, S., 2010. Petrological and geochemical constraints on the origin of the Nehbandan ophiolitic complex (eastern Iran): Implication for the evolution of the Sistan Ocean. Lithos, 117(1-4), pp.209-228.

Sadegh, H.R., Moeinzadeh, H. and Moazzen, M., 2021. Geochemistry and geochronology of amphibolites from the Sirjan area, Sanandaj-Sirjan zone of Iran: Jurassic metamorphism prior to Arabia and Eurasia collision. Journal of Geodynamics, 143, p.101786.

Safari, H.O., Ghassemi, M.R. and Razavi-Pash, R., 2013. Determination and structural analysis of the Lahijan transverse fault in forestall region of Alborz Mountains, Iran: a geospatial application. International Journal of Remote Sensing Applications, 3(4), p.215-224.

Saintot, A., Brunet, M.-F., Yakovlev, F., Sébrier, M., Stephenson, R., Ershov, A., Chalot-Prat, F. and McCann, T., 2006. The Mesozoic-Cenozoic tectonic evolution of the Greater Caucasus. Geological Society, London, Memoirs, 32(1): 277-289.

Samadi, R., Torabi, G., Dantas, E.L., Morishita, T. and Kawabata, H., 2022. Ordovician crustal thickening and syn-collisional magmatism of Iran: Gondwanan basement along the north of the Yazd Block (Central Iran). International Geology Review, 64(15), pp.2151-2165.

Savostin, L.A., Sibuet, J.C., Zonenshain, L.P., Le Pichon, X. and Roulet, M.J., 1986. Kinematic evolution of the Tethys belt from the Atlantic Ocean to the Pamirs since the Triassic. Tectonophysics, 123(1-4), pp.1-35.

Schoenbohm, L.M., Burchfiel, B.C., Liangzhong, C. and Jiyun, Y. 2006. Miocene to present activity along the Red River fault, China, in the context of continental extrusion, upper-crustal rotation, and lower-crustal flow. Geological Society of America Bulletin, 118, 672-688, https://doi.org/10.1130/b25816.1.

Schreiber, A., Weippert, D., Wittekindt H-P. and Wolfart, R., 1972. Geology and petroleum potentials of central and south Afghanistan. AAPG Bulletin, 56(8), pp.1494-1519.

Schwab, M., Ratschbacher, L., Siebel, W., McWilliams, M., Minaev, V., Lutkov, V., Chen, F., Stanek, K., Nelson, B., Frisch, W. and Wooden, J.L. 2004. Assembly of the Pamirs: Age and origin of magmatic belts from the southern Tien Shan to the southern Pamirs and their relation to Tibet. Tectonics, 23, https://doi.org/10.1029/2003tc001583.

Searle, M. and Cox, J., 1999. Tectonic setting, origin, and obduction of the Oman ophiolite. Geological Society of America Bulletin, 111(1), pp.104-122.

Şengör, A.C., 1979. Mid-Mesozoic closure of Permo–Triassic Tethys and its implications. Nature, 279, pp.590-593.

Şengör, A.C., 1984. The Cimmeride orogenic system and the tectonics of Eurasia. Geological Society of America Special Paper, 195, p.82.

Şengör, A.M.C., 1987. Tectonics of the Tethysides: orogenic collage development in a collisional setting. Annual Review of Earth and Planetary Sciences, 15(1), pp.213-244.

Şengör, A.M.C., 1990a. A new model for the late Palaeozoic—Mesozoic tectonic evolution of Iran and implications for Oman. Geological Society, London, Special Publications, 49(1), pp.797-831.

Şengör, A.M.C., 1990b. Plate Tectonics and Orogenic Research after 25 Years: A Tethyan Perspective

Şengör, A.C. and Yılmaz, Y., 1981. Tethyan evolution of Turkey: a plate tectonic approach. Tectonophysics, 75(3-4), pp.181-241.

Şengör, A.M.C., Cin, A., Rowley, D.B. and Shangyou, N., 1991. Magmatic evolution of the Tethysides: a guide to reconstruction of collage history. Palaeogeography, Palaeoclimatology, Palaeoecology, 87(1-4), pp.411-440.

Şengör, A.M.C., Altıner, D., Cin, A., Ustaömer, T. and Hsü, K.J., 1988. Origin and assembly of the Tethyside orogenic collage at the expense of Gondwana Land. Geological Society, London, Special Publications, 37(1), pp.119-181.

Şengör, A.C., Lom, N., Sunal, G., Zabcı, C. and Sancar, T., 2019. The phanerozoic palaeotectonics of Turkey. Part I: an inventory. Mediterranean Geoscience Reviews, 1, pp.91-161.

Şengör, A.M.C., Tüysüz, O., İmren, C., Sakınç, M., Eyidoğan, H., Görür, N., Le Pichon, X. and Rangin, C., 2005. The North Anatolian Fault: A New Look. Annual Review of Earth and Planetary Sciences, 33(1): 37-112. https://doi.org/10.1146/annurev.earth.32.101802.120415.

Şengör, A.M.C., Yılmaz, Y. and Sungurlu, O., 1984. Tectonics of the Mediterranean Cimmerides: nature and evolution of the western termination of Palaeo-Tethys. Geological Society, London, Special Publications, 17(1), pp.77-112.

Sepahi, A.A., Salami, S., Lentz, D., McFarlane, C. and Maanijou, M., 2018. Petrography, geochemistry, and U–Pb geochronology of pegmatites and aplites associated with the Alvand intrusive complex in the Hamedan region, Sanandaj–Sirjan zone, Zagros orogen (Iran). International Journal of Earth Sciences, 107, pp.1059-1096.

Sepidbar, F., Shafaii Moghadam, H., Li, C., Stern, R.J., Jiantang, P. and Vesali, Y., 2020. Cadomian magmatic rocks from zarand (SE Iran) formed in a retro-arc basin. Lithos, 366, p.105569.

Seton, M., Müller, R.D., Zahirovic, S., Gaina, C., Torsvik, T., Shephard, G., Talsma, A., Gurnis, M., Turner, M., Maus, S. and Chandler, M., 2012. Global continental and ocean basin reconstructions since 200 Ma. Earth-Science Reviews, 113(3-4), pp.212-270.

Shabanian, E., Siame, L., Bellier, O., Benedetti, L. and Abbassi, M.R., 2009. Quaternary slip rates along the northeastern boundary of the Arabia-Eurasia collision zone (Kopeh Dagh Mountains, Northeast Iran). Geophysical Journal International, 178(2), pp.1055-1077.

Shafaii Moghadam, H. and Stern, R.J., 2011. Geodynamic evolution of Upper Cretaceous Zagros ophiolites: formation of oceanic lithosphere above a nascent subduction zone. Geological Magazine, 148(5-6): 762-801.

Shafaii Moghadam, H. and Stern, R.J., 2014. Ophiolites of Iran: Keys to understanding the tectonic evolution of SW Asia:(I) Paleozoic ophiolites. Journal of Asian Earth Sciences, 91, pp.19-38.

Shafaii Moghadam, H. and Stern, R.J., 2015. Ophiolites of Iran: Keys to understanding the tectonic evolution of SW Asia:(II) Mesozoic ophiolites. Journal of Asian Earth Sciences, 100, pp.31-59.

Shafaii Moghadam, H., Bröcker, M., Griffin, W.L., Li, X.H., Chen, R.X. and O'Reilly, S.Y., 2017. Subduction, high-P metamorphism, and collision fingerprints in South Iran: Constraints from zircon U-Pb and mica Rb-Sr geochronology. Geochemistry, Geophysics, Geosystems, 18(1), pp.306-332.

Shafaii Moghadam, H., Corfu, F., Chiaradia, M., Stern, R.J. and Ghorbani, G., 2014. Sabzevar Ophiolite, NE Iran: Progress from embryonic oceanic lithosphere into magmatic arc constrained by new isotopic and geochemical data. Lithos, 210, pp.224-241.

Shafaii Moghadam, H., Corfu, F., Stern, R.J. and Bakhsh, A.L., 2019. The Eastern Khoy metamorphic complex of NW Iran: a Jurassic ophiolite or continuation of the Sanandaj–Sirjan Zone?. Journal of the Geological Society, 176(3), pp.517-529.

Shafaii Moghadam, H., Li, X.H., Santos, J.F., Stern, R.J., Griffin, W.L., Ghorbani, G. and Sarebani, N., 2017. Neoproterozoic magmatic flare-up along the N. margin of Gondwana: The Taknar complex, NE Iran. Earth and Planetary Science Letters, 474, pp.83-96.

Shafaii Moghadam, H., Li, X.H., Ling, X.X., Stern, R.J., Santos, J.F., Meinhold, G., Ghorbani, G. and Shahabi, S., 2015. Petrogenesis and tectonic implications of Late Carboniferous A-type granites and gabbronorites in NW Iran: Geochronological and geocoemical constraints. Lithos, 212, pp.266-279.

Shafaii Moghadam, H., Stern, R.J. and Rahgoshay, M., 2010. The Dehshir ophiolite (central Iran): Geochemical constraints on the origin and evolution of the Inner Zagros ophiolite belt. Bulletin, 122(9-10), pp.1516-1547.

Shafaii Moghadam, H., Stern, R.J., Chiaradia, M. and Rahgoshay, M., 2013. Geochemistry and tectonic evolution of the Late Cretaceous Gogher–Baft ophiolite, central Iran. Lithos, 168, pp.33-47.

Shafaii Moghadam, H., Whitechurch, H., Rahgoshay, M. and Monsef, I., 2009. Significance of Nain-Baft ophiolitic belt (Iran): Short-lived, transtensional Cretaceous back-arc oceanic basins over the Tethyan subduction zone. Comptes Rendus Geoscience, 341(12), pp.1016-1028.

Shafiei Bafti, S. and Mohajjel, M., 2015. Structural evidence for slip partitioning and inclined dextral transpression along the SE Sanandaj–Sirjan zone, Iran. International Journal of Earth Sciences, 104, pp.587-601.

Shahabpour, J., 2010. Tectonic implications of the geochemical data from the Makran igneous rocks in Iran. Island Arc 19 (4), 676–689.

Shahbazi, H., Siebel, W., Pourmoafee, M., Ghorbani, M., Sepahi, A.A., Shang, C.K. and Abedini, M.V., 2010. Geochemistry and U–Pb zircon geochronology of the Alvand plutonic complex in Sanandaj–Sirjan Zone (Iran): New evidence for Jurassic magmatism. Journal of Asian earth sciences, 39(6), pp.668-683.

Shakerardakani, F., Neubauer, F., Bernroider, M., Von Quadt, A., Peytcheva, I., Liu, X., Genser, J., Monfaredi, B. and Masoudi, F., 2017. Geochemical and isotopic evidence for

Carboniferous rifting: mafic dykes in the central Sanandaj-Sirjan zone (Dorud-Azna, West Iran). Geologica Carpathica, 68(3), pp.229-247.

Shakerardakani, F., Neubauer, F., Liu, X., Dong, Y., Monfaredi, B., and Li, X., 2021. New detrital zircon U–Pb insights on the palaeogeographic origin of the central Sanandaj–Sirjan zone, Iran. Geological Magazine, 158(12), 2165-2186. doi:10.1017/S0016756821000728

Shakerardakani, F., Neubauer, F., Masoudi, F., Mehrabi, B., Liu, X., Dong, Y., Mohajjel, M., Monfaredi, B. and Friedl, G., 2015. Panafrican basement and Mesozoic gabbro in the Zagros orogenic belt in the Dorud–Azna region (NW Iran): laser-ablation ICP–MS zircon ages and geochemistry. Tectonophysics, 647, pp.146-171.

Sheikholeslami, M.R., 2015. Deformations of Palaeozoic and Mesozoic rocks in southern Sirjan, Sanandaj–Sirjan Zone, Iran. Journal of Asian Earth Sciences, 106, pp.130-149.

Sheikholeslami, M.R., 2016. Tectono-stratigraphic evidence for the opening and closure of the Neo-Tethys Ocean in the southern Sanandaj-Sirjan zone, Iran. Geological Society of America Special Papers, 525, pp.SPE525-09.

Sheikholeslami, M.R. and Kouhpeyma, M., 2012. Structural analysis and tectonic evolution of the eastern Binalud Mountains, NE Iran. Journal of Geodynamics, 61, pp.23-46.

Shirdashtzadeh, N., Torabi, G. and Schaefer, B., 2018. A magmatic record of Neoproterozoic to Paleozoic convergence between Gondwana and Laurasia in the northwest margin of the Central-East Iranian Microcontinent. Journal of Asian Earth Sciences, 166, pp.35-47.

Shnizai, Z. 2020. Mapping of active and presumed active faults in Afghanistan by interpretation of 1-arcsecond SRTM anaglyph images. *Journal of Seismology*, **24**, 1131-1157.

Shojaat, B., Hassanipak, A.A., Mobasher, K. and Ghazi, A.M., 2003. Petrology, geochemistry and tectonics of the Sabzevar ophiolite, North Central Iran. Journal of Asian Earth Sciences, 21(9), pp.1053-1067.

Siddiqui, N.K., 2012. A prospective Neoproterozoic-Cambrian hydrocarbon/exploration play in the Kirthar Fold Belt, Pakistan. Geological Society, London, Special Publications, 366(1), pp.123-130.

Siehl, A., 2017. Structural setting and evolution of the Afghan orogenic segment–a review. Geological Society, London, Special Publications, 427(1), pp.57-88.

Soffel, H.C., Schmidt, S., Davoudzadeh, M. and Rolf, C., 1996. New palaeomagnetic data from Central Iran and a Triassic palaeoreconstruction. *Geologische Rundschau*, *85*, pp.293-302.

Soffel, H.C. and Förster, H.G., 1984. Polar wander path of the Central-East-Iran Microplate including new results. Neues Jahrbuch für Geologie und Paläontologie-Abhandlungen, pp.165-172.

Soleimani, M., Faghih, A. and Kusky, T., 2021. Mesozoic compressional to extensional tectonics in the Central East Iranian Microcontinent: evidence from the Boneh Shurow metamorphic core complexM. Soleimani et al. Compressional to extensional tectonics in the CEIM. Journal of the Geological Society, 178(6).

Song, P., Ding, L., Zhang, L., Cai, F., Zhang, Q., Li, Z., Wang, H., Jafari, M.K. and Talebian, M., 2023. Paleomagnetism From Central Iran Reveals Arabia-Eurasia Collision Onset at the Eocene/Oligocene Boundary. Geophysical Research Letters, 50(12), p.e2023GL103858.

Song, P., Ding, L., Li, Z., Lippert, P.C. and Yue, Y. 2017. An early bird from Gondwana: Paleomagnetism of Lower Permian lavas from northern Qiangtang (Tibet) and the geography of the Paleo-Tethys. Earth and Planetary Science Letters, 475, 119-133, https://doi.org/10.1016/j.epsl.2017.07.023.

Stampfli, G.M., 2000. Tethyan oceans. Geological Society, London, Special Publications, 173 (1), pp.1-23.

Stampfli, G.M. and Borel, G.D., 2002. A plate tectonic model for the Paleozoic and Mesozoic constrained by dynamic plate boundaries and restored synthetic oceanic isochrons. Earth and Planetary Science Letters, 196(1-2), pp.17-33.

Stern, R.J., Moghadam, H.S., Pirouz, M. and Mooney, W. 2021. The geodynamic evolution of Iran. Annual Review of Earth and Planetary Sciences, 49, 9-36.

Stöcklin, J., 1968. Structural history and tectonics of Iran: a review. AAPG bulletin, 52(7), pp.1229-1258.

Stöcklin, J., 1974a. Possible ancient continental margins in Iran. In: Burk, C. A. & Drake, C. L. (eds) *The Geology of Continental Margins*. Springer-Verlag, Berlin, 873-887.

Stöcklin, J., 1974b. Northern Iran: Alborz mountains. In: Spencer, A. (Ed.), Mesozoic–Cenozoic orogenic belts: data for orogenic studies. Geological Society Special Publication 4, pp. 213–234.

Stöcklin, J., 1977. Structural correlation of the Alpine ranges between Iran and Central Asia. In: Livra à la Mémoire de Albert F. de Lapparent. Mémoire hors-série 8, Société Géologique de France, 333-353.

Stöcklin, J., 1989. Tethys Evolution in the Afghanistan-Pamir-Pakistan Region. In Şengör A.M.C. (ed) Tectonic Evolution of the Tethyan Region. NATO ASI Series (Series C: Mathematical and Physical Sciences), vol 259. Springer, Dordrecht. https://doi.org/10.1007/978-94-009-2253-2_13

Tadayon, M., Rossetti, F., Zattin, M., Calzolari, G., Nozaem, R., Salvini, F., Faccenna, C. and Khodabakhshi, P., 2019. The long-term evolution of the Doruneh Fault region (Central Iran): A key to understanding the spatio-temporal tectonic evolution in the hinterland of the Zagros convergence zone. Geological Journal, 54(3), pp.1454-1479.

Taheri, J., Fürsich, F.T. and Wilmsen, M., 2009. Stratigraphy, depositional environments and geodynamic significance of the Upper Bajocian–Bathonian Kashafrud Formation, E Iran. Geological Society, London, Special Publications, 312(1), pp.205-218.

Takin, M., 1972. Iranian geology and continental drift in the Middle East. Nature, 235, pp.147-150.

Tapponnier, P., Mattauer, M., Proust, F. and Cassaigneau, C. 1981. Mesozoic ophiolites, sutures, and large-scale tectonic movements in Afghanistan. Earth and Planetary Science Letters, 52, 355-71.

Tapponnier, P., Peltzer, G., Le Dain, A.Y., Armijo, R. and Cobbold, P., 1982. Propagating extrusion tectonics in Asia: New insights from simple experiments with plasticine. Geology, 10(12).

Taraz, H., Golshani, F., Nakazawa, K., Shimizu, D., Bando, Y., Ishii, K.I., Murata, M., Okimura, Y., Sakagami, S., Nakamura, K. and Tokuoka, T., 1981. The Permian and the Lower Triassic systems in Abadeh region, central Iran. Memoirs of the Faculty of Science, Kyoto University. Series of geology and mineralogy, 47(2), p.61-133.

Tchalenko, J.S., 1975. Seismicity and structure of the Kopet Dagh (Iran, USSR). Philosophical Transactions of the Royal Society of London. Series A, Mathematical and Physical Sciences, 278(1275), pp.1-28.

Termier, H. and Termier, G., 1974. Distribution des faunes marines dans le Sud de la Téthys et sur la bordure septentrionale du Gondwana au cours du Paléozoïque supérieur. Annales de la Société géologique de Belgique.

Tillman, J.E., Poosti, A., Rossello, S. and Eckert, A., 1981. Structural evolution of Sanandaj-Sirjan Ranges near Esfahan, Iran. AAPG Bulletin, 65(4), pp.674-687.

Tirrul, R., Griffis, R. J., and Camp, V. E., 1980, Geology of the Zabol Quadrangle, 1.250,000: Report submitted to the Geological and Mineral Survey of Iran, 180 p.

Tirrul, R., Bell, I.R., Griffis, R.J. and Camp, V.E., 1983. The Sistan suture zone of eastern Iran. Geological Society of America Bulletin, 94(1), pp.134-150.

Torsvik, T.H. and Cocks, L.R.M., 2017. Earth history and palaeogeography. Cambridge University Press. 317p.

Treloar, P.J. and Izatt, C.N., 1993. Tectonics of the Himalayan collision between the Indian plate and the Afghan block: A synthesis. Geological Society, London, Special Publications, 74(1), pp.69-87.

Treloar, P.J., Petterson, M.G., Jan, M.Q. and Sullivan, M. 1996. A re-evaluation of the stratigraphy and evolution of the Kohistan arc sequence, Pakistan Himalaya: implications for magmatic and tectonic arc-building processes. Journal of the Geological Society, 153, 681-693.

Ul-Hadi, S., Khan, S.D., Owen, L.A., Khan, A.S., Hedrick, K.A. and Caffee, M.W., 2013. Slip-rates along the Chaman fault: Implication for transient strain accumulation and strain partitioning along the western Indian plate margin. Tectonophysics, 608, pp.389-400.

Ulmishek, G.F., 2004. Petroleum geology and resources of the Amu-Darya basin, Turkmenistan, Uzbekistan, Afghanistan, and Iran (Vol. 2201). Iran: US Department of the Interior, US Geological Survey. vi+32 p.

Vaes, B., van Hinsbergen, D.J.J., van de Lagemaat, S.H.A., van der Wiel, E., Lom, N., Advokaat, E., Boschman, L.M., Gallo, L.C., Greve, A., Guilmette, C., Li, S., Lippert, P.C., Montheil, L.,

Qayyum, A. and Langereis, C.G. 2023. A global apparent polar wander path for the last 320 Ma calculated from site-level paleomagnetic data. Earth-Science Reviews, 245, 104547.

VahdatiRad, M., Vahidinia, M. and Sadeghi, A., 2016. Early Eocene planktonic and benthic foraminifera from the Khangiran formation (northeast of Iran). Arabian Journal of Geosciences, 9, pp.1-13.

Van der Boon, A., van Hinsbergen, D.J.J., Rezaeian, M., Gürer, D., Honarmand, M., Pastor-Galán, D., Krijgsman, W. and Langereis, C.G., 2018. Quantifying Arabia–Eurasia convergence accommodated in the Greater Caucasus by paleomagnetic reconstruction. Earth and Planetary Science Letters, 482, pp.454-469.

van der Boon, A., Kuiper, K., Villa, G., Renema, W., Meijers, M., Langereis, C., Aliyeva, E. and Krijgsman, W., 2017. Onset of Maikop sedimentation and cessation of Eocene arc volcanism in the Talysh Mountains, Azerbaijan. Geological Society, London, Special Publications, 428(1): 145-169.

Van der Meer, D.G., Van Hinsbergen, D.J.J. and Spakman, W., 2018. Atlas of the underworld: Slab remnants in the mantle, their sinking history, and a new outlook on lower mantle viscosity. Tectonophysics, 723, pp.309-448.

Van der Voo, R., 1993. The Tethys blocks. In Paleomagnetism of the Atlantic, Tethys and Iapetus Oceans (pp. 143-228). Cambridge: Cambridge University Press. doi:10.1017/CBO9780511524936.008

Van der Voo, R., van Hinsbergen, D.J.J., Domeier, M., Spakman, W. and Torsvik, T.H. 2015. Latest Jurassic–earliest Cretaceous closure of the Mongol-Okhotsk Ocean: A paleomagnetic and seismological-tomographic analysis Late Jurassic Margin of Laurasia–A Record of Faulting Accommodating Plate Rotation. Geological Society of America Special Papers, 513, 589-606, https://doi.org/10.1130/2015.2513(19).

van Hinsbergen, D.J.J. and Schmid, S.M., 2012. Map view restoration of Aegean-West Anatolian accretion and extension since the Eocene. Tectonics, 31(5): n/a-n/a.

Van Hinsbergen, D.J. and Schouten, T.L., 2021. Deciphering paleogeography from orogenic architecture: constructing orogens in a future supercontinent as thought experiment. American Journal of Science, 321(6), pp.955-1031.

van Hinsbergen, D.J.J., Kapp, P., Dupont-Nivet, G., Lippert, P.C., DeCelles, P.G. and Torsvik, T.H. 2011. Restoration of Cenozoic deformation in Asia and the size of Greater India. Tectonics, 30, https://doi.org/10.1029/2011tc002908.

van Hinsbergen, D.J.J., Lippert, P.C., Li, S., Huang, W., Advokaat, E.L. and Spakman, W., 2019. Reconstructing Greater India: Paleogeographic, kinematic, and geodynamic perspectives. Tectonophysics, 760: 69-94.

van Hinsbergen, D.J., Steinberger, B., Guilmette, C., Maffione, M., Gürer, D., Peters, K., Plunder, A., McPhee, P.J., Gaina, C., Advokaat, E.L. and Vissers, R.L., 2021. A record of plume-induced plate rotation triggering subduction initiation. Nature Geoscience, 14(8), pp.626-630.

van Hinsbergen, D.J.J., Torsvik, T., Schmid, S.M., Matenco, L., Maffione, M., Vissers, R.L.M., Gürer, D. and Spakman, W., 2020. Orogenic architecture of the Mediterranean region and kinematic reconstruction of its tectonic evolution since the Triassic. Gondwana Research, 81: 79-229.

van Hinsbergen, D.J.J., Gürer, D., Koç, A. and Lom, N. 2024. Shortening and extrusion in the East Anatolian Plateau: How was Neogene Arabia-Eurasia convergence tectonically accommodated? Earth and Planetary Science Letters, 641, 118827.

van Hinsbergen, D.J., Granot, R., Vaes, B. and Vissers, R.L.M. 2025. Tectonic mode switches in the Pyrenees caused by Africa-Eurasia rotation pole drift. *Nature Geoscience*, in review; preprint at https://doi.org/10.21203/rs.3.rs-8017726/v1.

Vaziri, H., 2001. The Triassic Nakhlak Group, an exotic succession in central Iran. Proceedings, pp, 53, p.68.

Verdel, C., Wernicke, B.P., Hassanzadeh, J. and Guest, B., 2011. A Paleogene extensional arc flare-up in Iran. Tectonics, 30(3).

Vernant, P., Nilforoushan, F., Chery, J., Bayer, R., Djamour, Y., Masson, F., Nankali, H., Ritz, J.F., Sedighi, M. and Tavakoli, F., 2004a. Deciphering oblique shortening of central Alborz in Iran using geodetic data. Earth and planetary science letters, 223(1-2), pp.177-185.

Vernant, P., Nilforoushan, F., Hatzfeld, D., Abbassi, M.R., Vigny, C., Masson, F., Nankali, H., Martinod, J., Ashtiani, A., Bayer, R. and Tavakoli, F., 2004b. Present-day crustal deformation

and plate kinematics in the Middle East constrained by GPS measurements in Iran and northern Oman. Geophysical Journal International, 157(1), pp.381-398.

Vincent, S.J., Allen, M.B., Ismail-Zadeh, A.D., Flecker, R., Foland, K.A. and Simmons, M.D., 2005. Insights from the Talysh of Azerbaijan into the Paleogene evolution of the South Caspian region. Geological Society of America Bulletin, 117(11-12), pp.1513-1533.

Walker, F. and Allen, M.B., 2012. Offset rivers, drainage spacing and the record of strike-slip faulting: The Kuh Banan Fault, Iran. Tectonophysics, 530, pp.251-263.

Walker, R. and Jackson, J., 2002. Offset and evolution of the Gowk fault, SE Iran: a major intra-continental strike-slip system. Journal of structural Geology, 24(11), pp.1677-1698.

Walker, R. and Jackson, J., 2004. Active tectonics and late Cenozoic strain distribution in central and eastern Iran. Tectonics, 23(5).

Walker, R.T., Bezmenov, Y., Begenjev, G., Carolin, S., Dodds, N., Gruetzner, C., Jackson, J.A., Mirzin, R., Mousavi, Z. and Rhodes, E.J., 2021. Slip-rate on the Main Köpetdag (Kopeh Dagh) strike-slip fault, Turkmenistan, and the active tectonics of the South Caspian. Tectonics, 40(8), p.e2021TC006846.

Walker, R.T., Gans, P., Allen, M.B., Jackson, J., Khatib, M., Marsh, N. and Zarrinkoub, M., 2009. Late Cenozoic volcanism and rates of active faulting in eastern Iran. Geophysical Journal International, 177(2), pp.783-805.

Wang, S., Tang, W., Liu, Y., Liu, X. and Yao, X. 2020. Rushan-Pshart Paleo-Tethyan suture deduced from geochronological, geochemical, and Sr-Nd-Hf isotopic characteristics of granitoids in Pamir. Lithos, 364, 105549.

Walpersdorf, A., Manighetti, I., Mousavi, Z., Tavakoli, F., Vergnolle, M., Jadidi, A., Hatzfeld, D., Aghamohammadi, A., Bigot, A., Djamour, Y. and Nankali, H., 2014. Present-day kinematics and fault slip rates in eastern Iran, derived from 11 years of GPS data. Journal of Geophysical Research: Solid Earth, 119(2), pp.1359-1383.

Wellman, H. W., 1966. Active wrench faults of Iran, Afghanistan and Pakistan." Geologische Rundschau 55, no. 3, 716-735.

Wensink, H., 1982. Tectonic inferences of paleomagnetic data from some Mesozoic formations in Central Iran. Journal of Geophysics, 51(1), pp.12-23.

Wensink, H. and Varekamp, J.C., 1980. Paleomagnetism of basalts from Alborz: Iran part of Asia in the Cretaceous. Tectonophysics, 68(1-2), pp.113-129.

Wensink, H., Zijderveld, J.D.A. and Varekamp, J.C., 1978. Paleomagnetism and ore mineralogy of some basalts of the Geirud Formation of Late Devonian-Early Carboniferous age from the southern Alborz, Iran. Earth and Planetary Science Letters, 41(4), pp.441-450.

Whitney, J.W., 2006. Geology, water, and wind in the lower Helmand Basin, southern Afghanistan: U.S. Geological Survey Scientific Investigations Report 2006–5182, 40 p.

Whitney, D.L., Delph, J.R., Thomson, S.N., Beck, S.L., Brocard, G.Y., Cosca, M.A., Darin, M.H., Kaymakcı, N., Meijers, M.J. and Okay, A.I. 2023. Breaking plates: Creation of the East Anatolian fault, the Anatolian plate, and a tectonic escape system. Geology 51, 673-677.

Whitney, D.L., Bezada, M., Hansen, L.N., Teyssier, C., Wada, I. and Zhou, X. 2025. Escape tectonics. Tectonophysics, 231029.

Wilmsen, M., Fürsich, F.T. and Majidifard, M.R., 2013. The Shah Kuh Formation, a latest Barremian–Early Aptian carbonate platform of Central Iran (Khur area, Yazd Block). Cretaceous Research, 39, pp.183-194.

Wilmsen, M., Fürsich, F.T. and Seyed-Emami, K., 2003. Revised lithostratigraphy of the Middle and Upper Jurassic Magu Group of the northern Tabas Block, east-central Iran. Newsletters on Stratigraphy, pp.143-156.

Wilmsen, M., Fürsich, F.T. and Majidifard, M.R., 2015. An overview of the Cretaceous stratigraphy and facies development of the Yazd Block, western Central Iran. Journal of Asian Earth Sciences, 102, pp.73-91.

Wilmsen, M., Fürsich, F.T., Seyed-Emami, K. and Majidifard, M.R., 2009. An overview of the stratigraphy and facies development of the Jurassic System on the Tabas Block, east-central Iran. Geological Society, London, Special Publications, 312(1), pp.323-343.

Wittekindt, H. and Weippert, D., 1973.Geological Map of Central and Southern Afghanistan. 1:500.000. Geological Survey of the Federal Republic of Germany.

Wittekindt H.P., Wolfart K. and Moores E.M.,1997. Afghanistan. In: Encyclopedia of European and Asian Regional Geology. Encyclopedia of Earth Science. Springer, Dordrecht. https://doi.org/10.1007/1-4020-4495-X_1

Wolfart, R. and Wittekindt, H., 1980. Geologie von Afghanistan: Gebrüder Borntraeger, Berlin and Stuttgart, p.167.

Woodward, N.B., Boyer, S.E. and Suppe, J., 1989. Balanced geological cross-sections. American Geophysical Union, Short Courses in Geology, 6, p.132.

Wu, L., Kravchinsky, V.A., Gu, Y.J. and Potter, D.K. 2017. Absolute reconstruction of the closing of the Mongol-Okhotsk Ocean in the Mesozoic elucidates the genesis of the slab geometry underneath Eurasia. Journal of Geophysical Research: Solid Earth, 122, 4831-4851.

Xu, S., Li, Y.-X., van Hinsbergen, D.J., Liu, X., Li, B., Li, X. and Wang, T. 2025. An asymmetric Late Cretaceous back-arc basin south of Tibet? Geology, 53, 392-397.

Yarahmadzahi, H., Ernst, A. and Gorgij, M.N., 2012. Fistulipora Microparallela (Yang and Lu, 1962) from Lower Permian Bryozoans of Lut Block, Central Iran. Iranian Journal of Earth Sciences, 4(2), pp.120-124.

Yeats, R., 2012. Active faults of the world. Cambridge University Press. xii+621 p.

Yin, A., 2010. Cenozoic tectonic evolution of Asia: A preliminary synthesis. Tectonophysics, 488(1-4), pp.293-325.

Yogibekov, D., Sang, M., Xiao, W., Mamadjonov, Y., Zhou, C., Yang, H., Mao, Q., Aminov, J., Khalimov, G. and Ashuraliev, S. 2023. Post-collisional magmatism associated with the final closure of the Rushan-Pshart Meso-Tethys Ocean in Pamir, Tajikistan: Inference from Cretaceous igneous rocks of the Pshart accretionary complex. Frontiers in Earth Science, 10, 1090952.

Zanchetta, S., Berra, F., Zanchi, A., Bergomi, M., Caridroit, M., Nicora, A. and Heidarzadeh, G., 2013. The record of the Late Palaeozoic active margin of the Palaeo-Tethys in NE Iran: constraints on the Cimmerian orogeny. Gondwana Research, 24(3-4), pp.1237-1266.

Zanchetta, S., Zanchi, A., Villa, I., Poli, S. and Muttoni, G., 2009. The Shanderman eclogites: a Late Carboniferous high-pressure event in the NW Talesh Mountains (NW Iran). Geological Society, London, Special Publications, 312(1), pp.57-78.

Zanchi, A., Zanchetta, S., Balini, M. and Ghassemi, M.R., 2016. Oblique convergence during the Cimmerian collision: evidence from the Triassic Aghdarband Basin, NE Iran. Gondwana Research, 38, pp.149-170.

Zanchi, A., Zanchetta, S., Berra, F., Mattei, M., Garzanti, E., Molyneux, S., Nawab, A. and Sabouri, J., 2009a. The Eo-Cimmerian (Late? Triassic) orogeny in North Iran. Geological Society, London, Special Publications, 312(1), pp.31-55.

Zanchi, A., Zanchetta, S., Garzanti, E., Balini, M., Berra, F., Mattei, M. and Muttoni, G., 2009b. The Cimmerian evolution of the Nakhlak–Anarak area, Central Iran, and its bearing for the reconstruction of the history of the Eurasian margin. Geological Society, London, Special Publications, 312(1), pp.261-286.

Zarrinkoub, M.H., Chung, S.L., Chiu, H.Y., Mohammadi, S., Khatib, M., Lin, I.J., 2010. Zircon U–Pb age and geochemical constraints from the northern Sistan suture zone on the Neotethyan magmatic and tectonic evolution in eastern Iran. Abst. to GSA Conference on “Tectonic Crossroads: Evolving Orogens in Eurasia–Africa–Arabia”, Oct. 4–8, 2010, Ankara, Turkey.

Zarrinkoub, M.H., Pang, K.N., Chung, S.L., Khatib, M.M., Mohammadi, S.S., Chiu, H.Y. and Lee, H.Y., 2012. Zircon U–Pb age and geochemical constraints on the origin of the Birjand ophiolite, Sistan suture zone, eastern Iran. Lithos, 154, pp.392-405.

Zhao, L., Nissen, E., Xu, W., Jamalreyhani, M., Bergman, E.A., Zhao, D. and Xie, L. 2025. Variable fault geometry controls the cascading 2023 Herat, Afghanistan multiplet sequence. Communications Earth & Environment, 6, 135.

Zonenshain, L.P. and Pichon, X., 1986. Deep basins of the Black Sea and Caspian Sea as remnants of Mesozoic back-arc basins. Tectonophysics, 123(1-4), pp.181-211.

Authors' CVs.

Nalan Lom (PhD, Istanbul Technical University, 2017) is Assistant Professor of Earth and Environmental Sciences, University of Central Asia, Tajikistan, where she taught since 2025. Lom is a geologist with a background in geophysics whose research focuses on the large-scale evolution of orogenic systems and the plate-kinematic reconstruction of ancient tectonic domains. Her work integrates paleomagnetism, stratigraphy, mantle tomography, and field geology to understand the deformation and dynamics of convergent margins from Precambrian to Cenozoic.

Douwe van Hinsbergen (PhD, Utrecht University, 2004) is Professor of Global Tectonics and Paleogeography at Utrecht University, the Netherlands, where he has taught since 2012. Van Hinsbergen studies global plate tectonics, orogenesis, and paleogeography across the globe, and closely collaborates with scholars of geodynamics, paleoclimate, and (paleo)biology to advance understanding in the drivers of geological processes, particularly of crustal deformation and paleogeographic change, and their co-evolution with climate and life.

Figure Captions

Figure 1: Simplified geological map of the area of interest in Iran, Afghanistan, Pakistan, Turkmenistan, Uzbekistan and Tajikistan.

Figure 2: Tectonic units in Iranian and Afghan segment. 1: South Caspian Basin, 2: Kopet Dagh, 3: Alborz Mountains, 4: Central Basin, 5: Sanandaj-Sirjan Zone, 6-9: Central-East Iranian Microcontinent, 6: Yazd Block, 7: Posht-e Badam Block, 8: Tabas Block, 9: Lut Block, 10: Band-e Turkestan, 11-12: Farah-Rud Block, 13: Waras-Panjao suture, 14: Helmand Block, 15: Kabul Block, 16: Sistan Basin, 17: Chagai Hills-Raskoh Magmatic Arc, 18: Kharan Basin, 19: Sistan suture, 20: Makran Accretionary Complex, 21: Zagros Fold-Thrust Belt, 22: Katawaz Basin, 23: Southern Pamir-Hindu-Kush, 24: North Pamir, 25: Central Pamir, AF: Andarab Fault, AlF: Altimur Fault, AnF: Anar Fault, ArF: Araks Fault, AS: Apsheron Sill Fault, CF: Chaman Fault, ChF: Chapedony Fault, DF: Doruneh Fault, DSF: Dehshir Fault, GaF: Gardez Fault, GoF: Gowk Fault, HF: Herat Fault, HeF: Helmand Fault, HRF: Hari-Rud Fault, JF: Jovain Fault, KF: Kalmard Fault, KBF: Kuh-Banan Fault, MKDF: Main Kopet Dagh Fault, MoF: Moqor Fault, M-ZF: Minab-Zendan Fault, NF: Nayband Fault, O-NF: Ornach-Nal Fault, SF: Sabzevaran Fault, SBF: Shahr-e Babak Fault, SiF: Siahan Fault, WCF: West Caspian Fault, ZF: Zahedan Fault

Figure 3: Generalized stratigraphic columns from the Cimmerian blocks of Iran and Afghanistan. The figure represents a synthesis of published data and interpretations from the literature cited in the manuscript.

Figure 4: Geological map of northeastern Iran and southern Turkmenistan. The map includes the Kopet Dagh in the north, the Sabzevar Suture Zone in the south and easternmost part of the Central Basin in the west. DM: Darrehanjir Mountain, OBO: Oryan-Bardaskan Ophiolite, ShK-BiC: Shotor Kuh-Biarjmand metamorphic core complex, SO: Sabzevar Ophiolite, Ta: Taknar, THO: Torbat-e-Heydarieh Ophiolite

Figure 5: Geological map of the Alborz-Talesh Mountains and western Iran. GC: Gasht Metamorphic Complex, KD: Kura depression, KMO: Khoy-Maku Ophiolite, KO: Kermanshah Ophiolite, PSO: Piranshahr-Serow Ophiolite, Sh: Shanderman Complex, T-V: Talysh–Vandam gravity high.

Figure 6: Geological map of the Central Basin, the Yazd Block, the Posht-e Badam Block, the Sanandaj-Sirjan Zone and Zagros Mountains. Ai: Airekan, AO: Ashin Ophiolite, B-SC: Boneh-Shurow Complex, BaO: Balvard Ophiolite, CC: Chapedony Complex, DM: Daranjir Mountain, DO: Dehshir Ophiolite, Gs: Godar-e-Siah Complex, JC: June Complex, NO: Nain Ophiolite, SBO: Shahr-e Babak Fault, SC: Sarkuh Complex, ShC: Sheikh Chupan granodiorite, ShK-BiC: Shotor Kuh-Biarjmand metamorphic core complex, SK: Shahrekord, Zg: Zarigan Leucogranite

Figure 7: Simplified geological map of the Lut and Tabas blocks and the Sistan suture. AB: Abdoughi Basin, Bag: Bazman Granodiorite, BaO: Balvard Ophiolite, BiO: Birjand Ophiolite, Bjg: Bajestan granitoid, BO: Baft Ophiolite, DS: Deh-Salm Complex, EO: Esfandagheh

Ophiolite, Ggr: Gazu Granodiorite, KaO: Kahnuj Ophiolite, KBR: Kuh-e-Bam Range, MRC: Mahi Rud Complex, NAO: Nostrabad Ophiolite, NO: Nehbandan Ophiolite, QO: Qayen Ophiolite, ShC: SK: Shah-Kuh pluton, SO: Siahjangal Ophiolite, SR: Shotori Range, TB: Tabas Basin, TKO: Tchehel-Kureh Ophiolite, UDMA: Urumieh-Dokhtar Magmatic Arc, ZKg: Zeber-Kuh Granite.

Figure 8: A structural cross-section of South-Central Iran. Redrawn from Afagi et al. (1977). For location see Supplementary Information I.

Figure 9: Geological map of Afghanistan and Pakistan. DT: Dalbandin through, LC: Laghman granitoid complex, NC: Nilaw igneous complex, MuBO: Muslim Bag Ophiolite, RO: Raskoh Ophiolite, WO: Waziristan Ophiolite.

Figure 10: A composite structural cross-section of Central Afghanistan. For location see Fig. 9. The Farah Rud Block is adopted from Blaise et al. (1978) and Girardeau et al. (1989). The Helmand Block is adopted from Siehl (2017) and Abdullah and Chmyriov (2008). The whole section is correlated with Wittekind and Weippert (1973) and Doebrich and Wahl (2006).

Figure 11: Paleomagnetic vector compilation. Data compiled from Wensink et al. (1978), Wensink and Varekamp (1980), Conrad et al. (1981), Wensink (1982), Bazhenov and Burtman (1986), Bina et al. (1986), Bazhenov 1987, Besse (1988), Soffel et al. (1989 (as cited in Mattei et al. 2015); 1996), Mattei et al. (2012, 2014), Cifelli et al (2015), Rashid (2016), van der Boon et al. (2018), Ruh et al. (2019), Rezaeien et al. (2020), Song et al. (2023). See Supplementary Information 2 for details.

Figure 12: Tectonic map of the Central Tethysides used as basis for our kinematic reconstruction. For key to tectonic units, see Fig. 2.

Figure 13: Paleotectonic map of the Central Tethyan region for the late Oligocene (25 Ma). Map is projected in a Europe fixed reference frame. GPlates rotation files are provided in Supplementary Material. For key to tectonic units, see Fig. 2.

Figure 14: Paleotectonic map of the Central Tethyan region for the late Oligocene (40 Ma). Map is projected in a Europe fixed reference frame. GPlates rotation files are provided in Supplementary Material. For key to tectonic units, see Fig. 2.

Figure 15: Paleotectonic map of the Central Tethyan region for the late Oligocene (65 Ma). Map is projected in a Europe fixed reference frame. GPlates rotation files are provided in Supplementary Material. For key to tectonic units, see Fig. 2.

Figure 16: Paleotectonic map of the Central Tethyan region for the late Oligocene (90 Ma). Map is projected in a Europe fixed reference frame. GPlates rotation files are provided in Supplementary Material. For key to tectonic units, see Fig. 2.

Figure 17: Paleotectonic map of the Central Tethyan region for the late Oligocene (140 Ma). Map is projected in a Europe fixed reference frame. GPlates rotation files are provided in Supplementary Material. For key to tectonic units, see Fig. 2.

Figure 18: Paleotectonic maps of the Central Tethysides in context of the wider Tethyan region from the Mediterranean region to the Tibetan region. The focus of our paper is on the central Tethysides - the reconstruction of the Mediterranean region follows van Hinsbergen et al. (2020) and the reconstruction of the Tibetan segment of the Tethys is compiled from various sources (van der Voo et al., 2015; Song et al., 2017; Li et al., 2016; van Hinsbergen et al., 2019; Advokaat and van Hinsbergen, 2024).

Supplementary Information

Supplementary Information 1: Geological map of the region that merges Figures 4,5,6,7 and 9.

Table S1: Paleomagnetic data compilation used to plot paleomagnetic vectors in Figure 11.

Supplementary Information 2: GPlates shape and rotation file of the reconstruction presented in this paper. These consist of a Gplates project file, a rotation file, and a series of shape files (in gpml format).

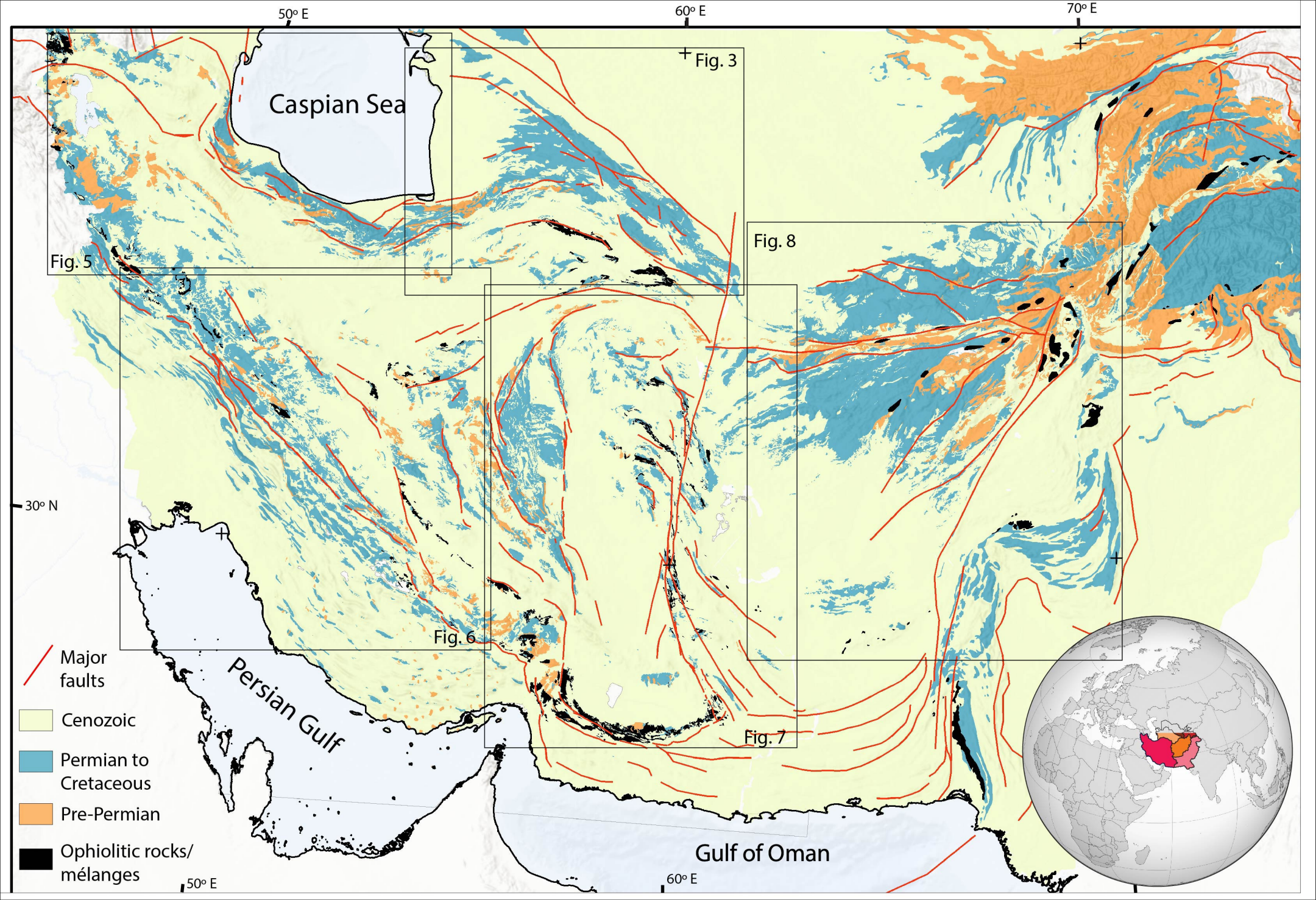
50° E
60° E
70° E
30° N
Caspian Sea
Fig. 3
Fig. 5
Fig. 8
Fig. 6
Fig. 7
Persian Gulf
Gulf of Oman
Major faults
Cenozoic
Permian to Cretaceous
Pre-Permian
Ophiolitic rocks/ mélanges

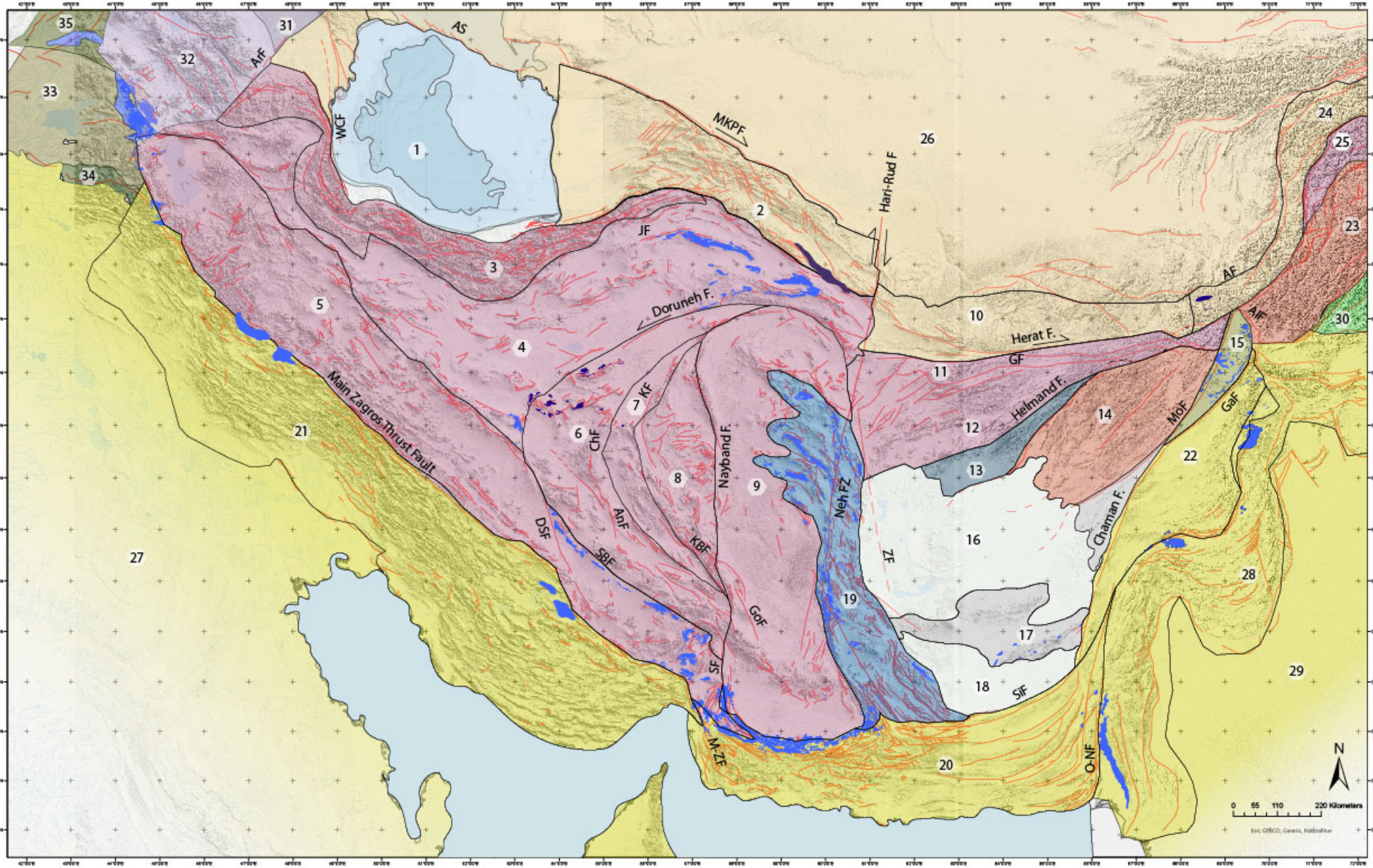
AS
WCF
MKPF
Hari-Rud F
JF
Doruneh F.
Herat F.
AF
AfF
GF
Helmand F.
Main Zagros Thrust Fault
KF
ChF
AnF
KBF
Nayband F.
Neh FZ
ZF
Chaman F.
MöF
GaF
DSF
SBF
GoF
SF
SjF
M-ZF
O-NF
1
2
3
4
5
6
7
8
9
10
11
12
13
14
15
16
17
18
19
20
21
22
23
24
25
26
27
28
29
30
31
32
33
34
35
N
0 55 110 220 Kilometers

AGE (Ma)

PERIOD / EPOCH

- QUATERNARY
- NEOGENE: PLIOCENE, MIOCENE
- PALEOGENE: OLIGOCENE, EOCENE, PALEOCENE
- CRETACEOUS: UPPER, LOWER
- JURASSIC: UPPER, MEDIAL, LOWER
- TRIASSIC: UPPER, MEDIAL, LOWER
- PERMIAN: LOPINGIAN, GUADALUPIAN, CISURALIAN
- CARBONIFEROUS: PENNSYLVANIAN, MISSISSIPPIAN
- DEVONIAN: UPPER, MEDIAL, LOWER
- SILURIAN: PRIDOLI, LUDLOW, WENLOCK, LLANDOVERY
- ORDOVICIAN: UPPER, MEDIAL, LOWER

Kopet Dagh

Alborz Mountains

Sanandaj-Sirjan Zone

Central and East Iranian Microcontinent

Anarak

Yazd

Tabas

Lut

Farah Rud Block

Band-e Bayan Block

Farah Basin

Helmand Block

N

S

215+-15

?

?

?

- sandy silty shale
- quartz sandstone
- marl, shale
- evaporites
- marl, silty limestone
- shale
- coal
- sandstone
- conglomerate
- limestone
- cherty limestone
- shale sandstone siltstone w. ripple marks
- dolomite
- recrystallised limestone, marble
- bauxite
- silty sandstone
- sandy limestone
- basic volcanism
- intermediate volcanism
- mafic magmatism
- acidic magmatism
- volcanoclastics
- schist
- metamorphosed accretionary prism (metacarbonate, metasandstone, marble, phyllite, metavolcanics, quartzite)
- diabase dyke
- fosilliferous strata

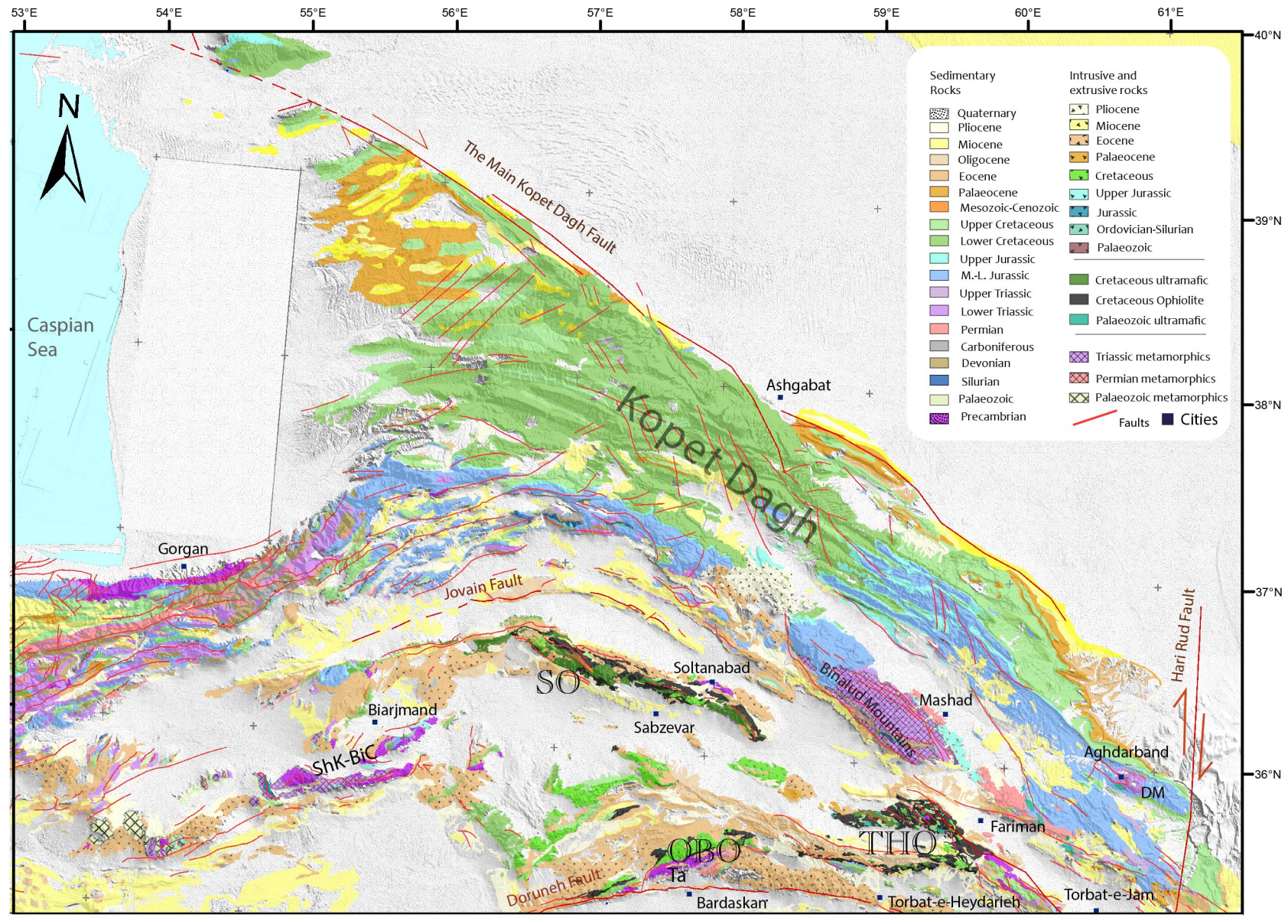
53°E
54°E
55°E
56°E
57°E
58°E
59°E
60°E
61°E
40°N
39°N
38°N
37°N
36°N
N
Caspian Sea
The Main Kopet Dagh Fault
Kopet Dagh
Ashgabat
Gorgan
Jovain Fault
Soltanabad
Binalud Mountains
Mashad
Hari Rud Fault
SO
Biarjmand
Sabzevar
ShK-BiC
Aghdarband
DM
Fariman
THO
OBO
Ta
Doruneh Fault
Bardaskan
Torbat-e-Heydarieh
Torbat-e-Jam
Sedimentary Rocks
Quaternary
Pliocene
Miocene
Oligocene
Eocene
Palaeocene
Mesozoic-Cenozoic
Upper Cretaceous
Lower Cretaceous
Upper Jurassic
M.-L. Jurassic
Upper Triassic
Lower Triassic
Permian
Carboniferous
Devonian
Silurian
Palaeozoic
Precambrian
Intrusive and extrusive rocks
Pliocene
Miocene
Eocene
Palaeocene
Cretaceous
Upper Jurassic
Jurassic
Ordovician-Silurian
Palaeozoic
Cretaceous ultramafic
Cretaceous Ophiolite
Palaeozoic ultramafic
Triassic metamorphics
Permian metamorphics
Palaeozoic metamorphics
Faults
Cities

45°E 46°E 47°E 48°E 49°E 50°E 51°E 52°E 53°E 54°E

40°N 39°N 38°N 37°N 36°N 35°N

KMO

PSO

KO

TZC

ShC

Araks F.

T-V

KD

West Caspian Fault

Talesh Mountains

Sh

GC

Lahijan Fault

Alborz Mountains

South Caspian Basin

Tabriz

Ardabil

Urumieh

Urumieh Lake

Bonab

Takab

Zanjan

Rasht

Gasht

Lahijan

Sanandaj

Qorveh

Karaj

Tehran

Gorgan

N

Sedimentary Rocks

- Quaternary
- Pliocene
- Miocene
- Oligocene
- Eocene
- Palaeocene
- Mesozoic-Cenozoic
- Upper Cretaceous
- Lower Cretaceous
- Jurassic- Cretaceous
- Upper Jurassic
- M.-L. Jurassic
- Upper Triassic
- Lower Triassic
- Permian-Triassic
- Permian
- Carboniferous
- Devonian
- Silurian
- Cambrian
- Palaeozoic
- Precambrian

Intrusive and extrusive rocks

- Pliocene
- Miocene
- Oligocene
- Eocene
- Palaeocene
- Upper Cretaceous
- Lower Cretaceous
- Upper Jurassic
- Jurassic
- Triassic
- Permian
- Carboniferous
- Ordovician-Silurian
- Palaeozoic
- Cretaceous ultramafic
- Cretaceous Ophiolite
- Palaeozoic ultramafic

Metamorphics

- Oligocene
- Eocene
- Palaeocene
- U. Jurassic
- L-M. Jurassic
- Triassic
- Mesozoic
- Permian
- Devonian
- Palaeozoic

Faults

Cities

Sedimentary Rocks

- Quaternary
- Pliocene
- Miocene
- Oligocene
- Eocene
- Palaeocene
- Mesozoic-Cenozoic
- Upper Cretaceous
- Lower Cretaceous
- Jurassic- Cretaceous
- Upper Jurassic
- M.-L. Jurassic
- Upper Triassic
- Lower Triassic
- Permian-Triassic
- Permian
- Carboniferous
- Devonian
- Silurian
- Cambrian
- Palaeozoic
- Precambrian

Metamorphics

- Oligocene
- Eocene
- Palaeocene
- U. Jurassic
- L-M. Jurassic
- Triassic
- Mesozoic
- Permian
- Devonian
- Palaeozoic

Faults — Sistan Suture

Sea — Lake — Cities

Intrusive and extrusive rocks

- Pliocene
- Miocene
- Oligocene
- Eocene
- Palaeocene
- Upper Cretaceous
- Lower Cretaceous
- Upper Jurassic
- Jurassic
- Triassic
- Permian
- Carboniferous
- Ordovician-Silurian
- Palaeozoic
- Cretaceous ultramafic
- Cretaceous Ophiolite
- Palaeozoic ultramafic

Sanandaj
Hamadan
Kermanshah
Urumieh-Dokhtar Magmatic Arc
Sanandaj-Sirjan Zone
Zagros Mountains
Main Zagros Thrust
Garmsar Basin
Qom Basin
Great Kavir Basin
Doruneh Fault
Ai
Jandaq
GS
Nakhlak
AO
Anarak
Nain
NO
Yazd Block
Bayazeh
Posht-e Badam
Kalmard F.
Esmailabad
Chapedony F.
CC
Posht-e-Badam F.
SC
Ardekan
DM
Zg
Yazd
Kuh Banan F.
Dehshir F.
Abadeh
DO
Anar F.
Shahr-e-Babak F.
SBO
Sirjan
BaO
Balvard
Golpaygan
Esfahan
SK
Azna
JC
Dorud
Persian Gulf

36° N
35° N
34° N
33° N
32° N
31° N
30° N
29° N
49° E
50° E
51° E
52° E
53° E
54° E
55° E
56° E

56° E
57° E
58° E
59° E
60° E
61° E
62° E
35° N
34° N
33° N
32° N
31° N
30° N
29° N
28° N
27° N
Doruneh Fault
Doruneh
Kashmar
ZKg
KBR
Bjg
Gonabad
Herat Fault
Boshruyeh
SR
Kalmard Fault
Tabas
TB
Ggr
Qayen
QO
Gazik
Birjand
BiO
Hari Rud Fault
Nayband
Nayband Fault
NO
Sistan Suture
East Neh Fault
MRC
SK
Neh
AB
DS
Sefidabeh
Kuh Banan Fault
Kerman
Dasht-E Lut
West Neh Fault
Sistan Basin
TKO
Gowk Fault
Nostrabad
Kahurak Fault
NAO
Siahan Fault
Zahedan
UDMA
BaO
BO
Nostrabad Fault
SO
Sabzevaran Fault
EO
KaO
Bag
Minab-Zendan Fault
Durkan Complex
Jaz Murian Depression
Iranshahr
Fannuj
Makran Accretionary Complex

Sedimentary Rocks

- Quaternary
- Pliocene
- Miocene
- Oligocene
- Eocene
- Palaeocene
- Mesozoic-Cenozoic
- Upper Cretaceous
- Lower Cretaceous
- Jurassic- Cretaceous
- Upper Jurassic
- M.-L. Jurassic
- Upper Triassic
- Lower Triassic
- Permian-Triassic
- Permian
- Carboniferous
- Devonian
- Silurian
- Cambrian
- Palaeozoic
- Precambrian

Intrusive and extrusive rocks

- Pliocene
- Miocene
- Oligocene
- Eocene
- Palaeocene
- Upper Cretaceous
- Lower Cretaceous
- Upper Jurassic
- Jurassic
- Triassic
- Permian
- Carboniferous
- Ordovician-Silurian
- Palaeozoic
- Cretaceous ultramafic
- Cretaceous Ophiolite
- Palaeozoic ultramafic

Metamorphics

- Oligocene
- Eocene
- Palaeocene
- U. Jurassic
- L-M. Jurassic
- Triassic
- Mesozoic
- Permian
- Devonian
- Palaeozoic

Faults
Sistan Suture
Sea
Lake
Cities


Zagros Ranges
Sanandaj-Sirjan Zone
Nain-Baft Suture Zone
Urumieh Dokhtar Magmatic Arc
Yazd Block
Posht-e Badam Block
Tabas Block
A
A'
Lavar Maidan
Zagros Main thrust
Dehshir Fault
Shahr-e Babak Fault
Anar Fault
Kuh Banan Fault
0
5
10 km
25 km
Central-East Iranian Microcontinent
Q Alluvium, lake deposits, Dasht fans, terraces
QPl Plio-Pleistocene gravels, lake deposits
N Neogene redbeds and conglomerates
EJ Eocene-Oligocene limestone, dolomite
El Eocene limestone
Pgc Paleogene conglomerates
EF Palaeogene flysch
KB Cenomanian carbonate shelf/ platform deposits (Sarvak Fm.)
Ka Aptian-Albian Orbitolina Limestone
K Crushed Cretaceous limestone
KR Radiolarite Group
CM Coloured Melange
u Ultramafics
JK Jurassic-Aptian limestone, dolomite and shale
Js Lower Jurassic Shemshak Fm.
Trk Triassic limestone and dolomite
Undiff. Mesozoic limestone
PK Permian Dolomite/limestone (Khuff Fm.)
MT Precambrian Metamorphics
Precambrian Marbles
a Neogene acidic intrusives
Jurassic-Cretaceous igneous rocks
Q Alluvium, lake deposits, Dasht fans, terraces
QPlc Plio-Pleistocene conglomerates
Plc Pliocene-Neogene conglomerates
Nc Neogene conglomerates
Oc Oligocene conglomerates
EOv Eocene-Oligocene tuffs/ Vc.
Ev Eocene lavas
Evt Eocene tuffs/ Vc.
Ef Eocene flysch
Pgv Palaeocene tuffs/ Vc
Pgc Paleogene conglomerates
Km Maastrictian limestone
K2 Upper Cretaceous
Ka Aptian-Albian Orbitolina Limestone
Kf Cretaceous flysch
KBf Lower Cretaceous shales (Biabanak Fm.)
Kc Lower Cretaceous conglomerates
JKc Upper Jurassic-Cretaceous conglomerates
Jev Jurassic evaporites, salt plugs
JB Upper Jurassic Baghamshah Fm.
JBd Middle Jurassic Badamu limestone
Js Lower Jurassic Shemshak Fm.
TrE Triassic dolomite, limestone (Elika Fm.)
TrS Triassic Dolomite (Shotori Fm.)
TrP Permo- Triassic limestone-/ dolomite
PJ Permian dolomite, limestone (Jamal Fm.)
D Devonian
PZ1 Upper Palaeozoic undiff.
PZ2 Lower Palaeozoic undiff.
PZ Palaeozoic undiff.
€ Lower Cambrian siltstone
Ediacaran-Cambrian volcanics
E€ Ediacaran-Cambrian dolomites, shale, sandstone (Soltanieh and Rizu fm.
Ed Upper Neoproterozoic-Cambrian diapirs
P€M Pre-Cambrian Morad series
b Quaternary-Neogene basalt
Quaternary-Neogene andesite-rhyodacite
d Neogene dacite plug
Neogene intermediate intrusives
Eocene lavas
Jurassic basic igneous
Ediacaran-Cambrian magmatics (Zarigan granite)
Ediacaran-Cambrian diorite
Fault

62°E 63°E 64°E 65°E 66°E 67°E 68°E 69°E 70°E

36°N 35°N 34°N 33°N 32°N 31°N 30°N 29°N

N

Paropamisus Range

Herat

Herat Fault

Band-e Turkestan Mountains

Andarab Fault

Panjshir Fault

Altimur F.

Konar F.

Spin Gawh F.

NC

LC

Kabul

Garghanaw Fault

A

A′

A″

Farah Rud Block

Farah Fault

Helmand Block

Helmand Fault

Tirin Fault

Moqor Fault

Gardez Fault

Katawaz Basin

Sulaiman Ranges

WO

MuBO

Farah

Kandahar

Chaman Fault

Sistan Basin

Chagai Arc

DT

Dalbandin

RO

Raskoh Arc

Sedimentary Rocks

- Quaternary
- Pliocene
- Miocene
- Oligocene
- Eocene
- Palaeocene
- Mesozoic-Cenozoic
- Upper Cretaceous
- Lower Cretaceous
- Jurassic- Cretaceous
- Upper Jurassic
- M.-L. Jurassic
- Upper Triassic
- Lower Triassic
- Permian-Triassic
- Permian
- Carboniferous
- Devonian
- Silurian
- Cambrian
- Palaeozoic
- Precambrian

Intrusive and extrusive rocks

- Pliocene
- Miocene
- Oligocene
- Eocene
- Palaeocene
- Upper Cretaceous
- Lower Cretaceous
- Upper Jurassic
- Jurassic
- Upper Triassic
- Triassic
- Permian
- Carboniferous
- Ordovician-Silurian
- Palaeozoic

Metamorphics

- Oligocene
- Eocene
- Palaeocene
- U. Jurassic
- L-M. Jurassic
- Triassic
- Mesozoic
- Permian
- Devonian
- Palaeozoic

- Cretaceous ultramafic
- Cretaceous Ophiolite
- Palaeozoic ultramafic

- Faults
- Cities

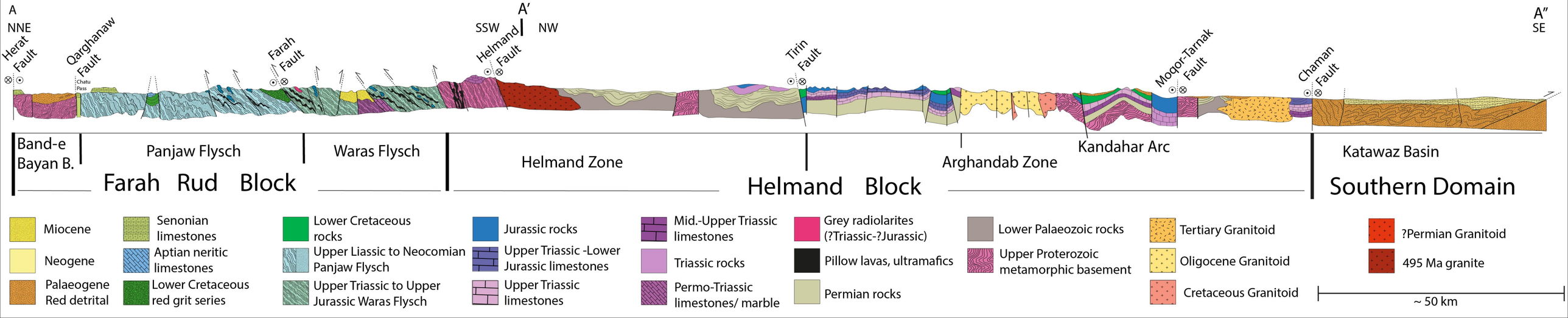
A
NNE
A′
SSW
NW
A″
SE
Herat Fault
Qarghanaw Fault
Chatu Pass
Farah Fault
Helmand Fault
Tirin Fault
Moqor-Tarnak Fault
Chaman Fault
Band-e Bayan B.
Panjaw Flysch
Waras Flysch
Helmand Zone
Arghandab Zone
Kandahar Arc
Katawaz Basin
Farah Rud Block
Helmand Block
Southern Domain
Miocene
Neogene
Palaeogene Red detrital
Senonian limestones
Aptian neritic limestones
Lower Cretaceous red grit series
Lower Cretaceous rocks
Upper Liassic to Neocomian Panjaw Flysch
Upper Triassic to Upper Jurassic Waras Flysch
Jurassic rocks
Upper Triassic -Lower Jurassic limestones
Upper Triassic limestones
Mid.-Upper Triassic limestones
Triassic rocks
Permo-Triassic limestones/ marble
Grey radiolarites (?Triassic-?Jurassic)
Pillow lavas, ultramafics
Permian rocks
Lower Palaeozoic rocks
Upper Proterozoic metamorphic basement
Tertiary Granitoid
Oligocene Granitoid
Cretaceous Granitoid
?Permian Granitoid
495 Ma granite
~ 50 km

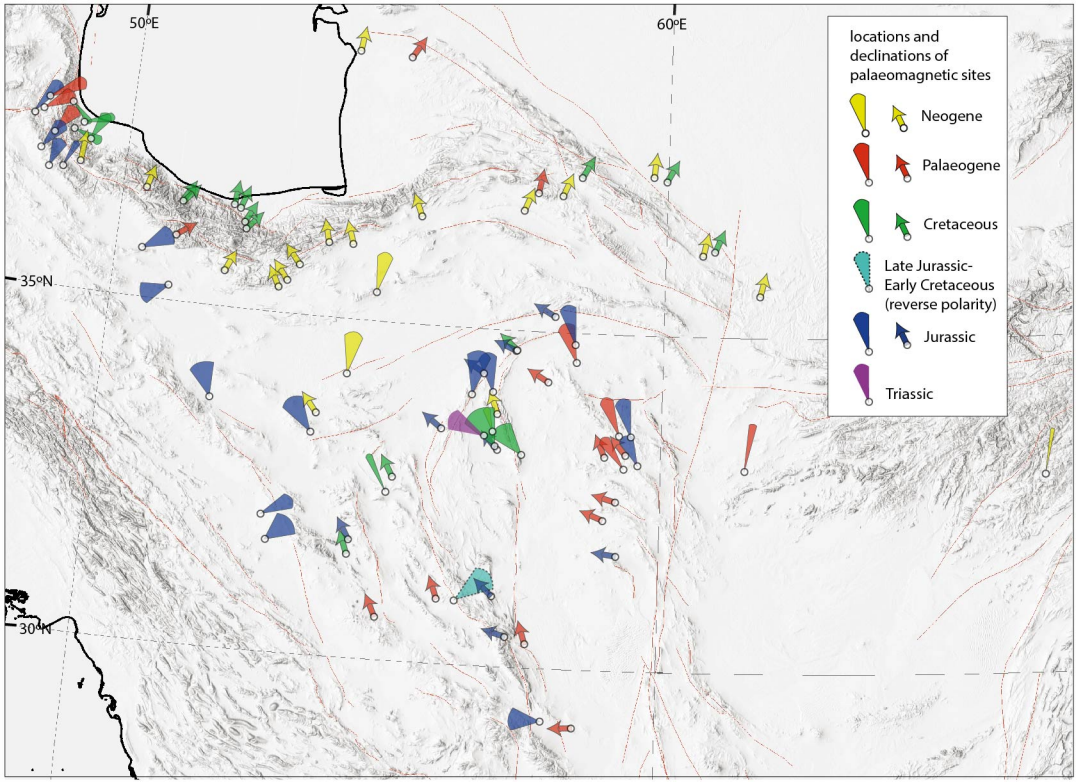
50ºE
60ºE
35ºN
30ºN
locations and declinations of palaeomagnetic sites
Neogene
Palaeogene
Cretaceous
Late Jurassic-Early Cretaceous (reverse polarity)
Jurassic
Triassic

Present Day

EURASIAN PLATE

ARABIAN PLATE

INDIAN PLATE

Greater Caucasus

Pontides

S. Armenian

Greater Adria

Talesh

S. Caspian

Kopet Dagh

Alborz

Central Basin

Sanandaj-Sirjan

Zagros

Band-e Turkestan

Farah-Rud

Waser Suture

Central-East Iranian Microcontinent

Helmand

Sistan Suture

Makran

K.B.

Suleiman Ranges

Tarim Craton

E. Kunlun

Songpan Ganzi

N. Pamirs

C. Pamirs

R

P

S. Pamirs

W. Kunlun

Qiantang

Kohistan

Ladakh

Lhasa

Himalaya

28° 46° 32° 36° 40° 44° 48° 52° 56° 60° 64° 68° 72° 76° 80° 46° 84° 88° 92° 42°

28° 42° 38° 32° 30° 26° 22° 18° 14°

92° 34° 30° 88° 26° 22° 18° 14° 84° 10°

36° 40° 44° 48° 52° 56° 60° 64° 68° 72° 76° 80° 10°

Late Oligocene - 25 Ma

(Eurasia-fixed frame)

EURASIAN PLATE

ARABIAN / AFRICAN PLATE

INDIAN PLATE

Greater Caucasus Basin

Pontides

Greater Adria

S. Armenian

Talesh

S. Caspian

Kopet Dagh Basin

Alborz

Central Basin

Sanandaj-Sirjan

Central-East Iranian Microcontinent

Sistan Suture

Band-e Turkestan

Farah-Rud

Waser Suture

Helmand

RCA

KaB

K.B.

Makran

Tarim Craton

E. Kunlun

Songpan Ganzi

N. Pamirs

?

Pamir Embayment

C. Pamirs

P

R

S. Pamirs

W. Kunlun

Qiantang

Kohistan

Ladakh

Lhasa

Himalaya

Mid-Eocene - 40 Ma

(Eurasia-fixed frame)

EURASIAN PLATE

AFRICAN / ARABIAN PLATE

INDIAN PLATE

Greater Caucasus

Pontides

Greater Adria

S. Armenian

S. Caspian

Kopet Dagh

Talesh

Alborz

Central Basin

Sanandaj-Sirjan

Central-East Iranian Microcontinent

Sistan Suture

Band-e Turkestan

Farah-Rud

Waser Suture

Helmand

RCA

N. Pamirs

?

C. Pamirs

P

R

S. Pamirs

W. Kunlun

Tarim Craton

E. Kunlun

Songpan Ganzi

Qiantang

Kohistan

Ladakh

Lhasa

Himalaya

Danian- 65 Ma

(Eurasia-fixed frame)

EURASIAN PLATE

AFRICAN/ ARABIAN PLATE

INDIAN PLATE

Greater Caucasus

Pontides

Greater Adria

S. Armenian

S. Caspian

Kopet Dagh

Talesh

Alborz

Central Basin

Sanandaj-Sirjan

Sabzevar Ocean

Nain-Baft Suture

Central-East Iranian Microcontinent

Sistan Ocean

Band-e Turkestan

Farah-Rud

Waser Suture

Helmand

RAC

N. Pamirs

?

Tarim Craton

E. Kunlun

Songpan Ganzi

C. Pamirs

W. Kunlun

Rushan-Pshart

S. Pamirs

Qiantang

Kohistan

Ladakh

Lhasa

Himalaya

Turonian- 90 Ma

(Eurasia-fixed frame)

EURASIAN PLATE

Pontides

Greater Caucasus

S. Caspian

Kopet Dagh

Talesh

Alborz

Central Basin

Sanandaj-Sirjan Zone

Sabzevar Nain-Baft Ocean

Sabsevar Nain-Baft SSZ forearc

Central-East Iranian Microcontinent

Sistan Ocean

Sistan SSZ forearc

S. Armenian

Greater Adria

N. Pamirs

?

Tarim Craton

E. Kunlun

Songpan Ganzi

Central Pamirs

W. Kunlun

Rushan-Pshart

Farah-Rud

Waser Suture

Helmand

Southern Pamirs

Qiantang

Lhasa

RAC

Ladakh

Kohistan

NEOTETHYS

AFRICAN/ ARABIAN PLATE

JM

Berriasian- 140 Ma

(Eurasia-fixed frame)

EURASIAN PLATE

NEOTETHYS

Pontides

Greater Caucasus Basin

Talesh

S. Caspian

Kopet Dagh

Alborz

Central Basin

Sanandaj-Sirjan

Sabzevar Ocean

S. Armenian

N. Pamirs

?

Tarim Craton

Mongol-Okhotsk Ocean

?

Central Pamirs

W. Kunlun

E. Kunlun

Farah-Rud

Rushan-Pshart

Songpan Ganzi

Waser Suture

Central-East Iranian Microcontinent

Southern Pamirs

Sistan Rifting

Helmand

Qiantang

Bangong-Nujiang Ocean

Lhasa

Kohistan-Ladakh

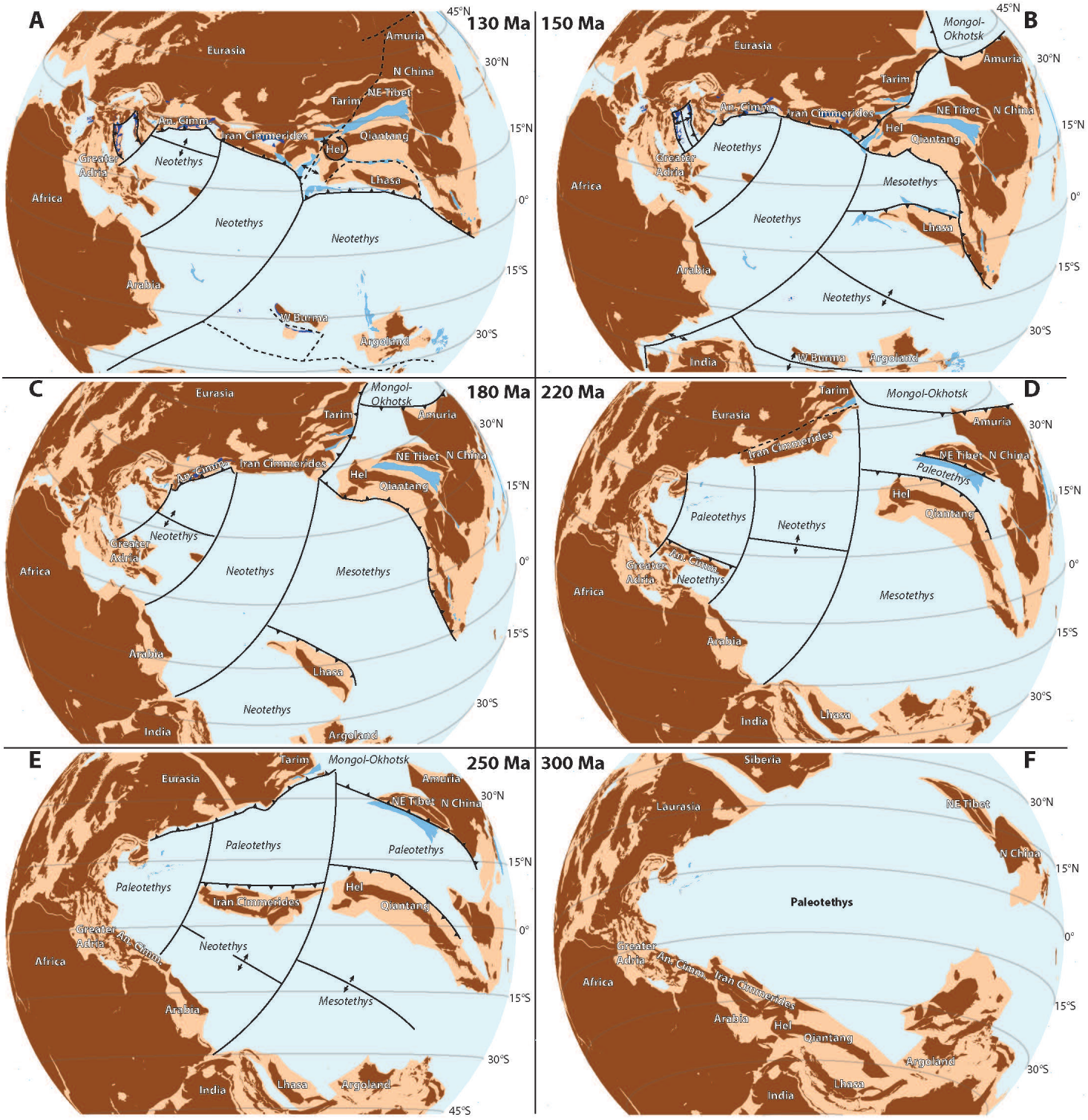
A
130 Ma
Eurasia
Amuria
N China
NE Tibet
Tarim
An. Cimm.
Iran Cimmerides
Qiantang
Hel
Greater Adria
Neotethys
Lhasa
Africa
Neotethys
Neotethys
Arabia
W Burma
Argoland
45°N
30°N
15°N
0°
15°S
30°S
B
150 Ma
Mongol-Okhotsk
Eurasia
Amuria
Tarim
An. Cimm.
Iran Cimmerides
NE Tibet
N China
Hel
Qiantang
Greater Adria
Neotethys
Mesotethys
Africa
Neotethys
Lhasa
Arabia
Neotethys
India
W Burma
Argoland
C
180 Ma
Eurasia
Mongol-Okhotsk
Tarim
Amuria
An. Cimm.
Iran Cimmerides
NE Tibet
N China
Hel
Qiantang
Neotethys
Greater Adria
Africa
Neotethys
Mesotethys
Arabia
Lhasa
Neotethys
India
Argoland
D
220 Ma
Tarim
Mongol-Okhotsk
Eurasia
Amuria
Iran Cimmerides
NE Tibet
N China
Paleotethys
Hel
Qiantang
Paleotethys
Neotethys
An. Cimm.
Greater Adria
Neotethys
Africa
Mesotethys
Arabia
India
Lhasa
E
250 Ma
Tarim
Mongol-Okhotsk
Eurasia
Amuria
NE Tibet
N China
Paleotethys
Paleotethys
Paleotethys
Iran Cimmerides
Hel
Qiantang
Greater Adria
An. Cimm.
Neotethys
Africa
Mesotethys
Arabia
India
Lhasa
Argoland
F
300 Ma
Siberia
Laurasia
NE Tibet
N China
Paleotethys
Greater Adria
An. Cimm.
Iran Cimmerides
Africa
Arabia
Hel
Qiantang
Argoland
India
Lhasa


Caspian Sea
Persian Gulf
Kopet Dagh
The Main Kopet Dagh Fault
Alborz Mountains
Talesh Mountains
West Caspian Fault
Garmsar Basin
Qom Basin
Great Kavir Basin
Doruneh Fault
Urumieh-Dokhtar Magmatic Arc
Sanandaj-Sirjan Zone
Zagros Mountains
Main Zagros Thrust
Yazd Block
Tabas Block
Lut Block
Sistan Suture
Dasht-E Lut
Jaz Murian Depression
Makran Accretionary Complex
Sistan Basin
Kharan Basin
Chagai Arc
Raskoh Arc
Sulaiman Ranges
Chaman Fault
Helmand Block
Farah Rud Block
Band-e Turkestan Mountains
Paropamisus Range
Herat Fault
Hari Rud Fault
Andarab Fault
Gardez Fault
Katawaz Basin
Mokor Fault
UDMA
Nayband Fault
Gowk Fault
Sabzevaran Fault
Nostrabad Fault
Kahurak Fault
West Neh Fault
East Neh Fault
Siahan Fault
Dehshir F.
Shahr-e Babak F.
Anar F.
Kalmard Fault
Joyain Fault
Tabriz
Urumieh
Urumieh Lake
Bonab
Takab
Zanjan
Ardabil
Rasht
Lahijan
Gorgan
Ashgabat
Mashad
Sabzevar
Soltanabad
Biarjmand
Karaj
Tehran
Sanandaj
Qorveh
Hamadan
Kermanshah
Doruneh
Bardaskan
Kashmar
Torbat-e-Heydarieh
Torbat-e-Jam
Fariman
Aghdarband
Jandaq
Nakhlak
Anarak
Nain
Esfahan
Golpaygan
Azna
Dorud
Bayazeh
Posht-e Badam
Esmailabad
Tabas
Boshruyeh
Gonabad
Qayen
Birjand
Gazik
Nayband
Ardekan
Yazd
Abadeh
Kerman
Sirjan
Balvard
Sefidabeh
Nostrabad
Zahedan
Bazman
Iranshahr
Fannuj
Herat
Farah
Kandahar
Kabul
Dalbandin
Spin
Sedimentary Rocks
Quaternary
Pliocene
Miocene
Oligocene
Eocene
Palaeocene
Mesozoic-Cenozoic
Upper Cretaceous
Lower Cretaceous
Jurassic-Cretaceous
Upper Jurassic
M.-L. Jurassic
Upper Triassic
Lower Triassic
Permian-Triassic
Permian
Carboniferous
Devonian
Silurian
Ordovician-Silurian
Ordovician
Cambrian
Palaeozoic
Precambrian
Faults
Sea
Lake
Cities
Metamorphics
Oligocene
Eocene
Palaeocene
U. Jurassic
L-M. Jurassic
Triassic
Mesozoic
Permian
Devonian
Palaeozoic
Intrusive and extrusive rocks
Quaternary
Pliocene
Miocene
Oligocene
Eocene
Palaeocene
Upper Cretaceous
Lower Cretaceous
Upper Jurassic
Jurassic
Upper Triassic
Triassic
Permian
Carboniferous
Devonian
Ordovician-Silurian
Palaeozoic
Cretaceous ultramafic
Cretaceous Ophiolite
Palaeozoic ultramafic
N
0 50 100 200 Kilometers
A
A'